Ubiquitin-proteasome dependent mitochondrial protein quality control

Inauguraldissertation

zur

Erlangung der Würde eines Doktors der Philosophie

vorgelegt der

Philosophisch-Naturwissenschaftlichen Fakultät

der Universität Basel

von

Anne-Sophie Benischke

aus Basel-Stadt

Basel, 2014

Genehmigt von der Philosophisch-Naturwissenschaftlichen Fakultät auf Antrag von

Prof. Christoph Handschin

PD Dr. Albert Neutzner

Prof. Jörg Huwyler

Basel, den 18.02.2014

Prof. Dr. Jörg Schibler

Dekan

Acknowledgments

My first thanks go to PD Dr. Albert Neutzner for giving me the opportunity to perform my doctoral thesis in his laboratory. It was a great privilege to work under his supervision. I want to thank him for introducing me to the fascinating world of mitochondria, for guiding me through these years with enthusiasm and scientific support and for taking time whenever I needed help.

I would like to thank Prof. Christoph Handschin for having accepted the role of the faculty representative and for taking time for my PhD committee meeting.

I am very grateful to Prof. Jörg Huwyler for joining my PhD committee as a co-referee. I also want to thank Prof. Christoph Meier for offering me to be the chairman of my defense.

I want to thank the whole members of the eye clinic, especially Prof. Josef Flammer and Prof. David Goldblum for their scientific and personal support.

I would like to thank Beat and Mike for introducing me to the microscopy and for their support and helpful suggestions concerning questions.

A special thank goes to all my lab members of the Ocular Pharmacology and Physiology. It was a pleasure working with all of them in the laboratory and watching how this laboratory group was growing and developing over the last years. Therefore, big thanks go to Esther for supporting me so much in several protein purifications. Also special thanks go to Corina, Claudia, Lei, Jia, Charles, Kathrin, Tatjana, Roy and Reto for supporting me with good advise during my thesis.

Furthermore, I would like to thank the members of the Department of Biomedicine, especially Niklaus Vogt and Ilija Lujic for their IT support.

I would like to thank the Freiwillige Akademische Gesellschaft (FAG), especially the August Collin-Fonds for their financial support.

Most importantly I would like to express my deepest gratitude to my family. A special thank goes to my boyfriend Cornelius for his limitless support, love and for always

believing in me. My sincerest thanks are addressed to my parents, who provided me the opportunity to be where I am now and to do what I love the most.

Abstract

Dysfunctional mitochondria cause many neurodegenerative disorders and with aging in general, mechanisms of mitochondrial quality control are essential for cellular function. Keeping mitochondria in a healthy state is a complex process, which is tightly regulated by several mitochondrial quality control systems. An ubiquitin-mediated proteasome-dependent protein degradation pathway, termed outer mitochondrial-associated degradation (OMMAD), was recently described. OMMAD provides mitochondrial protein quality control to prevent mitochondrial damage. Up until now, four outer mitochondrial membrane-anchored RING finger ubiquitin ligases as well as the AAA-ATPase p97 were described as OMMAD components. Here, we further characterize the mitochondrial RING finger protein MARCH9. We found that MARCH9 is an unstable protein degraded in a proteasomal-dependent manner. Furthermore MARCH9 interacts physically with both mitofusins, Mfn1 and Mfn2, both involved in the mitochondrial fusion. The dominant-negative mutant of MARCH9 was found to block mitochondrial fusion and cause mitochondrial fragmentation. Taken together, our result suggests a role for MARCH9 in mitochondrial quality control and further integrates OMMAD into mitochondrial physiology.

Not only reactive oxygen species are involved in the aging process and in neurodegeneration, other stressors such as reactive nitrogen species, especially nitric oxide (NO) also cause such damage. Constant low level damage caused by NO to mitochondria eventually results in the loss of mitochondrial integrity and ultimately mitochondrial dysfunction. NO can directly modify mitochondrial proteins in a reaction, called S-nitrosylation. In response to low level of exogenous NO but also in the absence of such exogenous nitrosative stress, S-nitrosylated proteins are present in mitochondria. Furthermore, we found that upon inhibition of the proteasome, levels of S-nitrosylated proteins are increased and that the AAA-ATPase p97 is involved in the translocation of such S-nitrosylated proteins from mitochondria into the cytosol.

Taken together, OMMAD components are necessary for maintaining mitochondrial integrity on the molecular and on the organellar level through the removal of damaged proteins and through regulating mitochondrial morphology.

Table of Contents

List of Figures

List of Tables

Abbreviations

-SH	thiol group
-SNO	S-nitrosothiol
°C	celsius
AA	amino acid
AAA-ATPase	ATPase associated with various cellular activities
ActD	actinomycin D
ADOA	autosomal dominant optic atrophy
ADP	adenosindiphosphate
ALS	amyotrophic lateral sclerosis
AMP	adenosine monophosphate
AMPK	AMP-activated protein kinase
APC2	anaphase promoting complex 2
APS	ammonium persulfate
ATP	adenosintriphosphate
Bax	BCL2-associated X protein
Bcl-2	B-cell lymphoma 2
BSA	bovine serum albumin
Ca^{2+}	calcium
Cam	chloramphenicol
CCCP	carbonyl cyanide m-chlorophenyl hydrazone
CD4	cluster of differentiation 4
Cdk1	cyclin-dependent kinase 1
ClpXP	caseinolytic mitochondrial matrix peptidase
CMT2A	Charcot-Marie-Tooth neuropathy type 2A
CRL	cullin-RING ubiquitin ligases
Cys	cysteine
ddH_2O	double-distilled water
DMEM	Dulbecco's Modified Eagle's Medium
DMSO	dimethylsulfoxid
DNA	deoxyribonucleic acid
Dnm1	dynamin 1
dNTP	deoxynukleosidtriphosphate

Drp1	dynamin-related protein 1
DTT	dithiothreitol
E2	ubiquitin-conjugating enzyme
E3	ubiquitin protein ligase
EDTA	ethylenediaminetetraacetic acid
eNOS	endothelial nitric oxide synthase
ER	endoplasmic reticulum
ERAD	endoplasmic reticulum-associated degradation
ETC	electron transport chain
FA	Friedreich's ataxia
FAD	flavin adenine dinucleotide
FZO	fuzzy onion
GED	GTPase effector domain
GFP	green fluorescent protein
Gly	glycine
GSH	reduced glutathione
GSK3β	glycogen synthase kinase 3 beta
GSNO	S-nitrosoglutathione
GSNOR	S-nitrosoglutathione reductase
GST	glutathion-S-transferase
GTPase	guanine triphosphatease
H_2O_2	hydrogen peroxide
HA-epitop	hemagglutinin-epitop
HECT	homologous to the E6-AP carboxyl terminus
hFis	human mitochondrial fission 1 protein
His_6-tag	hexahistidin-tag
HLA-DOβ	human leukocyte antigen
HR	heptad repeat
HRP	horseradish peroxidase
IBRDC2	in-between-ring (IBR)-type RING-finger domain
ICAM-1	intercellular adhesion molecule 1
IMM	inner mitochondrial membrane
IMS	intermembrane space

IPTG	isopropyl-ß-D-thiogalactopyranosid
Kan	kanamycin
kD	kilo Dalton
l	liter
LB	Luria-Bertani
LHON	Leber hereditary optic neuropathy
Lys	lysine
MAP1B	microtubule-associated protein 1B
MARCH	membrane-associated RING CH
MAVS	mitochondrial antiviral signaling protein
MBP	maltose binding protein
Mcl-1	myeloid cell leukemia sequence 1
Mdv1	mitochondrial DiVision
MELAS	mitochondrial myopathy, encephalopathy, lactic acidosis, and stroke
Mff	mitochondrial fission factor
Mfn	mitofusin
mg	milligram
MiD49/MiD51	mitochondrial dynamic protein of 49/51 kDa
MIEF1	mitochondrial elongation factor 1
ml	milliliter
mM	millimolar
MMTS	S-methylmethane thiolsulfonate
MOMP	outer membrane permeabilization
MPP	matrix processing peptidase
mSOD1	mutant superoxide dismutase 1
mtDNA	mitochondrial deoxyribonucleic acid
MTS	matrix-targeting signal
MULAN	mitochondrial ubiquitin ligase activator of NF-κB
Myc	c-myc epitop
N_2O_3	dinitrogen trioxide
NADH	nicotinamide adenine dinucleotide
NDMA	N-methyl-D-aspartate
NLRX1	NOD-like receptor (NLR) family member X1

nNOS	neuronal nitric oxide synthase
iNOS	inducible nitric oxide synthase
NO	nitric oxide
NO_2	nitrogen dioxide
NOS	nitric oxide synthase
O_2	oxygen
OH^-	hydroxide
O_2^-	superoxide
OD	optical density
OMA1	zinc metallopeptidase
OMM	outer mitochondrial membrane
OMMAD	outer mitochondrial membrane-associated degradation
$ONOO^-$	peroxynitrite
OPA1	optic atrophy 1
OXPHOS	oxidative phsphorylation
PARL	presenilin-associated rhomboid-like protease
PCR	polymerase chain reaction
PD	Parkinson's disease
PDI	protein-disulfide isomerase
PEI	polyethylenimine
P_i	inorganic phosphate
PINK1	PTEN induced putative kinase 1
polyQ	polyglutamine
PP_i	pyrophosphates
RING	really interesting new gene
RNS	reactive nitrogen species
ROCK1	rho-associated, coiled-coil containing protein kinase 1
ROS	reactive oxygen species
rpm	revolutions per minute
rRNA	ribosomal ribonucleic acid
RNAi	ribonucleic acid interference
RS-NO	S-nitrosothiol
RT	room temperature

SDS	sodium dodecyl sulfate
SEM	standard error of the mean
SENP5	SUMO1/sentrin specific peptidase 5
Skp1	S-phase kinase-associated protein 1
SNP	sodium nitroprusside
Strep	streptomycin
SUMO	small ubiquitin-like modifier
TANK	TRAF family member-associated NFKB Activator
TCA	tricarboxylic acid
TEMED	tetramethylethylenediamine
tRNA	transfer ribonucleic acid
TrxR	thioredoxin reductase
Uba1/E1	ubiquitin activating enzyme
UCP2	uncoupling protein 2
UPS	ubiquitin proteasome system
V	volt
VDAC	voltage-dependent anion channel
XIAP	X-linked inhibitor of apoptosis
XO	xanthine oxidase
YME1L	YME1-like 1
Zn^{2+}	zinc
zVAD-fmk	benzyloxycarbonyl-Val-Ala-DL-Asp-fluoromethylketone
ΔCT	delta C-terminus
µl	microliter
µM	micromolar

1. Introduction

1.1. Mitochondria

1.1.1. Mitochondrial structure and function

Mitochondria are essential eukaryotic organelles, which play an important role in different cellular functions. While mitochondria are known for their role in adenosine triphosphate (ATP) generation through oxidative phosphorylation (OXPHOS), they are also involved in the synthesis of lipids (*1*), the buffering of Ca^{2+} ions (*2*) and they act as a central player in apoptosis (Figure 1) (*3*). Mitochondria are thought to be derived from an endosymbiotic event, 1.5 billion years ago, between an archaeal ancestor and an α-proteobacteria, together building the first eukaryotic cells (*4*). Reminiscent of their endosymbiotic origin, mitochondria are double-membraned organelles giving rise to four distinct mitochondrial compartments (*5*). First an outer mitochondrial membrane (OMM), second an inner mitochondrial membrane (IMM), third the intermembrane space (IMS) between OMM and IMM and finally the matrix compartment contained within the inner mitochondrial membrane (*6*).

The outer mitochondrial membrane delimits mitochondria towards the cytosol, but also allows rapid exchanges of metabolites via channels forming porins. The inner mitochondrial membrane is the membrane with the highest protein content (around 75%) of all cellular membranes due to the massive amounts of electron transport chain proteins (*7*). Also, the IMM is highly invaginated and forming so called cristae greatly increasing membrane surface area (*8*). The mitochondrial matrix contains soluble enzymes, which are involved in fatty acid β-oxidation and in the citric acid cycle, essential for energy conversion. The matrix also holds the mitochondrial DNA (mtDNA) molecules and the machinery necessary for mtDNA replication and protein translation (*9*). The human mtDNA is a circular molecule, encoding 13 proteins of the respiratory chain and special rRNAs and tRNAs, important for translation of proteins encoded by the organellar genome. The mtDNA is organized in so called nucleotides containing 2-10 mtDNA copies with up to several thousand nucleotides per cell (*10*).

Almost all biochemical reactions of the cell depend on the hydrolysis of ATP to adenosine diphosphate (ADP + P_i) or ATP to adenosine monophosphate (AMP + PP_i). In order to

maintain ATP homeostasis, and therefore guarantee both cell integrity and cell function, ATP must be constantly replenished (*11*), as about 40 kilogram of ATP are turned over by the human body daily (*12*). Mitochondria are the main site of energy conversion from food into ATP via oxidative phosphorylation (OXPHOS). The electron transport chain (ETC) consists of five transmembrane complexes. Complexes I to IV are involved in the oxidation of nicotinamide adenine dinucleotide (NADH), electron transport and generation of a proton gradient across the IMM. While complex V, also known as F_0F_1-ATP synthase, uses this proton gradient to convert ADP + P_i to ATP (*13*). Each complex is made of multiple subunits, which are encoded by both the nuclear and the mitochondrial genomes, except for complex II, which is entirely encoded by the nuclear genome (*14*).

In detail, complex I (NADH: ubiquinone oxidoreductase) is the largest complex of the ETC and catalyzes the reduction of ubiquinone by NADH effectively transferring reduction equivalents from the tricarboxylic cycle (Krebs) and β-oxidation of fatty acid. Complex I translocates four protons for one oxidized NADH molecule across the inner membrane, thereby producing an electrochemical gradient (*15*). Complex II (succinate:quinone oxidoreductase) consists of four subunits, all encoded by the nuclear genome (*16*). During succinate oxidation, electrons are transported by flavin-adenine dinucleotide (FAD) coenzyme through the Fe-S clusters to reduce ubiquinone to ubiquinol. This reaction is not associated with proton transfer (*17*). Complex III (ubiquinol-cytochrome *c* oxidoreductase) consists of eleven subunits with only one subunit (cytochrome *b*) encoded by mtDNA (*18, 19*). Complex III catalyzes the oxidation of ubiquinol and the reduction of cytochrome *c* also generating a proton gradient across the inner mitochondrial membrane through the transfer of four electrons (*20*).

Finally, complex IV (cytochrome *c* oxidase; COX) is the last enzyme of the electron transport chain and consists of 13 subunits encoded by both the mitochondrial and nuclear DNA (*21*). The four electrons are transferred from cytochrome *c* to the heme center of CuA and from there, on to the heme center of CuB, also generating an additional proton gradient across the inner mitochondrial membrane (*22*).

Complex V (ATP synthase, F_0F_1-ATPase) is the enzyme that converts the proton gradient across the IMM generated by the ETC into ATP. This complex consists of a globular F_1

domain, localized in the matrix, and a F_0 domain, embedded in the inner mitochondrial membrane (*23*). The F_0 domain resembles a rotor composed of several subunits. Protons travel through a channel along the electrochemical potential thereby causing the rotation of this rotor and leading to the generation of ATP from ADP and inorganic phosphate (P_i) for every 120° turn (*24, 25*).
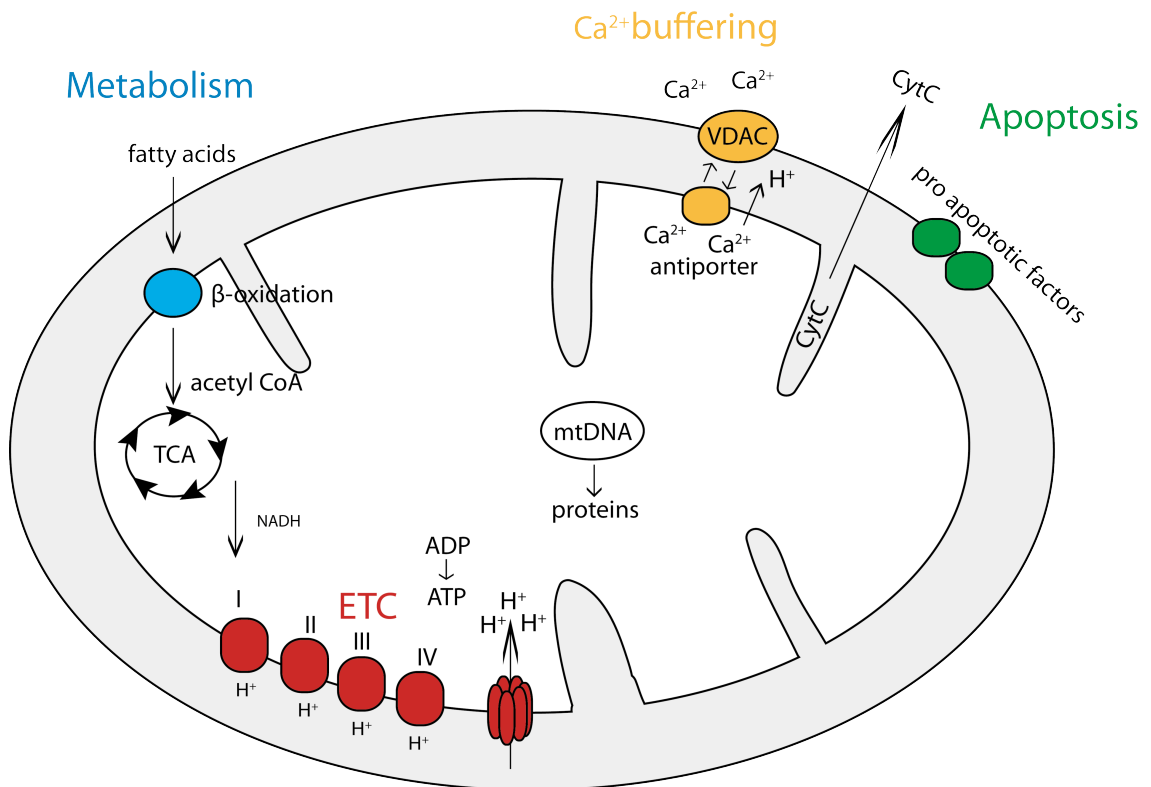
Figure 1: Functions of mitochondria
Mitochondria are involved in different cellular functions. Their main function is energy conversion in the process of β-oxidation, tricarboxylic acid (TCA) cycle and the electron transport chain all leading to the production of ATP. Additionally, mitochondria are involved in calcium homeostasis via the VDAC dependent transfer of Ca^{2+} across the outer mitochondrial membrane and the Ca^{2+}/H^+ antiporter-mediated Ca^{2+} transport across the inner mitochondrial membrane. Mitochondria are as well involved in the apoptotic pathway with pro-apoptotic signals triggering cytochrome *c* release from the mitochondria (*26*).

1.2. Mitochondrial and cellular stressors

1.2.1. Oxidative stress

Mitochondria are not only the powerhouse of the cell, they are also the major source of endogenous reactive oxygen species (ROS). Mitochondria are the main consumers of oxygen in the body as final electron acceptor during OXPHOS. Mitochondria strictly control oxygen handling, however, due to the reactive nature of O_2, the generation of ROS,

such as superoxide (O_2^-), hydrogen peroxide (H_2O_2) and hydroxyl radicals (OH^-), is an avoidable consequence of aerobic metabolism. These oxidants are highly reactive molecules and therefore capable of damaging mtDNA, proteins and lipids (*27*). As the generation of ROS is unavoidable, several defense mechanisms, including ROS converting enzymes or ROS scavengers (*28*) help to reduce oxidative stress. However, oxidative stress exists despite the antioxidant defense, and it has been almost 50 years since Harman proposed the "free radical theory" of aging (*29*). This hypothesis suggests that free radicals lead to aging, as well as to age-related neurodegenerative disorders (*30*). A "vicious cycle" of ROS production during ageing has been postulated (*31*). Miquel et al. (*32*) first suggested that mtDNA might be damaged during aging by enhanced ROS production. The production of hydrogen peroxide (H_2O_2), superoxide (O_2^-) and hydroxyl radicals (OH^-) products causes accumulation of mtDNA mutations giving rise to mutated and therefore sub par ETC components, in turn, increasing ROS production, which leads to an increased rate of mtDNA mutations (*33*). During ageing, this vicious cycle would cause an ever increasing mitochondrial ROS production, leading to ever more oxidized proteins and mtDNA mutations (*34*) and finally resulting in cell death.

However, the "vicious cycle" hypothesis is still controversial and it is unclear, whether mitochondrial ROS production indeed increases with age. This view was challenged by the so called mtDNA-mutator mouse. This mouse model contains a point mutation in the proof-reading domain of the mtDNA polymerase causing an increased mtDNA mutation rate. This increased mutation rate leads to increased levels of mutated respiratory chain subunit proteins resulting in elevated ROS production. These mice displayed premature aging associated with hair loss, graying and kyphosis at nine months (*35*). However, the point mutations observed in the mutator mouse mtDNA accumulated in a linear manner and no an exponential increase of ROS production was observed as predicted by the "vicious cycle" hypothesis (*36*). Rather, these results indicate that the profound aging phenotypes in mtDNA mutator mice are not produced by a "vicious cycle" of increased oxidative stress but still support the involvement of mitochondria-derived ROS in aging.

1.2.2. Reactive nitrogen species

Besides reactive oxygen species, other reactive intermediates are known to cause cellular damage. One of them is nitric oxide (NO), a small free radical synthesized from L-arginine by the nitric oxide synthase (NOS) (*37*). Three different genes encode the three isoforms of

the NOS enzymes. Two of these isoforms, endothelial NOS (eNOS) and neuronal NOS (nNOS), are constitutively expressed. In endothelial cells, NO produced by eNOS plays an important role in the regulation of vascular tone (*38*), while inducible NO synthase (iNOS) production is promoted by certain cytokines or bacterial lipopolysaccharides. In macrophages, iNOS produce a high amount of NO as part of the host defense mechanism (*39*).

However, besides these functions of NO in normal cellular physiology, NO is also able to form highly active intermediates with O_2, or various transition metals, such as iron. These NO-intermediates quickly support additional nitrosative reactions, such as S-nitrosothiol (RS-NO) formation with cysteine residues in proteins (*40*). Accordingly, NO can react with many different metal- and thiol-containing proteins and modify them via S-nitrosylation. NO can also react with superoxide (O_2^-), which leads to the formation of peroxynitrite anion ($ONOO^-$), a highly unstable and reactive compound with great potential for cellular damage (*41, 42*).

1.2.3. S-nitrosylation of proteins

Whether NO acts as regulatory protein modification in cellular signaling or causes protein damage associated stress depends on the specific biological environment. Various proteins are regulated by a posttranslational modification with NO-induced S-nitrosylation. S-nitrosylation is a reversible process where a NO reacts with a cysteine thiol group (-SH) of a specific protein to regulate its function. This S-nitrosylation reaction forms an S-nitrosothiol (-SNO), and a S-nitrosylated protein is therefore called a SNO-protein (*43*). Under certain physiological conditions, S-nitrosylation changes the function of a target protein and can therefore play an important role in different regulatory processes. Like other posttranslational modifications, S-nitrosylation can promote conformational changes, modulate channels and trigger protein interactions (*44, 45*). NO is a signal molecule with a broad aspect of functions, but in excess it can lead to cellular damage, including neuronal cell damage, and cell death (Figure 2). There are some specific examples where S-nitrosylation plays a key role and affects neuronal survival. Overactivation of NDMA-receptors leads to excessive release of Ca^{2+}, which produces ROS and activates nNOS resulting in massive NO production and cell damage (*46*). However, S-nitrosylation of NMDA receptor itself decreases its activity resulting in an attenuation of the process (*47*).

In another example, the ubiquitin ligase X-linked inhibitor of apoptosis (XIAP) targets activated caspases for ubiquitination and degradation therefore leading to the degradation and inactivation of caspases (*48*), thus inhibiting caspase-mediated apoptosis and promoting cell survival (*49*). In animal models of Parkinson's diseases and also in patients, an increase of S-nitrosylated XIAP was shown, consistent with insufficient attenuation of caspase function and increased apoptotic cell death (*50*). On the other hand, it was also demonstrated that NO can modify the catalytic cysteine of almost all caspases, thus inhibiting their protease activity and subsequently, preventing apoptotic cell death (*51*).

Another area where S-nitrosylation plays an important role is the S-nitrosylation of the protein-disulfide isomerase (PDI). PDI is an oxidireductase of the endoplasmatic reticulum (ER), and belongs to the Trx family, which is responsible for proper protein folding by inducing disulfide bond formation, breaking disulfide bonds or catalyzing thiol exchange (*52*). Under conditions of nitrosative stress, the isomerase activity of PDI is decreased due to S-nitrosylation leading to the accumulation of misfolded proteins and subsequently ER stress (*53*).

S-nitrosylation also plays an important role in the inhibition of the activity of the ubiquitin ligase Parkin in Parkinson's disease (*54*). Parkin, together with PINK1, are involved in the mitophagic clearance of mitochondria (*55*). Several studies have shown that excessive nitrosative stress induces S-nitrosylation of Parkin (*54*). Parkin has several target cysteine residues that can react with NO to form S-nitrosylated Parkin resulting in its inactivation (*56*). The inhibition of Parkin activity may cause deficits for example in mitophagy or other Parkin-mediated quality control systems ultimately causing cell death (*54*).

In addition to these targets for S-nitrosylation, it was shown that increased levels of NO cause modification of the mitochondrial fission factor dynamin-related protein 1 (Drp1) at cysteine residue 644 (*57*). Formation of SNO-Drp1 influences its guanosine triphosphatase (GTPase) activity and contributes to an excessive mitochondrial fragmentation and neuronal damage (section 1.4.3.).

There are mechanisms in place, such as the thioredoxin and the GSNO reductase systems that play an important role in the S-denitrosylation (*58*).

For example, S-nitrosoglutathione (GSNO) is formed by the reaction between a S-nitrosylated protein and glutathione (GSH) leaving the protein with reduced thiol group. To restore glutathione, GSNO reductase (GSNOR) catalyzes the denitrosylation of GSNO to GSH. It was shown that mice lacking GSNO reductase have an accumulation of S-nitrosothiols (*59, 60*). Consistent with these findings, the addition of GSH to S-nitrosylated proteins results to the fast denitrosylation of proteins *in vitro (61)*.

Another major reductase system involved in denitrosyaltion is the thioredoxin (Trx) system consisting of Trx proteins, thioredoxin reductase (TrxR) proteins and NADPH (*62*). The Trx/TrxR system is involved in the detoxification of free radicals and regeneration of antioxidant compounds such as ascorbic acid and ubiquinones (*63*). The active site of Trx contains a Cys-Gly-Pro-Cys motif (*62*). It was recently found that S-nitrosylated caspase 3 is denitrosylated by Trx1 resulting in caspase activation, while inhibition of Trx1 increased the levels of S-nitrosylated caspase 3 in lymphocytes and macrophages (*64*). There are two mechanisms of Trx-mediated denitrosylation. Either by formation of an intermolecular disulphide intermediate in which Trx is covalent bound to the S-nitrosylated protein through a disulphide bridge or via transnitrosylation in which Trx is transiently S-nitrosylated and NO transferred to another protein (*60*).

Additional to the GSNOR and Trx systems, other enzymes are also involved in the denitrosylation processes, although their physiological function has to be further established. For example, xanthine oxidase (XO) is a flavin-containing enzyme, which is expressed in both prokaryotic and eukaryotic organisms. It was found that CysNO and GSNO are decomposed by XO in the presence of purine substrates (*65*).

In summary, homeostasis of S-nitrosylation is crucial for the maintenance of cellular integrity with excessive S-nitrosylation causing cellular stress. Therefore, denitrosylated systems dealing with S-nitrosylated proteins are very important to cope with low levels of stress and to keep cells and mitochondria in a healthy state.
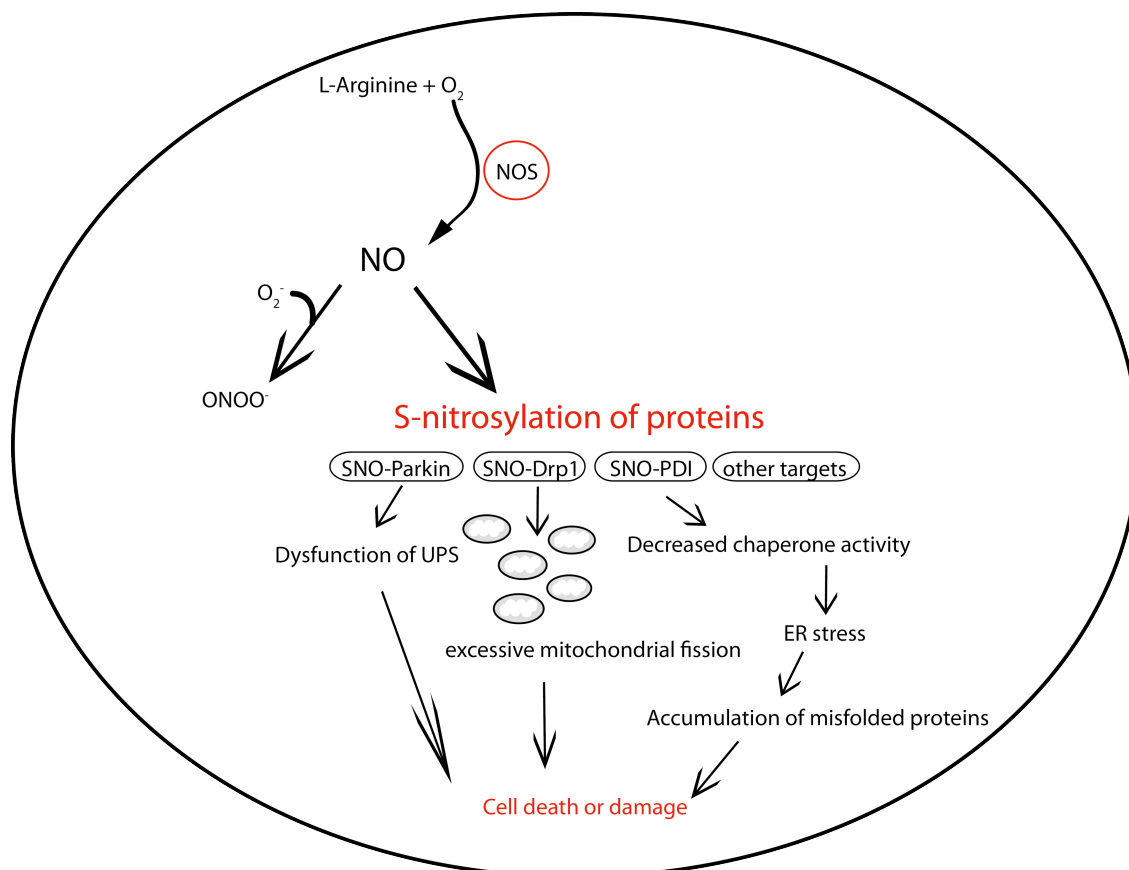
Figure 2: NO triggers formation of S-nitrosylation
Possible mechanism whereby NO can induce S-nitrosylation of different target proteins. NO is produced from L-arginine by NOS and can modify cysteine residues of proteins. For example S-nitrosylation of Parkin, Drp1, PDI and other proteins can contribute to neuronal cell death and damage.

1.3. Mitochondrial Quality Control

Due to the complex mitochondrial structure and exposure to various stressors, tightly regulated defense and quality control systems have evolved to deal with mitochondrial damage (Figure 3). Each of the four-mitochondrial compartments is monitored by its own control system and multi-tiered damage-correlated repair mechanisms are in place to keep mitochondria in a healthy state. Based on the severity of the damage an appropriate response is mounted, including apoptotic clearance of entire cells, mitophagic digestion of individual mitochondria or degradation of mitochondrial proteins in case of less severe damage.

1.3.1. Apoptosis – mitochondrial quality control on the cellular level

Apoptosis, the last line of defense in mitochondrial quality control, is a process whereby cells are induced by either intrinsic or extrinsic signals. Dysregulation of this process leads to several diseases ranging from neurodegenerative disease to cancer and viral infections

(*66*). A wide variety of neurological disorders such as Alzheimer's disease, Parkinson's disease, amyotrophic lateral sclerosis and others are characterized by a loss of neuronal cells. In these diseases, inappropriate apoptosis results in the untimely death of neurons causing ultimately dysfunction of the central nervous system (*67*). On the other hand cancer cells are able to survive due to their decreased ability to undergo apoptosis in response to cytotoxic conditions (*68*). Thus, apoptosis is an essential process for the removal of damaged or harmful cells, so that the organism as a whole can survive (*69*). As opposed to death-receptor induced apoptosis not discussed here (*70*), intrinsic programmed cell death is initiated by the release of apoptotic factors such as cytochrome *c* from the mitochondria to the cytosol. The release of these apoptotic factors requires mitochondrial outer membrane permeabilization (MOMP) modulated by various pro- and anti-apoptotic proteins (*71*). It was found that cytochrome *c*, a 15kD redox carrier protein, usually responsible for the electron transfer between complex III and IV in the electron respiratory chain, is essential for the activation of caspases (*72*). In summary, mitochondria play an important role in integrating different apoptotic signals by release of proapoptotic factors and are themselves the target for quality control in case of extensive mitochondrial damage.

1.3.2. Mitophagy – a quality control on the organellar level

In contrast to the complete removal of mitochondrial networks by apoptosis, in the case of less severe damage to the mitochondrial network, single damaged mitochondrial subunits are targeted by a special quality control system, named mitophagy (*73*).

Mitophagy is a type of autophagy, which was recently found to be governed by the ubiquitin ligase Parkin whereby mitochondria are selectively removed. The translocation of Parkin to the mitochondria is induced by loss of mitochondrial membrane potential, suggesting that collapse of the membrane potential is a signal for Parkin recruitment (*55*). The activity of mitochondrial kinase PINK1 is necessary to recruit Parkin to the mitochondria to induce mitophagy. Recent studies showed that PINK1 is expressed in mitochondria and is rapidly degraded by proteolysis. When mitochondria become damaged, the proteolysis process is inhibited and PINK1 accumulates in the cell thus recruiting Parkin to the affected mitochondria (*74*). Furthermore it was shown that loss of Parkin and PINK1 in *Drosophila* resulted in mitochondria swelling and dysfunction (*75*). These findings suggest that Parkin is important in the elimination of damaged mitochondria from the mitochondrial network to maintain mitochondrial integrity (*74, 76*). Beside the quality

control function, mitophagy is as well needed to adjust mitochondrion numbers, in order to adapt to changes in metabolic requirements (*77*) as well as during specialized development stages of red blood cells where mitochondria need to be completely eliminated (*78*). Taken together, failed mitophagy may be linked to Parkinson's disease and therefore Parkin-mediated mitophagy most likely plays a critical role in maintaining mitochondrial integrity.

1.3.3. Mitochondrial quality control on the molecular level

Moderate damage to mitochondrial compartments might not necessitate complete removal of a mitochondrial subunit by mitophagy. Such damage might be dealt with on the molecular level through either repair or degradation mechanisms.

1.3.3.1. Proteases involved in mitochondrial protein quality control

Molecular chaperones and proteases provide this first line of defense by monitoring mitochondrial protein folding and by mediating the immediate removal of damaged proteins. The quality control system in the mitochondrial matrix contains two bacterial type ATP-dependent proteases. The first is Lon, a serine protease and a member from the ATPase associated with diverse cellular activities (AAA^+) family of proteins, which degrades denatured and oxidized proteins in the mitochondrial matrix (*79*). The second ATP-dependent protease, less well characterized, is ClpXP, which is localized in the matrix space of mitochondria and is also involved in the degradation of damaged proteins (*80*). As the mitochondrial inner membrane contains both the respiratory chain and several proteins, there are multiple possible target proteins for oxidative and nitrosative stress and other protein damage. The quality control of the inner mitochondrial membrane is mediated by the membrane-embedded two metalloprotease complexes, called AAA proteases, which play an important role in the degradation of immature and harmful proteins (*81*). One is the *i*-AAA protease, which faces towards intermembrane space, while the second protease complex, the *m*-AAA protease, exposes the catalytic domain to the matrix side of the inner membrane. Both, *i*-AAA and *m*-AAA are involved in the processing as well as in the degradation of proteins localized either in the matrix, inner mitochondrial membrane or inner mitochondrial space (*82*).
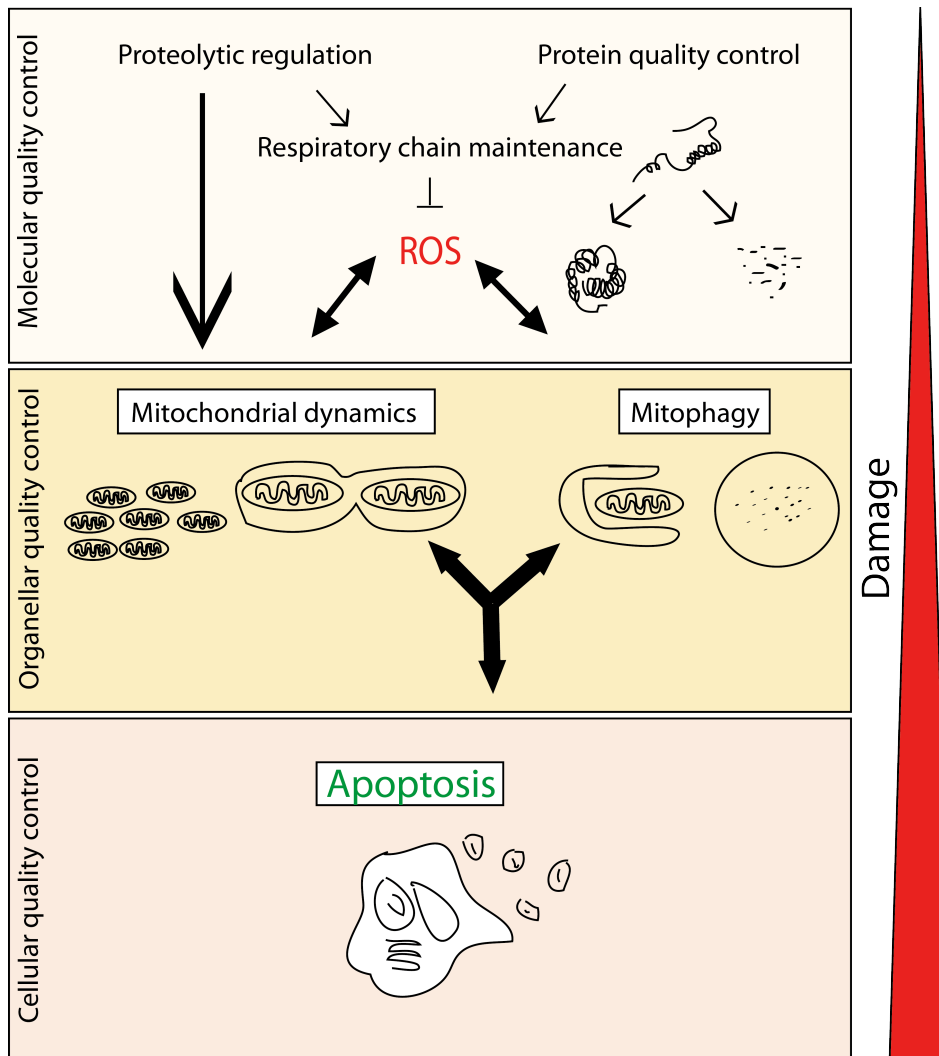
Figure 3: Quality control system of mitochondria
The molecular quality control is the first line of defense and is provided by an intraorganellar proteolytic system. The second line of defense is on the organellar level, where damaged mitochondria can either be recovered by the fusion process or removed by mitophagy. As last quality step, apoptosis will be induced, in case of excessive damage (*82*).

1.3.3.2. Ubiquitin-proteasome system (UPS) and mitochondrial quality control

The ubiquitin-proteasome system is a primarily cytosolic multi-component system, responsible for the removal of damaged proteins and therefore involved in protein quality control (*83*). Recently, a role for the UPS in mitochondrial protein degradation was described (*84-87*).

1.3.3.2.1. The ubiquitin-proteasome system

The main function of the UPS is the recognition, tagging and degradation of substrate proteins (*84*). To this end, the small protein modifier ubiquitin, a 76 amino acid protein, is attached to substrate proteins catalyzed by a three-step enzymatic cascade (Figure 4). In the

first step ubiquitin-activating enzyme (Uba1) or E1 forms an energy-rich thioester bond (energy provided by ATP) with the C-terminal glycine residue of ubiquitin and the active site cysteine of the E1. The second step involves a carrier protein, termed ubiquitin-conjugative enzyme E2, which transfers ubiquitin from the high-energy thioester bond on the E1 to another high-energy thioester bond on E2. From there, with the help of an ubiquitin ligase or E3 enzyme, ubiquitin is attached to the ϵ-NH$_2$ group of a lysine residue in the substrate protein forming an isopeptide bond. As ubiquitin itself can be modified by ubiquitination, this cascade results in the formation of a polyubiquitin chain, mostly via the lysine 48 (K48) of ubiquitin. This newly built chain is then recognized by the proteasome and the proteasome degrades the ubiquitin tagged proteins (*88*). However, other lysine residues in the ubiquitin protein such as Lys 63 (*89*) or Lys 11 (*90*) can serve as acceptor to form polyubiqutin chains mediating other processes aside from proteasomal degradation.

As ubiquitin-mediated proteasomal degradation is an irreversible process, substrate recognition has to be very specific and tightly regulated (*91*). While only about fifty E2 proteins are found in the mammalian genome, the presence of several hundred potential ubiquitin ligases implies that the specificity of ubiquitination lies with this class of proteins. Indeed, all E3's seem to have two functional domains, one is important for the interaction between E2 and E3, the other domain essential for target protein recognition (*92*).
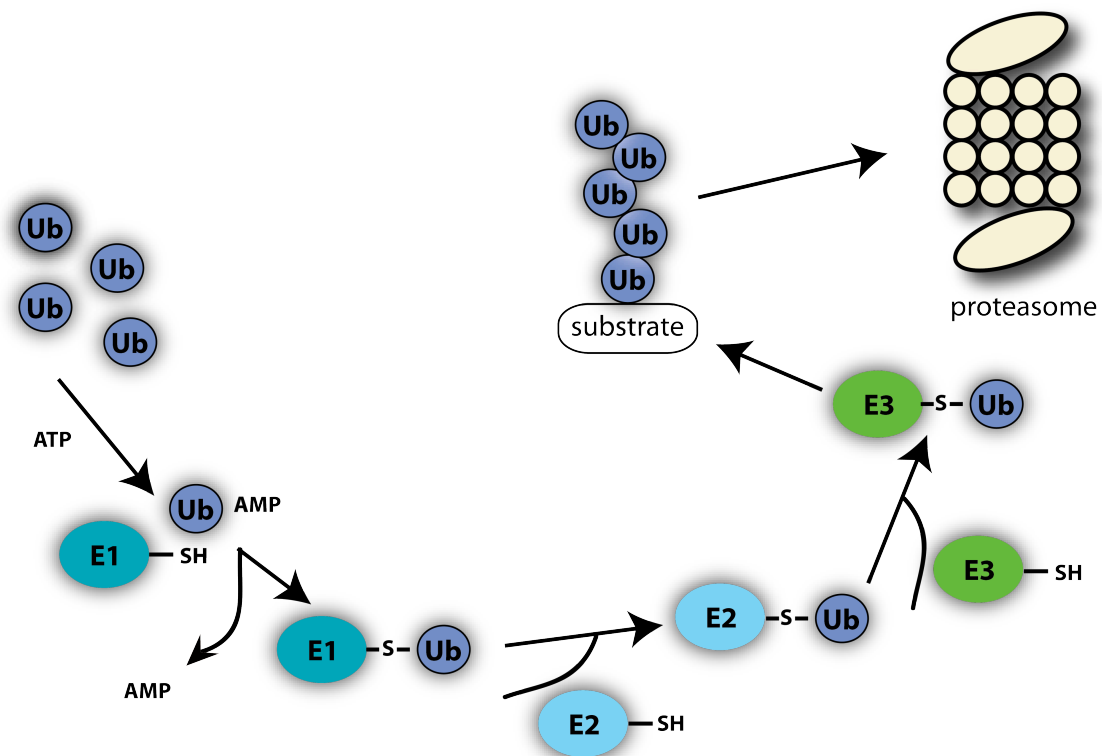
Figure 4: The ubiquitin-proteasome pathway
The three-step cascade start with the ATP-dependent activation of ubiquitin by the ubiquitin-activating enzyme E1, followed by the conjugation of the ubiquitin-activating enzyme (E2), from which ubiquitin is then transferred to Lys residues of a target protein mediated by an ubiquitin ligase E3. This ubiquitin cascade is repeated until a polyubiquitin chain is built. The ubiquitinated protein is then recognized by the 26S proteasome and degraded in an ATP-dependent process.

1.3.3.2.2. Classes of ubiquitin ligases

Two main classes of ubiquitin ligases can be distinguished. The homologous to E6-AP Carboxy Terminus (HECT)-type ubiquitin ligase was first reported in 1995 (*93*). The HECT domain encompasses an active-site cysteine residue, able to form an ubiquitin-ligase intermediate prior to transfer to the substrate protein (*94*).

The largest class of ubiquitin ligases contain a so called RING (Really Interesting New Gene) finger domain and was originally described by Freemont and colleagues (*95*). The canonical RING finger domain consists of a series of cysteine and histidine residues with the consensus sequence $Cys-X_2-Cys-X_{9-39}-Cys-X_{1-3}-His-X_{2-3}-Cys-X_2-Cys-X_{4-48}-Cys-X_2-Cys$ (*96*), which allows the coordination of two zinc ions in a so called cross-brace structure (Figure 5) (*97*). RING finger domains can further be classified into RING-CH or RING-H2, depending on whether the amino acid Cys or His occupies the fifth coordination site (*84*). Unlike the HECT domain, the RING finger domain does not form a catalytic intermediate

with ubiquitin. Rather RING finger containing ubiquitin ligases act as a scaffold that binds E2 to the sharable target protein, bringing them into close proximity, which results in a direct transfer of ubiquitin from the E2 to the substrate (*98*).

A subset of membrane-localized RING finger ubiquitin ligase contains a so called RING variant (RINGv) (Figure 5 and 6) domain and are referred to membrane-associated RING-CH or MARCH proteins. The RINGv domains are characterized by a typical seven amino acids gap between conserved cysteine on position four and histidine on position five of the RING scaffold (*99*). Two out of nine MARCH proteins were found to localize to the outer mitochondrial membrane (section 1.3.3.2.3.) (*100*).

There are other RING finger ubiquitin ligases that exist as multi-subunit protein complexes. A well-studied example is the cullin RING ligase (CRL) superfamily, which has an enormous plasticity in substrate specificity. The cullin RING ligase consists of a cullin protein, a RING protein and an adaptor protein (Skp1) that binds the substrate recognition element, F-box protein. While the cullin ligase exhibits the biggest range of substrate recognition, other multi-subunit E3s have an even greater structural complexity. For example, the anaphase-promoting complex (APC2) contains 13 subunits including a cullin like protein and a RING protein, and is responsible for regulating cell cycle transition (*101, 102*).
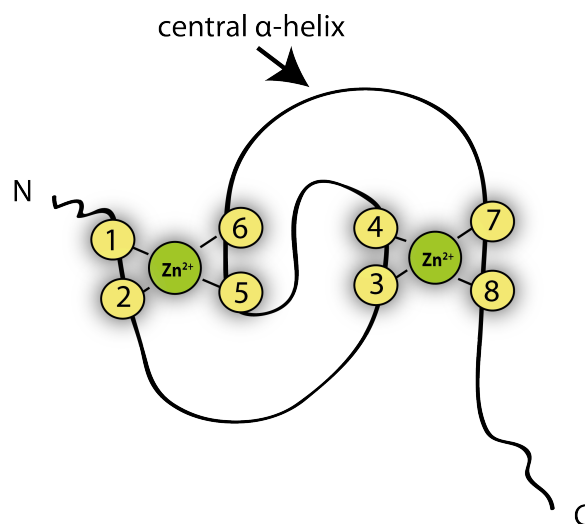
Figure 5: The RING finger structure
The RING finger domain coordinates Zn^{2+} ions in a cross-brace structure, which allows the interaction with specific E2 for ubiquitination. The two Zn^{2+} bind certain cysteine and histidine residues (yellow).

```
MARCH2    CRICHE-GA--NGENLLSPCGCTGTLGAVHKSCLEKWLSS------SNTSYCELC
MARCH4    CRIC-FQGPEQG--ELLSPCRCDGSVKCTHQPCLIKWISE------RGCWSCELC
MARCH6    CRVCRSEGTPE--KPLYHPCVCTGSIKFIHQECLVQWLKH------SRKEYCELC
MARCH8    CRICHCEGDDE--SPLITPCHCTGSLHFVHQACLQQWIKS------SDTRCCELC
MARCH9    CRICFQ-GP--EQGELLSPCRCDGSVRCTHQPCLIRWISE------RGSWSCELC
MARCH5    CWVCFATDEDDRTAEWVRPCRCRGSTKWVHQACLQRWVDEKQRGNSTARVACPQC
```

Figure 6: The RING-CH domain
The RING finger domains found in all MARCH proteins are highly conserved and were shown to possess ubiquitin ligase activity. Amino acid sequences of MARCH RING CH domains are aligned. Red letters show the conserved cysteine and histidine residues of RING finger motif, which are responsible for coordinating two zinc ions.

1.3.3.2.3. Outer mitochondrial membrane-associated degradation (OMMAD)

The UPS plays an important role in mitochondrial quality control. In addition to the different quality levels above, recent findings indicated that the ubiquitin-proteasome system is involved in the control of mitochondrial proteins, which are localized in the outer mitochondrial membrane (*103*). Recently, several ubiquitin ligases were found to locate to the outer mitochondrial membrane, namely the RING finger-containing proteins MULAN (*104*), MARCH5 (*105*), MARCH9 (Neutzner- personal communication) as well as the in-between-RING finger domain protein (IBR) IBRDC2 (*106*), and Parkin (*107*). Similar to the endoplasmatic reticulum (ER), which is quality controlled by ER-associated degradation (ERAD), mitochondrial proteins might be controlled by an analogous mechanism termed OMM-associated degradation (OMMAD) (*105*). During ERAD, chaperones and other factors, such as Hsp70-family members, calnexin, calreticulin and protein disulphide isomerase (*108*) recognize misfolded proteins. Substrates are ubiquitinated by the RING domain containing ubiquitin ligases, Hrd1 (*109*) and Doa1 (*110*) followed by retrotranslocation from the ER to the cytosol. The extraction from the ER requires the activity of the AAA-ATPase p97, which interacts with ubiquitinated substrates (*111*) followed by proteasomal degradation (*112*). Analogue to the ERAD, the same process takes place in the mitochondria. While ERAD is a well-studied mechanism of protein quality control, the OMMAD pathway and its role in mitochondrial maintenance has not been comprehensively studied. However, the presence of mitochondrial ubiquitin ligases, such as, IBRDC2 (*106*), MULAN (*104*) and MARCH5 (*105*) and their involvement in the ubiquitination of mitochondrial proteins support the existence of such a process. The involvement of these ubiquitin ligases in mitochondrial physiology is underlined by the following observations. MARCH5 was shown to be involved in mitochondrial fission by recruiting Drp1 to the mitochondria (*105*) (section 1.4.4.), IBRDC2 was found to regulate the levels of Bax during apoptosis (*106*), while MULAN seems to regulate the

mitochondrial fission machinery (*104*). In addition MARCH9 was implicated in the regulation of mitochondrial fusion (Neutzner- personal communication) (section 3.1.5.). The proteasomal degradation of membrane and organeller proteins takes place in the cytosol, therefore necessitating protein retrotranslocation for UPS-mediated mitochondrial protein degradation is likely involved. The AAA-ATPase p97, a known retrotranlocator of the ER, was found to be involved in the retrotranslocation and proteasomal degradation of ubiquitinated mitochondrial proteins (*115*). This further underlies the similarities of ERAD and OMMAD on the molecular level (Figure 7).

In addition to mitochondrial proteins as substrates for ubiquitination, several target proteins for OMMAD were recently identified. One such target, are the mitofusins, important for maintaining mitochondrial morphology (*113*). First in yeast and later in human cells, Fzo1 and Mfn2, respectively, were shown to be degraded in an ubiquitin-dependent proteasome-mediated manner (*105*) (section 1.4.2.). Another mitochondrial UPS substrate is the uncoupling protein 2 (UCP2) located on the inner mitochondrial membrane. It was shown that UPC2 is ubiquitinated by an unknown E3 ligase and extracted from the mitochondrial inner membrane by processes that are probably ATP dependent. UCP2 is then subsequently degraded by the proteasome (*114*). Another example for an OMMAD substrate is the apoptosis-related outer mitochondrial protein Mcl-1. Mcl-1 is ubiquitinated by the HECT-domain containing ubiquitin ligase Mule (*115*).
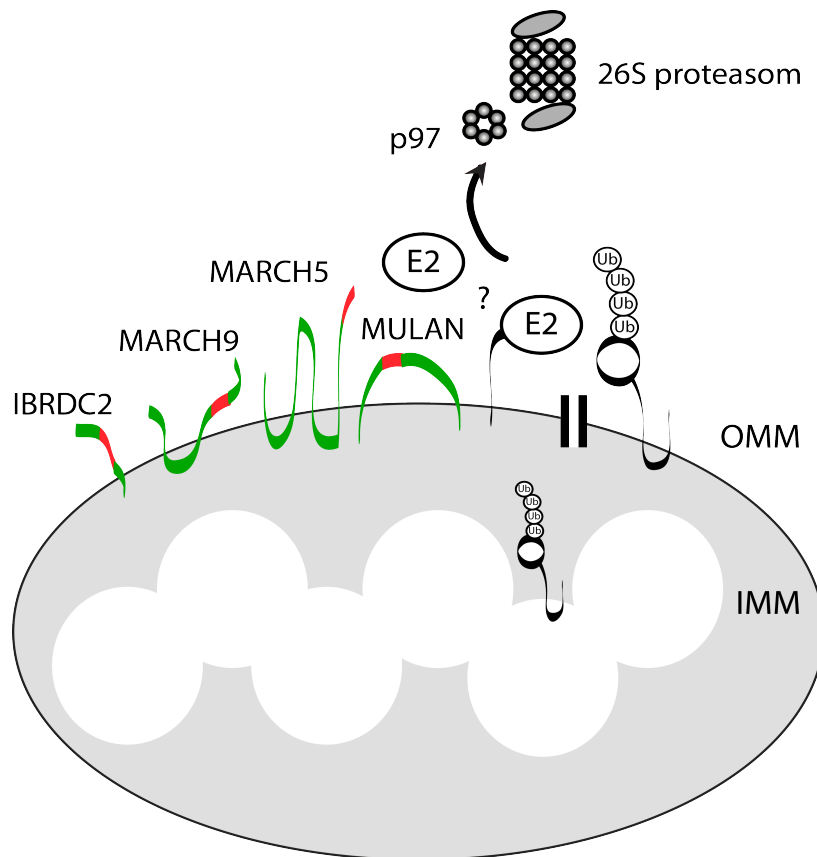
Figure 7: Outer mitochondrial membrane-associated degradation
Ubiquitin ligases (green) with the RING finger domain (red), facing towards the cytosol, are located on the outer mitochondrial membrane. Together with yet unknown ubiquitin conjugating enzyme (E2) the ubiquitin ligase (E3) conduct the ubiquitination of a substrate protein. The hexameric AAA-ATPase p97 translocates the polyubiquitinated protein from the mitochondria to the cytosol. The target protein is then degraded by the 26S proteasome.

1.4. Mitochondrial morphology

1.4.1. Mitochondrial dynamics

Mitochondria form a dynamic network, which is shaped by a constantly ongoing fission and fusion process (*116*). The balance between fission and fusion is very important for mitochondrial integrity. Excessive fission process leads to small spherical organelles, whereas a shift towards fusion results in an extended interconnected mitochondrial network. Extended mitochondria have, the advantage, compared to small isolated mitochondria (*117*), that they serve as a power transmission system from areas with high ATP demand to areas with low demand (*118*). Furthermore, a fused state of mitochondria helps to buffer Ca^{2+} more efficiently (*119*). In addition, mitochondrial fusion serves to unify and mix mitochondrial compartments, allowing for complementation and repair of mtDNA and helps to buffer local damage to proteins and lipids (*120-122*).

On the other hand, the fission process is important for the clearance of irreversibly damaged mitochondria. Mitochondrial damage leading to loss of membrane potential and ATP production excludes subunits from the mitochondrial network as the fusion process depends on mitochondrial membrane potential. On the other hand, mitochondrial fission is independent of membrane potential resulting in the separation of damaged mitochondria from an otherwise healthy mitochondrial network. This separation process aids the mitophagic removal of such damaged mitochondria (*123*) (section 1.3.2.). Beside this mechanism, the fission machinery is also involved in apoptosis by facilitating cytochrome *c* release and subsequent caspase activation (*124*) (section 1.4.5.).

Mitochondrial morphology is therefore essential to mitochondrial fidelity and has great influence on cellular functions.

1.4.2. Mitochondrial fusion

Mitochondria are double membrane-bound organelles and therefore fusing two mitochondrial subunits, which involves the coordinated fusion of two sets of membranes without losing organelle integrity to maintain mitochondrial membrane potential (*125*). The first mitochondrial morphogen identified is *fuzzy onion* (Fzo), which is required for mitochondrial fusion during the, so called onion stage of spermatogenesis in *Drosophila* (*126*).

Further studies of the fusion process in budding yeast identified Fzo1 as the homolog of fly *FZO* (*127, 128*). In the mammalian system, with the mitofusins Mfn1 and Mfn2, two homologs of Fzo1 were identified. Further characterization revealed a function of these mitofusins in the fusion of the outer mitochondrial membrane (*129*). The mitofusins are large proteins with a multidomain structure containing an N-terminal GTP-binding and two transmembrane domains, as well as two hydrophobic heptad repeat domains (HR). The HR1 domain is localized in the middle and HR2 on the C-terminal region, providing the basis for the coiled-coil intermolecular interactions. The transmembrane domains are important for targeting the protein to the mitochondria (*130*). Both the C-terminus and the N-terminus are exposed to the cytosol (*131*). It was shown that mutations in the GTPase domain block the formation of mitochondrial threads, therefore suggesting being important for the mitochondrial fusion process (*131*) (Figure 8). Furthermore, it was demonstrated that the hydrolysis of GTP by Mfn proteins regulates mitochondrial tethering through the

formation of a mitofusin complex in *trans* necessitating the presence of functional mitofusion on both mitochondrial fusion partners (*132*). Moreover, it seems that Mfn1 and Mfn2 have overlapping functions and are able to at least partially compensate their function. While the fusion process in single knock-out cells was comparable to the process in wildtype cells, loss of both Mfn1 and Mfn2 completely prevented mitochondrial fusion (*133*). Despite this observed complementation, both mitofusins seem to have some specialized functions. Mfn1 is crucial for mitochondrial docking and fusion, whereas Mfn2 has lower GTPase activity and is thought to stabilize the interaction between the two mitochondria (*134*). The docking event involves intermolecular interaction between Mfn proteins mediated by the coiled-coil domain (*135*). The GTPase domain likely provides energy, which is necessary to overcome the energy barrier involved in fusing lipid bilayers (*136*). Mfn2 is also rich in the ER-mitochondria interface and it was shown that Mfn2 regulates the shape of the ER and tethers it to mitochondria by complexes comprising Mfn2 at the ER and Mfn2 or Mfn1 on mitochondria (*137*). Ablation of Mfn2 causes the destruction of the ER structure, the detachment of mitochondria from ER and reduces the Ca^{2+} uptake (*137*).

Mitofusins are central to the fusion process and as such a target of several regulatory mechanisms. In budding yeast, Fzo1 is a substrate for ubiquitin-dependent degradation by at least two different mechanisms. During mating in response to mating pheromone, Fzo1 is destabilized by a yet unknown ubiquitin ligase to allow for mitochondrial fragmentation aiding mitochondrial mixing following zygote formation. During the fusion process itself, Fzo1 is the target of an ubiquitin ligase containing the F-box protein Mdm30. The ubiquitination and degradation of Fzo1 is thereby an essential part of the fusion process itself, likely rendering membrane fusion by Fzo1 irreversible (*138, 139*). A similar process has not been established in human cells and it is unclear how mitochondrial fusion is made irreversible.

The fusion of the inner mitochondrial membrane is performed by another large GTPase protein, the optic atrophy 1 (OPA1). OPA1 is a dynamin family member and contains a GTPase domain, a middle domain and a GTPase effector domain (GED), as well as a coiled-coil domain (*140*). The *OPA1* gene encodes 31 exons of which exons 4, 4b and 5b are involved in alternative splicing, which results in the generation of eight different mRNA variants (*141*). The splice variants are subsequently processed to form different

isoforms with distinct molecular sizes. OPA1 is located in the mitochondrial intermembrane space. Furthermore, OPA1 is synthesized as a preprotein and contains an N-terminal matrix-targeting signal (MTS). The MTS is removed by the mitochondrial processing peptidase (MPP) in the matrix during import to form the mature OPA1 isoforms (*142*), causing OPA1 to locate to the mitochondrial intermembrane space. Besides MPP involved in the maturation of OPA1, there are several proteases identified to date, which are involved in processing of OPA1 isoforms, based on the presence or absence of protease sites, namely the *m*-AAA protease, the *i*-AAA protease and the presenilin-associated rhomboid-like protease (PARL) (*143*). However, a number of other proteases, such as the metalloprotease human yme1-like protein (YME1L) (*144*) and the zinc metalloprotease OMA1 (*145*) can also perform OPA1 isoform processing. The mechanism of OPA1 processing can be different between different cell types and may be regulated by distinct stimuli such as low ATP levels or apoptotic stimuli (*146*). Mitochondrial fusion needs to be tightly coordinated to ascertain simultaneous fusion of the OMM and the IMM to prevent leakage of mitochondrial content. This tight coordination is evident in the strong interdependence of OPA1 and mitofusins. It has been shown that OPA1 requires mitofusins as a partner for mitochondrial fusion. Moreover, mitofusins are unable to promote mitochondrial elongation if OPA1 is unavailable. Beside its function in mitochondrial fusion, OPA1 is also essential for maintaining mitochondrial cristae formation (*147*). It was shown that lacking OPA1 results in highly disorganized and swollen cristae (*148*). Furthermore, it was found that OPA1 reduces cytochrome *c* release and regulates shape and length of mitochondrial cristae (*149*). It seems that OPA1 keeps the cristae junctions tight, which are involved in the cytochrome *c* release (*150*).
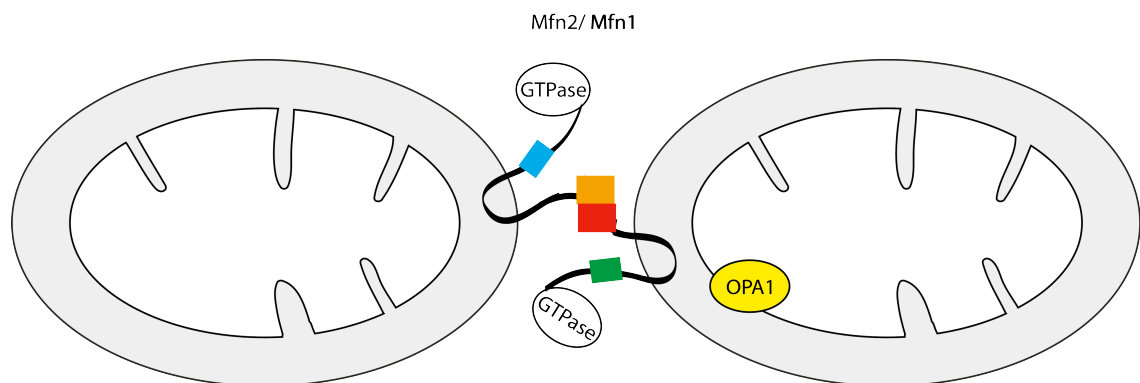
Figure 8: Proteins involved in the fusion machinery
GTPase proteins Mfn1 and Mfn2 are responsible for the fusion process of the outer mitochondrial membrane. The four squares show the coiled-coil region of the mitofusins. OPA1 is localized on the inner mitochondrial membrane and mediate fusion of the inner membrane.

1.4.3. Mitochondrial fission

The first gene that was identified as being involved in the mitochondrial fission process was *Dnm1*, in *S.cerevisiea* and *C.elegans,* and Drp1, its mammalian homolog (*151*). In general, mitochondrial fission requires the dynamin-related protein Drp1. The dynamin family members have a highly conserved N-terminal GTPase domain, a middle domain and GTPase effector domain (GED). Drp1 is mostly localized in the cytosol, however upon mitochondrial fission, it is recruited to the mitochondria forming distinct mitochondrial foci consistent with fission sites (*152*). Drp1 polymerizes into spirals around mitochondria, and is thought to be a mechanoenzyme, which upon GTP hydrolysis constricts and acts as pinchase similar to the dynamin during scission of endocytic vesicles (*153*). Consistent with its essential function during fission process, inhibition of Drp1 either by RNAi or a dominant-negative mutant leads to very elongated mitochondria that entangle and finally collapse (*154*). Drp1 does not possess a membrane-binding pleckstrin homology (PH) domain like dynamin, and thus relies on receptor-like mitochondrial membrane proteins for recruitment to the OMM (*155*). Four integral membrane proteins of the outer mitochondrial membrane have been suggested to act as receptors that recruit Drp1 to the mitochondria.

Human Fis1 is an integral membrane protein located around the OMM and it is important for the translocation of Drp1 from the cytosol to the mitochondria. The N-terminus of hFis1 faces the cytosol, whereas the C-terminus is exposed to the inner mitochondrial space (*156*). Loss of hFis1 results in fission defects and in failure to recruit Drp1. On the other hand, it was shown that knockdown of hFis1 in HeLa cells did not change mitochondrial morphology (*157*). The yeast Drp1 homolog, Dnm1, requires Fis1 to localize to mitochondria and interacts with Dnm1 via the adaptor protein Mdv1 or Caf4. As there are no mammalian homologs identified for Mdv1 and Caf4, this might be the reason for only a minor binding between Drp1 and hFis and that additional adaptor proteins are required for Drp1 recruitment (*158*).

One such recruitment factor is the mitochondria fission factor (Mff). Mff was identified in a RNAi screen in *Drosophila* for genes causing elongated mitochondria upon a knockdown (*159*). Mff is a tail-anchored protein and was shown to interact with Drp1, but does not build a complex with hFis1. These findings suggest that Mff and hFis act in different stages of the fission process. However, Mff helps to recruit Drp1 and it was shown that depletion

of Mff, inhibits recruitment to the mitochondria. Furthermore, Mff cannot induce mitochondrial fission in cells lacking Drp1 (*160*). These findings suggest Mff, like hFis1, acts as a pro-fission protein. Other fission factors are the mitochondrial dynamic protein of 49kDa (MiD49) and mitochondrial dynamic protein of 51kDA (MiD51) and the mitochondrial elongation factor 1 (MIEF1). These proteins are as well located on the outer mitochondrial membrane. Overexpression of these proteins cause elongated mitochondria and a collapse of the mitochondrial network (*161*). The exact role of MiD proteins is still unclear, however, recent studies suggest that MiD proteins are involved in Drp1 recruitment to the mitochondria and are able to promote fission in the absence of both hFis1 and Mff (*162*).

1.4.4. Regulation of mitochondrial fission

As mitochondrial fission is central for maintaining mitochondrial morphology and induction of apoptosis, this process is tightly regulated via modulation of Drp1 activity. It was found that Drp1 is post-translationally modified by SUMOylation, S-nitrosylation, ubiquitination as well as several phosphorylations and that these modifications can change the dynamic, localization and activity of Drp1 (Figure 9).

Phosphorylation of Drp1 by Calcium/calmodulin-dependent protein kinase 1a increases Drp1 recruitment to the mitochondria and interaction with hFis1 thus increasing mitochondrial fission (*163*). Another kinase, which translocates Drp1 to the mitochondria in response to hyperglycemia, is the serine/threonine kinase rho-associated protein kinase 1 (ROCK1). It was found that ROCK1 promotes phosphorylation of Drp1 at the serine residue and therefore contributes to induce mitochondrial fission (*164*). Drp1 is also targeted for phosphorylation by mitosis-promoting factor cyclin-dependent kinase Cdk1/cyclin B thereby activating Drp1 and allowing mitochondrial fragmentation during mitosis to ensure proper inheritance to daughter cells (*165*).

The glycogen synthase kinase 3 beta (GSK3β) (*166*) as well as AMP-activated protein kinase (AMPK) (*167*) mediate the inactivation of the phosphorylation of Drp1. GSK3β seems to be involved in the cellular response to oxidative stress, protecting neuronal as well as non neuronal cells from apoptosis by preventing excessive mitochondrial fission. Also phosphorylation of Dpr1 by the protein kinase A (PKA) seems to modulate the apoptotic threshold in response to various stimuli. Interestingly, dephosphorylation of Drp1 by the

phosphatase calcineurin increases mitochondrial fragmentation and the sensitivity to cell death (*168*).

Aside from phosphorylation, ubiquitination as well as SUMOylation are able to influence the mitochondrial fission machinery. The mitochondrial RING finger ubiquitin ligase MARCH5 was shown to bind and ubiquitinate hFis1 and Drp1. Silencing of MARCH5 and overexpression of MARCH5 mutant resulted in fragmented or elongated mitochondria (*105, 113*). However, the exact process remains unclear. Besides MARCH5, the ubiquitin ligase Parkin was also shown to regulate Drp1 by promoting ubiquitination and proteasomal degradation. Mutation in the second RING finger region leads to inactive Parkin, reducing levels of ubiquitination and enhanced mitochondrial fragmentation (*169*). Opposing ubiquitination is the SUMOylation of Drp1 by the ubiquitin ligase MAPL. Drp1 was shown to be protected from degradation following SUMOylation and to exhibit enhanced mitochondrial fragmentation activity (*170*). Interestingly, de-SUMOylation also plays a role in regulating Drp1 activity. The SUMO protease SENP5 catalyzes the removal of SUMO1 from Drp1. When SENP5 is up-regulated, it promotes the degradation of Drp1 and thereby inhibits the fission process. In contrast, knockout of SENP5 stabilized Drp1 and resulted in fragmented mitochondria (*171*).

1.4.5. Mitochondrial morphology and apoptotic induction

It has been shown that apoptosis and cytochrome *c* release is linked to the fragmentation of the mitochondrial network, by translocation of Drp1 from the cytosol to the mitochondria (*172*). The involvement of mitochondrial morphology in apoptosis is supported by the discovery that overexpression of a dominant-negative Drp1 (Drp1^{K38A}) mutant retards the release of cytochrome *c* and therefore inhibits apoptosis (*124*). In addition, inhibition of the fusion process often observed during apoptosis, results in mitochondrial fragmentation after activation of proapoptotic factors of the Blc-2 family (*173*). It has been shown that knockdown of the fusion protein optic atrophy 1 (OPA1) results in mitochondrial fragmentation and furthermore sensitizes cells to apoptotic stimuli suggesting an anti-apoptotic role for OPA1 (*154*).
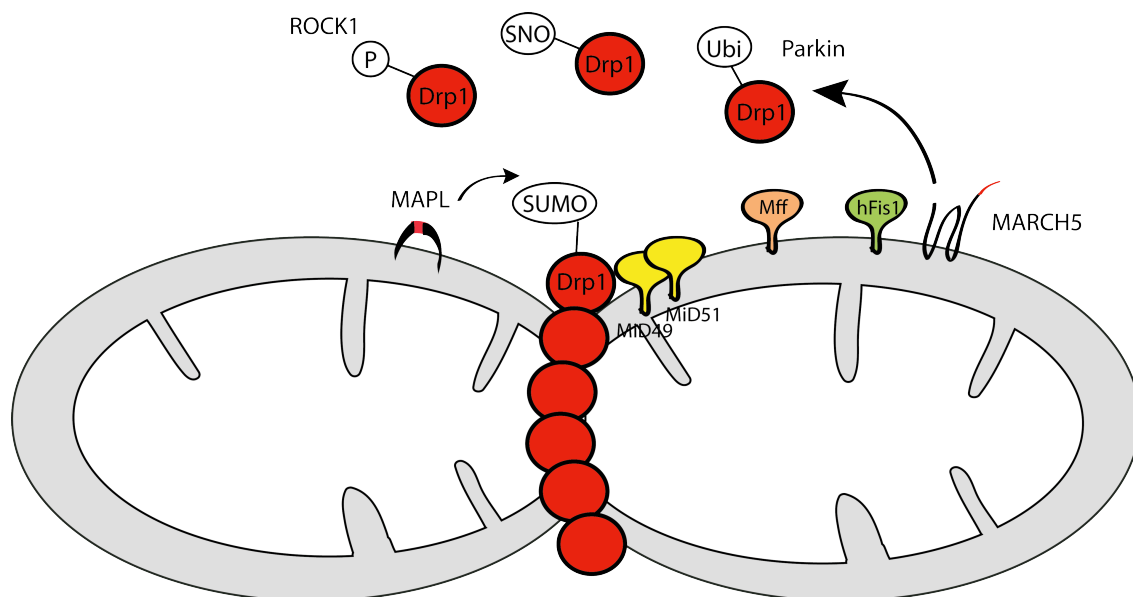
Figure 9: Proteins involved in the fission machinery
Drp1 is localized in the cytosol and is recruited to the mitochondria in the fission process. Drp1 oligomerizes into a contractile spiral around mitochondria and severs the mitochondria following GTP hydrolysis. Fission is mediated by outer membrane receptors, such as hFis1, Mff and MiD49/MiD51 that are proposed to act as recruiters for Drp1. Drp1 can be regulated by different modifications. The ubiquitin ligase MARCH5 and Parkin are known to ubiquitinate Drp1. SUMOylation by the ubiquitin ligase MAPL stabilizes Drp1 and promotes fission. Phosphorylation is another modification induced by several kinases and regulates Drp1.

1.5. Mitochondrial dysfunction in neurodegenerative diseases

Preserving the integrity of mitochondria is essential for cellular survival. For neuronal cells especially, a role for mitochondria in neurodegeneration is now widely accepted. Increased life expectancy during recent decades has resulted in a dramatic boost to the risk factors of neurodegenerative diseases (*174*). Defects in mitochondrial function have been implicated in neurodegenerative diseases (*175*). Mitochondrial dysfunction in neurodegenerative disorders is linked to mtDNA depletion, excessive ROS production, accumulation of misfolded proteins, mitochondrial morphology disturbances and losses in membrane potential (*176*).

1.5.1. ROS-dependent neurodegenerative disorders

One major factor for mitochondrial dysfunction is accumulating oxidative stress caused by the action of ROS (section 1.2.1.). Free radicals are produced constantly and must be balanced by antioxidant defenses to maintain cellular integrity. Imbalance of ROS and antioxidant systems result in oxidative stress and therefore causing damage, which leads to several neurodegenerative disorders (*177*). As an example of ROS-mediated neurodegeneration, Friedreich's ataxia (FA) is caused by a mutation in the gene coding for the protein frataxin (*178*). Frataxin acts as a chaperone in mitochondrial iron transport,

which leads to an accumulation of Fe(II) in mitochondria and finally to an increased ROS production (*179*) as Fe(II) is known to facility single electron reaction with oxygen. In another example, mutations in the subunits of NADH dehydrogenase (*180*) causing LHON (Leber's hereditary optic neuropathy) (*181*) are linked to optic nerve degeneration. As complex I is known to be the major source of ROS, LHON mutations seem to increase ROS production causing damage to retinal ganglion cells (*182*). Another such disorder, MELAS (mitochondrial myopathy, encephalopathy, lactic acidosis and stroke-like episodes) is also characterized by point mutations in mtDNA, which result in deficient expression of mitochondrial respiratory chain proteins and impaired OXPHOS (*183*).

1.5.2. Mitochondrial dysfunction following misfolded protein accumulation

Not only oxidative stress causes mitochondrial dysfunction leading to neurodegenerative disorders, but also accumulation of misfolded proteins is damaging mitochondria and therefore involved in various neurodegenerative diseases.

In the case of amyotrophic lateral sclerosis (ALS), a mutated superoxide dismutase was described to mislocalize to mitochondria, causing dramatic changes in the proteome of spinal cord mitochondria and mitochondrial failure (*184*). In addition, recent findings support the role of mSOD1 in disrupting axonal transport of mitochondria via aggregate formation with neurofilaments, thereby damaging neuronal cells (*185*). In addition, mSOD1 induces inhibition of mitochondrial protein import, therefore it could be explained that toxic proteins on the mitochondrial surface also affect the mitochondrial protein turnover (*186*).

In addition, mSOD1 was found to inhibit mitochondrial protein import further impacting mitochondria due to an unbalanced organellar proteome. A recent report connected the mitochondrial ubiquitin ligase MARCH5 to the degradation of mSOD1 further supporting a role for the UPS in mitochondrial maintenance and prevention of neurodegeneration (*187*). Polyglutamine (polyQ)-extension and associated misfolding of various proteins such as Huntingtin or ataxin-3 causing Machado-Josephs-Disease is also known to negatively impact mitochondrial fidelity. As it is for mSOD1 shown, MARCH5 is also involved in the decrease of polyQ toxicity by inducing ataxin-3 proteasomal degradation (*188*).

1.5.3. Failing mitophagic clearance and neurodegeneration

Many observations have implicated that mitochondria are involved in the pathogenesis of Parkinson's disease (PD). Mutations in both, the ubiquitin ligase Parkin and the mitochondrial kinase PINK1 were found to cause autosomal recessive juvenile PD (*189*). These proteins were first suggested to share a pathway based on the observation that the knock-out of both proteins Parkin and PINK1 in *Drosophila* showed similar phenotypes (*190*). PINK1 is located on the outer mitochondrial membrane and leads to recruitment of Parkin to the mitochondria. It was found that loss of Parkin and PINK1 leads to elongated mitochondria as a result of an excessive fusion process. This phenotype could be rescued by either overexpressing Drp1 or knock-down of OPA1 or mitofusins, indicating that Parkin and PINK1 promote the mitochondrial fission process or may inhibit mitochondrial fusion (*191*).

1.5.4. Neurodegeneration linked to mitochondrial morphogens

Dysfunction of the mitochondrial network results not only in aberrant morphology of the organelles, but it is also associated with a wide spectrum of neurodegenerative disorders (*122*). Mutation in OPA1 are linked to about 60% of autosomal dominant optic atrophy (ADOA) cases (*192*). ADOA is characterized by slow vision loss resulting from the degeneration of the retinal ganglion cells, whose axons are bundled to form the optic nerve. The mitochondrial fusion activity of OPA1 depends on an intact GTPase and C-terminal coiled-coil domain with mutations in these domains connected to ADOA (*192*). Insufficient mitochondrial fusion due to mutation in OPA1 likely leads to subpar mitochondria unable to completely fulfill the especially high energy requirement of retinal ganglion cells (*193*). In addition, loss of OPA1 function sensitizes cells to apoptotic stimuli (*194*). This mechanism might contribute to the death of retinal ganglion cells in ADOA patients ultimately leading to blindness.

Recent studies revealed that mutations close to or within the GTPase domain lead to Charcot-Marie-Tooth neuropathy type 2A (CMT2A) (*195*). Mutations in Mfn2 cause CMT2A, an autosomal-dominate disease characterized by axonal peripheral neuropathy sometimes associated with visual impairment (*195*). Patients suffer from weakness, muscle atrophy and hearing loss depending on the location of Mfn2 mutation (*196*). Although Mfn1 and Mfn2 share similar sequence homology, there is no known connection between Mfn1 and CMT2A to date.

While the connection between mitochondrial fusogens and neurodegeneration is well established, the connection between the fission process and the death of neuronal cells is less clear. A single case study reported a patient with a Drp1 mutation in the middle domain suffering from optic nerve degeneration, microencephaly and persistent lactic acidemia. The fibroblast of the patient showed elongated mitochondria and peroxisomes and the patient died 37 days after birth (*197*). These findings suggest that defects in the mitochondrial fission process lead to more severe consequences than defects in mitochondrial fusion.

In summary, mitochondrial dysfunction is the center of many neurodegenerative disorders. Not only deficiencies in mitochondrial respiration are responsible for neuron loss and cell death, mitochondrial quality control, mitochondrial dynamic and apoptosis all play important roles in the survival of neurons.

1.6. Aims of the thesis

1.6.1. First part of the thesis

The first part involves the characterization of MARCH9, a new potential mitochondrial ubiquitin ligase. The objectives are:

- To study the regulation of MARCH9
- To identify substrates of MARCH9
- To study the relation between MARCH9 and OMMAD

1.6.2. Second part of the thesis

The second part is a study of the degradation of S-nitrosylated proteins on the mitochondria, with special focus on the role of proteasomal degradation and the recently discovered OMMAD machinery in mitochondrial quality control. The objectives are:

- To study the turnover of S-nitrosylated proteins
- To establish the proteasomal degradation of S-nitrosylated proteins
- To study the role of OMMAD

2. Materials and Methods

2.1. Materials

2.1.1. Nucleic acids and enzymes

Nucleic acids and enzymes	Supplier
1-kb-DNA-marker	Invitrogen, Carlsbad, USA
dNTPs	Invitrogen, Carlsbad, USA
Oligonucleotides	Sigma, St. Louis, USA
Pfx-polymerase	Invitrogen, Carlsbad, USA
Restriction enzymes	New England Biolabs, Ipswich, USA
T4-DNA-ligase	New England Biolabs, Ipswich, USA

2.1.2. Antibodies

Antibodies	Supplier
goat α-mouse IgG DyLight800	Thermo Scientific, Waltham, USA
goat α-mouse IgG HRP	Thermo Scientific, Waltham, USA
goat α-mouse-IgG Alexa488	Invitrogen, Carlsbad, USA
goat α-mouse-IgG Alexa546	Invitrogen, Carlsbad, USA
goat α-rabbit IgG DyLight800	Thermo Scientific, Waltham, USA
goat α-rabbit IgG HRP	Thermo Scientific, Waltham, USA
mouse serum IgG	Sigma, St. Louis, USA
mouse α-cytochrome c	Abcam, Cambridge, UK
mouse α-GADH	Santa Cruz Biotechnology, USA
mouse α-GFP	Roche, Basel, Switzerland
mouse α-HA antibody clone 12CA5	Abcam, Cambridge, UK
mouse α-MBP	New England Biolabs, Ipswich, USA
mouse α-Myc	Sigma, St. Louis, USA
mouse α-myc antibody clone 9E10	Sigma, St. Louis, USA
mouse α-FLAG	Sigma, St. Louis, USA
rabbit α-GFP	Sigma, St. Louis, USA
rabbit α-Mfn2	Abcam, Cambridge, UK
rabbit α-ubiquitin	Enzo Life Science, Lausen, Switzerland
rabbit α-VDAC	Abcam, Cambridge, UK
streptavidin high sensitive HRP	Thermo Scientific, Waltham, USA

2.1.3. Reagents

Reagents	Supplier

1,4-dithiointhreitol	Roth, Karlsruhe, Germany
A/G plus-Agarose beads	Santa Cruz Biotechnology, Dallas, USA
Acetone	Sigma, St. Louis, USA
Acrylamide	Roth, Karlsruhe, Germany
Agarose	Sigma, St. Louis, USA
Amicon Ultra-4 Centrifugal Filter	Millipore, Billercia, USA
Ammoniumperoxodisulfate	Roth, Karlsruhe, Germany
Ampicillin	Roth, Karlsruhe, Germany
B-Per buffer	Thermo Scientific, Waltham, USA
BCA™ protein assay Kit	Thermo Scientific, Waltham, USA
Biotin-HDPD	Sigma, St. Louis, USA
Blasticidin	InvivoGen, San Diego, USA
Bovine serum albumine	Roth, Karlsruhe, Germany
Bromphenol blue	MP Biomedicals, Ohio, USA
Calcium chloride	Roth, Karlsruhe, Germany
Carbonyl cyanide *m*-chlorophenyl hydrazine	Sigma, St. Louis, USA
Coomassie-Brilliant Blue G250	Roth, Karlsruhe, Germany
DAPI	Roth, Karlsruhe, Germany
Digitonin	Sigma, St. Louis, USA
Dimethyl sulfoxide	Sigma, St. Louis, USA
Dulbecco's modified Eagle's medium	Sigma, St. Louis, USA
ECL plus Solution A and B	Thermo Scientific, Waltham, USA
EDTA-free protease tablets	Roche, Basel, Switzerland
Epoxomicin	Peptide Institute, Osaka, Japan
Ethanol	Merck, Darmstadt, Germany
Ethidium Bromide	Biorad, Berkley, USA
Ethylendiamintetraacetat	Sigma, St. Louis, USA
Fetal bovine serum (FBS)	Sigma, St. Louis, USA
Filter paper	Roth, Karlsruhe, Germany
Formaldehyde Solution	Thermo Scientific, Waltham, USA
FuGENE6	Qiagen, Venlo, Nederland
Fuji Film medical X-ray	Fuji, Tokyo, Japan
Glacial acetic acid	Roth, Karlsruhe, Germany
Glutathione sepharose beads	Thermo Scientific, Waltham, USA
Glycerin	Roth, Karlsruhe, Germany
Glycine	Roth, Karlsruhe, Germany
HEPES	Roth, Karlsruhe, Germany
Histrap HP column	GE Healthcare, St. Giles, USA
Hygromycin	Roth, Karlsruhe, Germany
Imidazole	Roth, Karlsruhe, Germany
Iodoacetamide	Sigma, St. Louis, USA
Isopropyl β-D-1-thiogalactopyranoside	Roth, Karlsruhe, Germany
L-glutamine	Sigma, St. Louis, USA

LB-Medium	Roth, Karlsruhe, Germany
Leupetine	Sigma, St. Louis, USA
Magnesium chloride	Roth, Karlsruhe, Germany
Magnesium sulfate	Roth, Karlsruhe, Germany
Methanol	Roth, Karlsruhe, Germany
MG132	Peptide Institute, Osaka, Japan
Mitochondrial Isolation Kit Macs	Milteny Biotec, Gladbach, Germany
Mounting medium, Vectashield, H-1000	Vector Laboratories, Burlingame, USA
N-ethylmalmeide	Sigma, St. Louis, USA
Neocuprine	Sigma, St. Louis, USA
Nitrocellulose membrane	GE Healthcare, St. Giles, UK
NucleoSpin® Extract II Gel Extraction kit	Macherey-Nagel, Düren, Germany
OPTI-MEM	Invitrogen, Carlsbad, USA
Pepstatine	Sigma, St. Louis, USA
Polyethylenimine	Polyscience, Philadelphia, USA
Potassium acetate	Roth, Karlsruhe, Germany
Potassium chloride	Sigma, St. Louis, USA
Potassium hydrogen phosphate	Merck, Darmstadt, Germany
QYAprep® spin Mini Prep Kit	Qiagen, Venlo, Nederland
RIPA buffer (Pierce)	Thermo Scientific, Waltham, USA
S-Methyl methanethiosulfonate	Sigma, St. Louis, USA
Sodium ascorbate	Sigma, St. Louis, USA
Sodium chloride	Roth, Karlsruhe, Germany
Sodium dodecylsulfate	Roth, Karlsruhe, Germany
Sodium lactate	Sigma, St. Louis, USA
Tetracycline free FBS	Clontech (Takara), Kyoto, Japan
Tetracycline hydrochloride	Roth, Karlsruhe, Germany
Trypsin-EDTA 1x	Sigma, St. Louis, USA
Tryptone	Roth, Karlsruhe, Germany
z-VAD-fmk	Peptide Institute, Osaka, Japan
Zinc chloride	Roth, Karlsruhe, Germany
β-Mercapthoethanol	Sigma, St. Louis, USA

2.1.4. Equipment

Equipment	Supplier
ÄktaPrime FPLC	GE Healthcare, St.Giles, UK
Centrifuge 5424	Eppendorf, Hamburg, Germany
Centrifuge Avanti J-25	Beckman, Brea, USA
Centrifuge Mikro 200R	Hettich, Tittlingen, Germany
Electrophoresis chamber Xcell mini	Invitrogen, Carlsbad, USA
HE33 mini horizontal agarose electrophoresis	Hoefer, Holliston, USA
Heating bloc	Labnet, Edison, USA
Microscope, BX 63, Apollo	Olympus, Japan

Nanodrop	Thermo Scientific, Waltham, USA
Scale PM1200	Mettler Toledo, Zurich, Switzerland
Sterile filter 0.2 μM	Roth, Karlsruhe, Germany
Thermomixer	Eppendorf, Hamburg, Germany
Transfer-blot Semi-Dry Transfer cell	Biorad, Berkley, USA
Water bath	Memmert, Büchenbach, Germany
Water purification system	Millipore, Billercia, USA

2.1.5. Plasmids

Plasmids	Description
pAN393	MARCH9^{YFP}, CMV promoter, promoter active in mammalian cells
pAN464	MARCH9^{H136WYFP}, CMV promoter, promoter active in mammalian cells
pAN515	MARCH9^{3xMyc}, CMV promoter, promoter active in mammalian cells
pAN516	MARCH9^{H136W3xMyc}, CMV promoter, promoter active in mammalian cells
pAN680	Bacterial expression of MARCH9 RING domain part with Myc/GST, T7 promoter, bacterial expression
pAN681	^{YFP}Mfn1, CMV promoter, promoter active in mammalian cells
pAN770	MARCH9-Halo, CMV promoter, promoter active in mammalian cells
pAN832	MARCH9, CMV promoter, promoter active in mammalian cells
pAN833	MARCH9^{H136W}, CMV promoter, promoter active in mammalian cells
pAN918	^{FLAG}-Ubiquitin, CMV promoter, promoter active in mammalian cells
pAN940	Parkin^{YFP}, SV40 promoter, promoter active in mammalian cells
pAN945	$^{GST-3xMyc}$MARCH9 , T7 promoter, bacterial expression
pAN968	^{his6}-UBE2G2, UBE1-S-Tag, T7 promoter, bacterial expression
pAN969	UBE2G2, T7 promoter, bacterial expression
pAN993	$^{GST-3xMyc}$MARCH9 ^{H136W}, T7 promoter, bacterial expression
pAN1117	MARCH9-GST, CMV promoter, promoter active in mammalian cells
pAN1356	Mfn2^{YFP}, CMV promoter, promoter active in mammalian cells
pAN1357	Mfn2RasG12V^{YFP}, CMV promoter, active in mammalian cells
pAN1370	Mfn1RasG12V^{YFP}, CMV promoter, active in mammalian cells
pAN1371	^{MBP}MARCH9-ΔC-terminus^{-his6}, P-lac promoter, bacterial expression
pAN1372	^{MBP}MARCH9^{H136W}-ΔC-terminus^{-his6}, P-lac promoter, bacterial expression
Vector	pcDNA 3.1, mammalian expression vector, CMV promoter
Vector	YFP-N1, mammalian expression vector, CMV promoter
Vector	pMAL-c5E, bacterial expression vector for MBP-fusion protein
Vector	pCDF-DUET, bacterial co.expression vector, for two genes, lacI promoter
Vector	pACYC-DUET, bacterial co-expression vector for two genes, lacI promoter

Table 1: Plasmids used in experiments

The described plasmids were a gift from Neutzner lab or cloned individually for the experiment.

2.2. Molecular Biology Methods

2.2.1. Bacterial strains

The *Escherichia coli (E.coli)* strains, DH5α and BL21 (DE3) served in both the cloning and the expression experiments. BL21 and DH5α were used for heat shock transformation. They were grown overnight in LB (Luria-Bertani) medium and later on LB agar plates supplemented with the appropriate antibiotic for selection.

2.2.2. Preparation of competent cells

A 6 ml overnight culture of either *E.coli* DH5α or BL21 was grown in 2YT medium (10 g/l NaCl, 10 g/l yeast extract, 12 g/l tryptone, 20 nM $MgSO_4$ and 10 mM KCl) and diluted 1:100 in 10 ml 2YT medium (*198*). Cells were grown to OD_{600} 0.5, diluted 1:100 and grown again to OD_{600} 0.5. The culture was chilled for 10 minutes on ice and then collected by centrifugation (7 min, 2000g, 4°C). The supernatant was discarded and the pellet resuspended in 20 ml ice-cold transformation buffer (30 mM $MgCl_2$, 100 mM RbCl, 10 mM $CaCl_2$, 15% (v/v) glycerol in ddH_2O (pH 5.8)) then incubated for 10 minutes on ice. After a second centrifugation (7 min, 2000g, 4°C), the pellet was resuspended in 4 ml ice-cold transformation buffer 2 (10 mM MOPS, 10 mM RbCl, 75 mM $CaCl_2$, 15% (v/v) glycerol in ddH_2O (pH 6.8)). Aliquots of 100 μl were immediately stored at -80°C.

2.2.3. High-fidelity polymerase chain reaction (PCR)

Polymerase chain reaction (PCR) serves for the exponential amplification of a defined DNA-sequence by a thermo stable DNA-Polymerase (*199*). The PCR reaction contains template DNA, DNA polymerase, primers, 10x buffer and deoxynucleotides triphosphate (Table 2). The PCR consists of 20-40 repeated cycles and the PCR reaction has the following thermal cycler:

1. Denaturation step: heating the reaction up to 94 °C.
2. Annealing step: DNA polymerase binds to the primer-template hybrid
3. Extension step: DNA polymerase synthesizes the new DNA strand

PCR products were separated on an agarose gel (section 2.2.9.) and purified from agarose gel blocks using NucleoSpin® Extract Gel Extraction according to the manufactures protocol.

Components	PCR1 µl	PCR2 µl	PCR3 µl	PCR4 µl	MasterMix µl
MARCH9^{YFP}	0.5	0.5	0.5	0.5	2.25
Pfx buffer	5	5	10	10	
dNTPs	7.5	7.5	7.5	7.5	33.75
MgSO$_4$	1	1	1	1	4.5
Enhancer	0	5	0	5	
Oligo 884	1.5	1.5	1.5	1.5	6.75
Oligo 1177	1.5	1.5	1.5	1.5	6.75
Pfx	0.5	0.5	0.5	0.5	2.25
Water	32.5	27.5	27.5	22.5	12.5

Table 2: Components for PCR
PCR for ^{MBP}MARCH9^{his6}, PCR1 to PCR4 are different conditions, which result in four different PCR products.

1x94°C 4'; 25x94°C 15", 56°C 30", 68°C 1'; 1x10°C indef

Components	PCR1 µl	PCR2 µl	PCR3 µl	PCR4 µl	MasterMix µl
MARCH9^{H136WYFP}	0.5	0.5	0.5	0.5	2.25
Pfx buffer	5	5	10	10	
dNTPs	7.5	7.5	7.5	7.5	33.75
MgSO$_4$	1	1	1	1	4.5
Enhancer	0	5	0	5	
Oligo 884	1.5	1.5	1.5	1.5	6.75
Oligo 1177	1.5	1.5	1.5	1.5	6.75
Pfx	0.5	0.5	0.5	0.5	2.25
Water	32.5	27.5	27.5	22.5	12.5

Table 3: Components for PCR
PCR for ^{MBP}MARCH9^{H136Whis6}, PCR1 to PCR4 are different conditions, which result in four different PCR products.

1x94°C 4'; 25x94°C 15", 56°C 30", 68°C 1'; 1x10°C indef

2.2.4. Cloning of ^{MBP}MARCH9^{-his6}

^{MBP}MARCH9^{-his6} was amplified from MARCH9^{YFP} wildtype or from MARCH9^{H136WYFP} using Pfx polymerase, oligo nucleotide OAN884 (GGTGGTCAT ATGCTCAAGTCTCGGCTCCG) and OAN117 (TAGTCCAAGCTTCTA GTGATGGTGATGGTGATGCTTCTCGATGACCGTCAGGGA). The resulting PCR

product was cut with *Nde*I/*Hind*III and ligated into pMAL-c5E vector cut with *Nde*I/*Hind*III to obtain MARCH9ΔCT or MARCH9[H136W]ΔCT, respectively (section 2.2.3. Table 2 and 3). The PCR generated fragments were purified from agarose gel using NucleoSpin® Extract II Gel Extraction according to the manufacture's protocol.

2.2.5. DNA digestion

1 μg DNA was incubated with 1 μl selected restriction enzymes, with 2 μl of the appropriate incubation buffer as suggested by the manufacturer, 2 μl 10x BSA and ddH$_2$O to reach the final volume of 20 μl. The reaction was incubated for 1-2 hours and purified using Quiagen MinElute Reaction® cleanup kit according to the manufacture's protocol.

2.2.6. DNA ligation

For ligation reactions a 1:3 vector to insert ratio was used. 1 μl insert and 3 μl vector were mixed with 1 μl ligase, 2 μl of 10x ligase buffer and ddH$_2$O to reach a final volume of 20 μl. The reaction was incubated overnight at 37°C before transformation into DH5α (section 2.2.7).

2.2.7. DNA transformations

For transformation into competent bacteria (*E. coli*), 5 μl of ligation reactions were added to the competent cells and incubated on ice for 30 minutes. After incubation the DNA-bacteria mixture was heated at 42°C for 45 seconds. Immediately after incubation the bacteria were placed one ice for 5 minutes followed by adding 1 ml of SOC medium (SOB medium (5 g/l yeast extract, 20 g/l tryptone, 0.186 g/L KCl, 2.4 g/l MgSO$_4$) with 20 mM sterile glucose, then shaken for 1 hour at 37° C. The mixture was spread on LB plates containing the appropriate antibiotic for selection followed by an overnight incubation at 37°C.

2.2.8. DNA plasmid isolation

After transformation several clones were picked for growing overnight at 37 °C in 5 ml LB medium containing the appropriate antibiotic. DNA was extracted from bacteria using the QIAprep® Spin Mini prep kit according to manufacturer's instructions. The isolated DNA was digested with the selected restriction enzymes and separated onto agarose gel (section 2.2.9) to verify clones with the correct insert length. The constructs were verified by sequencing (Microsynth, Basel, Switzerland).

2.2.9. Gel electrophoresis

For gel electrophoresis DNA samples were separated on 0.8 % (w/v) agarose gels in TAE buffer (48.4 g/l Tris-base, 10.9 g/l glacial acetic acide, 2.92 g/l ethylendiaminetetraacetic acid (EDTA), ddH$_2$O add 1 l) supplemented with 0.5 μg/ml ethidium bromide. DNA loading dye (10x 10 mM TrisHCl pH7.8, 1 mM EDTA, 2.5 mg/ml bromphenol blue, 2.5 mg/ml xylene cyanol, 300 mg glycerol) was added to the DNA samples and samples were separated using 85 V for 45 minutes. NucleoSpin® Extract II Gel Extraction kit was used to extract DNA fragments from agarose gels for further cloning steps according to the manufacturer's protocol.

2.3. Biochemical Methods

2.3.1. Sodium dodecyl sulfate polyacrylamide gel electrophoresis (SDS-PAGE)

SDS-PAGE is a method to separate protein samples according to their molecular weight (*200*). For detection of proteins, 9% or 12% (w/v) acrylamide resolving gel combined with 4% stacking gels was used (Table 4, 5, 6). Samples were run at 120 V for 110 minutes in Laemmli running buffer (10x 250 mM Tris base, 1.92 M glycine, 10 g/l SDS).

Resolving Gel (12%)	
1.5 M Tris/HCL pH 8.8	5 ml
10% (v/w) SDS	200 μl
30% (v/w) acrylamide	8 ml
25% (w/v) APS	54 μl
TEMED	13 μl
ddH$_2$O	6.7 ml

Table 4: Components for 12% resolving gel

Stacking Gel (4%)	
0.5 M Tris/HCL pH 6.8	2.5 ml
10% (v/w) SDS	100 μl
30% (v/w) acrylamide	1340 ml
25% (w/v) APS	80 μl
TEMED	10 μl
ddH$_2$O	6 ml

Table 5: Components for 4% stacking gel

Resolving Gel (9%)	
1.5 M Tris/HCL pH 8.8	5 ml
10% (v/w) SDS	200 μl
30% (v/w) acrylamide	6 ml
25% (w/v) APS	54 μl
TEMED	13 μl

ddH$_2$O	8.7 ml

Table 6: Components for 9% resolving gel

2.3.2. Coomassie staining

To detect proteins, SDS gels were washed in 30 ml ddH$_2$O, heated for 30 seconds in the microwave and shaken for 10 minutes at RT. This procedure was repeated 3 times. The gels were then stained using 15 ml Coomassie staining solution (60-80mg Coomassie Brilliant Blue G250 in 1 l ddH$_2$O, 35 mM 37% HCl) and heated for 10 seconds in a microwave. After 20-30 minutes of staining, gels were destained overnight with ddH$_2$O under constant shaking.

2.3.3. Protein sample preparation

Cells expressing target proteins were harvested, and protein lysates were prepared using RIPA buffer according to the manufacturer's instructions. The pellet was lysed on ice with RIPA buffer 5 minutes followed by centrifugation (14000 rpm, 4°C) for 10 minutes. Supernatants containing the protein were collected and mixed 1:1 in 2x Laemmli sample buffer (125 mM Tris/HCl pH 6.8, 4% (w/v) SDS, 20% (v/v/) glycerol, 0.04% (w/v) bromphenol blue) supplemented with 50 mM DTT and heated at 65°C for 10 minutes for samples containing MARCH9 or at 95°C for 5 minutes for all other samples.

2.3.4. Western blot

Using Western blot, proteins were transferred from SDS-PAGE gel onto a nitrocellulose membrane followed by the detection of target proteins using specific monoclonal antibodies against the protein (*201*). The membrane was washed with PBS-T and incubated with a secondary HRP antibody. Proteins were detected using chemiluminescent substrate. To perform quantitative Western blotting, samples were loaded in triplicate onto SDS-PAGE, and proteins were detected using primary antibodies followed by secondary reagent α-DyLight800-coupled α-rabbit and α-mouse antibodies. Bands were visualized using an infrared-based laser scanner (LiCor) and quantified using Odyssey software (LiCor). Detection of GAPDH served as a loading control.

2.3.5. Immunoprecipitation

Cells were harvested and lysed on ice in lysis buffer (25 mM Hepes, pH 7.5, 10 mM CaCl$_2$, 1% digitonin, 20 mM iodoacetamide, 20 mM N-ethylmaleimide, 1 µg/ml pepstatin, 1 µg/ml leupeptin, 1 mM PMSF) for 30 minutes (*202*). Cleared lysates were generated by centrifugation at 14000 rpm for 10 minutes. Proteins from the lysates were mixed either with 2 µg of rabbit α-Mfn2 or 2 µg of rabbit α-GFP antibodies, then incubated for 2 hours at 4°C. Lysates were then incubated with 50 µl of prewashed protein A/G sepharose beads and rotated for 2 hours at 4 °C. Beads were washed three times with washing buffer (25 mM Hepes, pH 7.5, 10 mM CaCl$_2$, 0.2 % digitonin) and heated at 65 °C in 1x Laemmli sample buffer supplemented with 50 mM DTT for 10 minutes. Immunopurified proteins were detected by Western blot.

2.3.6. Bacterial ubiquitination assay

E. coli T7 express were transformed with a pCDF-DUET-based expression plasmid containing the single ubiquitin activating enzyme 1 (E1) as Stag marked version, as well as a suitable conjugating enzyme E2, such as ^{his6}UBE2G2 under the control of the IPTG-inducible T7 promoter (*203*). These bacteria were transformed with a second plasmid based on pACYC-DUET containing ^{3xFLAG}ubiquitin and $^{GST-his6-3xMyc}$MARCH9AA1-182 or $^{GST-his6-3xMyc}$MARCH9$^{AA1-182H136W}$, lacking both transmembrane domains and both under the control of an IPTG-inducible promoter. Solubility of MARCH9 in this bacterial expression system was confirmed in previous experiments performed in our laboratory. To detect auto-ubiquitination of $^{GST-his6-3xMyc}$MARCH9$^{AA1-182}$, bacteria containing both expression vectors were induced for 3 hours with 1 mM IPTG and lysed using B-PER buffer supplemented with DNAse and lysozyme according to the manufacturer's protocol. GST-tagged proteins were then purified using immobilized glutathione sepharose beads. Samples were boiled at 95°C in 1x Laemmli sample buffer and affinity-purified proteins as well as lysates were detected by Western blot using mouse α-myc and mouse α-FLAG antibodies.

2.3.7. Ubiquitin activating assay

To measure ubiquitin activity of ^{MBP}MARCH9 and ^{MBP}MARCH9^{H136W}, an *in vitro* ubiquitin activity assay was performed. All components, which were used for the reaction (Table 7) were mixed in a 1.5 ml microtube and incubated for 1 hour at 37°C. Afterwards 50 µl of nonreducing 2x Laemmli sample buffer was added and samples were analyzed by Western blot using either α-ubiquitin or mouse α-MBP antibody.

Component in μl	Control	MARCH9	MARCH9[H136W]
ddH$_2$O	28	0	0
10xUbiquitinylation Buffer	5	5	5
IPP (100U/ml)	10	10	10
DTT (50 mM)	1	1	1
Mg-ATP (0.1 M)	2.5	2.5	2.5
Reticulocytes lysate	1	1	1
Ubiquitin (50 μM)	2.5	2.5	2.5

Table 7: Components of *in vitro* ubiquitination assay

2.3.8. Detection of S-nitrosylated proteins

HeLa cells were transfected overnight with a plasmid encoding ubiquitin-HA. After incubation, cells were harvested and mitochondria isolation was performed (section 2.4.4.). Mitochondria were resuspended in RIPA buffer and heated at 95°C for 5 minutes. To detect ubiquitinated proteins, samples were separated on a 12% SDS-PAGE and detected by Western blot using rabbit α-ubiquitin antibody.

2.3.9. Purification of MARCH9 proteins

BL21 cells containing plasmids pAN1371 ([MBP]MARCH9[-his6]) or pAN1372 ([MBP]MARCH9[H136W-his6]) were grown overnight at 37°C in LB medium containing 2% glucose, 100 μM ZnCl$_2$ and 100 μg/ml ampicillin. The next day, cells were diluted to an OD$_{600}$ of 0.08 in the same medium. After reaching an OD$_{600}$ of 0.8, 1 mM IPTG was added to the culture to induce protein expression. After 3 hours, cells were centrifuged (4000g, 15 minutes, 4°C), the supernatant was discarded and the pellet was frozen at -20°C. This pellet was resuspended in buffer A (20 mM NaPO$_4$, 10 mM imidazole, 500 mM NaCl, pH 7.4 and protease inhibitor cocktail (Roche)), sonicated on ice 10 times for 30 seconds and centrifuged at 15000 g for 40 minutes at 4°C. The supernatant was filtered through a 0.45 μm sterile filter and subjected to ÄktaPrime FPLC using 1 ml Histrap HP column, buffer A and buffer B (20 mM NaPO$_4$, 500 mM imidazole, 500 mM NaCl, pH 7.4). Fractions containing MARCH9 were pooled together. In the case of dual-affinity purification, [MBP]MARCH9 fractions were diluted 1:5 in column buffer (20 mM Tris/HCl pH 7.4, 200

mM NaCl and one protease inhibitor cocktail (Roche)). This sample was loaded to 1 ml amylose beads equilibrated with column buffer. Beads were washed with 12 ml column buffer. Proteins were eluted in fractions of 1 ml with column buffer containing 20 mM maltose. Protein fractions from Histrap HP column or from amylose beads were pooled together and dialyzed against buffer C (20 mM Tris/HCl, 300 mM NaCl and 1 mM DDT, pH 7.9) using dialysis tubing with a molecular weight cut of 4'000-6'000 kDa. The samples were gently removed from the dialysis tubing and centrifuged (30 minutes at 4°C) to remove precipitated proteins. Proteins were concentrated using the Amicon Ultra-4 Centrifugal Filter Devices and concentration was determined by measuring A280 using nanodrop. Protein size was confirmed by SDS-PAGE followed by Coomassie staining.

2.4. Cell Biology methods

2.4.1. Cell culture

HeLA cells, a human cervix carcinoma cell line, were maintained in Dulbecco's Modified Eagle's Medium (DMEM), supplemented with 10% (v/v) fetal bovine serum, 1 mM sodium pyruvate and 2 mM L-glutamine. Cells were grown in a humidified incubator at 5% CO_2 and 37°C. Stable transfected 293 FlpIn TRex cells were cultured in DMEM supplemented with 10% tetracycline-free fetal bovine serum, 2 mM L-glutamine, 50 mg/ml hygromycin and 5 mg/ml blasticidin. To express the requested protein, 293 FlpIn TRex cells were induced by addition of 1 μg/ml tetracycline. For splitting cells, medium was removed and cells were washed once with PBS. After washing, trypsin/EDTA was added for 5 minutes and the same volume of medium was added to the cells to stop trypsination. Cells were spin down at 900 g for three minutes and diluted in 1:4 ratio. This procedure was repeated every 2-3 days.

2.4.2. Transfection of cells

HeLa cells were transfected with plasmid DNA using polyethylenimine (PEI) as previously described (*204*). Briefly, DNA was mixed with PEI in a ratio of 1:5 and incubated in the presence of sodium lactate (LBS) for 20 minutes at room temperature. After 20 minutes OPTI-MEM medium was added to the solution and the DNA complex was directly dropped onto the cells and incubated overnight.

2.4.3. Heavy membrane

HeLa cells were harvested using trypsine/EDTA. For fractionation, fresh cells were resuspended in mitochondria isolation buffer (210 mM mannitol, 70 mM sucrose, 1 mM EDTA, 10 mM Hepes pH 7.5) supplemented with protease inhibitors (1 µg/ml pepstatin, 1 µg/ml leupeptin, 1 mM PMSF), and passed 15 times through a 25G needle. Samples were centrifuged for 5 minutes at 500 rpm at 4°C. The resulting supernatant was again centrifuged for 30 minutes at 10000 rpm to obtain the mitochondria-enriched heavy membrane fraction. This fraction was either resuspended in RIPA buffer supplemented with 2 mM DTT and analyzed by Western blot or used for biotin switch assay.

2.4.4. Mitochondria isolation

Mitochondria were isolated using a mitochondrial isolation kit according to the manufacturer's protocol. Briefly, cells were harvested with ice-cold PBS, lysed in 1 ml lysis buffer supplemented with protease inhibitors (1:1000) and subsequently homogenized with a 25G needle (stepwise using 15 strokes). After homogenizing, ice-cold 1x separation buffer and 50 µl α-TOM22 microbeads were added to the lysate for magnetic labeling of the mitochondria. This mixture was incubated for 1 hour at 4°C under gentle rotation. One LS column was placed in the magnetic field of a MACS separator and the column was prepared by rinsing with 3 ml of 1x separation buffer. The cell lysate was applied stepwise to the column. Mitochondria were eluted by firmly pushing the plunger into the column. After two centrifugation steps, mitochondria were resuspended in 100 µl RIPA buffer and sonicated for 10 seconds.

2.4.5. Micro BCA

Concentration of mitochondria was determined by using BCA^{TM} protein assay kit (*205*). After pipetting 9 µl of working solution to each well, 1 µl of each sample was added to the solution. The standard curve was prepared using BSA in the concentrations of 0, 125, 250, 500, 750, 1000, 1500 and 2000 µg/ml. The samples were incubated for 15 minutes at 37°C and protein concentration was measured at OD546 using micro photometer.

2.4.6. Biotin-switch

Based on previous work (*206*) detection of S-nitrosylated mitochondria was done using biotin-switch assay. Biotin switch consists of three steps: (1) blocking of free cysteine thiols by S-methylmethane thiolsulfonate (MMTS); (2) conversion of S-nitrosothiol (SNO)

to a free thiol via a transnitrosation reaction with ascorbate; (3) labeling by S-biotinylation of the newly formed thiols with biotin-HPDP. Mitochondria were isolated as described in section 2.4.4. For all experiments 0.1-0.2 mg of mitochondria were used. Different treatments were adjusted with fresh prepared HEN buffer containing 250 mM Hepes pH 7.4, 1 mM EDTA pH 8.0, 20 µl neocuprine (5 mg/ml in methanol), 10 µl MMTS and 2.5% SDS. Samples were incubated in the dark at 50°C for 20 minutes under constant shaking. After the blocking step, 3 ml of 100% ice-cold acetone was added to each sample and precipitated for 30 minutes at -20°C. The pellets were collected by centrifugation at 2000 g for 10 minutes (section 2.4.8.). The supernatant was aspirated and the mitochondria pellet was washed 3 times with cold 70% acetone. After precipitation the dry pellet was resuspended in 200 µl HENS buffer containing 250 mM Hepes pH 7.4, 1 mM EDTA pH 8.0, 20 µl neocuprine (5 mg/ml in methanol) and 1% SDS. The labeling reaction was initiated by adding 15 µl biotin-HDPD (2.5mg/ml) and 20 µl of 20 mM sodium ascorbate. All samples were rotated at RT for 1 hour while protected from light. After the biotinylation step, samples were precipitated with 900 µl ice-cold 100% acetone for 30 minutes at -20°C. The supernatant was aspirated and the mitochondria pellet was washed 3 times with cold 70% acetone. After complete resuspension of the protein pellet in 200 µl HENS/10 buffer, 750 µl of neutralization buffer containing 25 mM Hepes pH 7.4, 100 mM NaCl, 0.5% Triton X-100 and 100 µM EDTA pH 8.0 as well as 40 µl of prewashed neutravidin beads were added and the samples were gently rotated overnight at 4°C. Neutravidin beads were used to enrich the biotinylated proteins. After the enrichment of biotinylated proteins, neutravidin beads were washed 4 times with neutralization buffer containing 25 mM Hepes pH 7.4, 600 mM NaCl, 0.5% Triton X-100 and 100 µM EDTA pH 8.0 and 40 µl of nonreducing 1x Laemmli sample buffer was added to the samples. The elution of the biotin labeled protein was performed by heating the beads to 95°C for 5 minutes. To detect the S-nitrosylated proteins samples were separated on a 12% SDS-PAGE, transferred onto a nitrocellulose membrane, blocked with 3% Topblock and incubated for 2 hours with 1:6000 diluted streptavidin high sensitive- peroxidase.

2.4.7. Immunocytochemistry

A primary antibody binds specifically to the protein of interest and a secondary antibody, tagged with a fluorescent dye, binds to the primary antibody. This allows the detection of proteins by fluorescence microscope. To assess mitophagy, HeLa cells grown on glass cover slips were transfected overnight with Parkin[YFP] using FuGENE 6 transfection reagent

followed by different treatments. Cells were fixed using methanol-free electron microscopy grade 4% paraformaldehyde in PBS for 15 minutes at RT, permeabilized for 15 minutes at RT using 0.15% Trixon X-100 in PBS and blocked for 1 h in 10% BSA in PBS. To stain for cytochrome *c*, cells were incubated with mouse α-cytochrome *c* antibody and mouse α-Alexa546 antibody. Samples were mounted using mounting medium, observed using fluorescence microscopy and analyzed with Image J software.

2.4.8. Protein precipitation

Protein samples contain substances, which can interfere with some further applications. To eliminate those substances from the samples, a compound that causes protein precipitation has to be added. The protein pellet, which contains the precipitated proteins, was re-dissolved in a compatible buffer. To remove interfering substances, 4 times of the sample volume of 100% ice-cold acetone was used and incubated at -20°C for 30 minutes. After incubation, samples were centrifuged (5000 rpm, 5 minutes, 4°C) and washed 3 times with 70% acetone. The compatible buffer was added to the dry pellet and resuspended.

2.4.9. Statistical analysis

All experiments were performed at least three times independently. Statistical significance was analyzed using unpaired, two-tailed Student's t-test as implemented in Microsoft Excel. P-values of < 0.05 or smaller was considered statistically significant and are highlighted with *, p-values of <0.01 are highlighted with **, p-values of <0.001 are highlighted with ***. Error bars represent the standard error of the mean (SEM).

3. Results

3.1. MARCH9, a potential new mitochondrial ubiquitin ligase

3.1.1. Characterization of MARCH9- previous findings

Bioinformatic analysis revealed about 400 genes in the human genome to encode RING finger domains containing proteins with 54 of these predicted to contain one or more transmembrane domains (Figure 10). Containing a RING finger domain suggests a putative ubiquitin ligase activity. Using a large scale subcellular localization, it was found that of these 54 potential RING finger ubiquitin ligases, four localize to mitochondria in the presence of two alpha-helical transmembrane domains (*202*), termed MARCH5 (*105*), IBRDC2 (*106*), MAPL/MULAN (*104*) and MARCH9 (Neutzner- personal communication). Further experiments confirmed for MARCH9 localization to the outer mitochondrial membrane with the RING finger domain facing the cytosol. In addition, mutating, and thus inactivating the RING finger domain of MARCH9 by exchanging a crucial zinc-complexing histidine residue on position 136 to tryptophan generated a likely dominant-negative mutant of MARCH9 (MARCH9^{H136W}) (*105*). Analyzing the impact of MARCH9^{H136W} on mitochondrial morphology revealed that the dominant-negative mutant MARCH9^{H136W} blocks the mitochondrial fusion process and causes mitochondrial fragmentation, making a role of MARCH9 in the fusion process likely (Neutzner- personal communication).

Figure 10: Domain structure of the mitochondrial RING finger protein MARCH9
MARCH9 is a 346 amino acid protein containing a RINGv domain N-terminal and (red) two membrane-spanning alpha helices (green).

3.1.2. MARCH9 is a substrate of OMMAD

The presence of a RING finger domain in MARCH9 supports ubiquitin ligase function for this protein. Ubiquitin ligases are known to possess auto-ubiquitination activity in the absence of substrate proteins, thus regulating their levels via auto-degradation (*207*). During the auto-ubiquitination process, ubiquitin ligases catalyze the addition of poly-

ubiquitin chains to themselves resulting in their degradation or change of their cellular function (*208*). To test the stability and the degradation of MARCH9 and MARCH9^{H136W} by the proteasome, expression levels of these proteins were studied. To test whether MARCH9 levels might be regulated through auto-ubiquitination, the stability of MARCH9 and MARCH9^{H136W} was studied. The exchange of the histidine residue on position 136 in MARCH9^{H136W} to tryptophan is predicted to render MARCH9^{H136W} inactive, thus MARCH9^{H136W} might be more stable compared to wildtype MARCH9. To this end, cells stably expressing MARCH9 or MARCH9^{H136W} under control of a tetracycline-inducible promoter were induced for 24 hours with tetracycline, additionally treated for 6 hours with the proteasome inhibitor MG132 or DMSO as control and expression levels of MARCH9 and MARCH9^{H136W} were analyzed by quantitative Western blot (Figure 11). Comparing the expression levels of MARCH9 control (lane 1) with MARCH9^{H136W} control (lane 3) revealed MARCH9^{H136W} levels to be about 20% of wildtype MARCH9 levels. Upon inhibition of the proteasome by MG132 treatment the levels of MARCH9^{H136W} significantly increased compared to DMSO control treated cells (lane 3 and 4) and reached almost wildtype levels. Interestingly, proteasomal inhibition did not significantly increase wildtype MARCH9 levels. Thus, inactivation of the RING domain of MARCH9^{H136W} did not stabilize the protein but rather destabilized it, while wildtype MARCH9 does not seem to be a target for proteasomal degradation. The stabilization after treatment with the proteasome inhibitor MG132 suggests that MARCH9^{H136W} is a target for proteasomal degradation. Based on this data, wildtype MARCH9 does not seem to possess auto-ubiquitination activity.
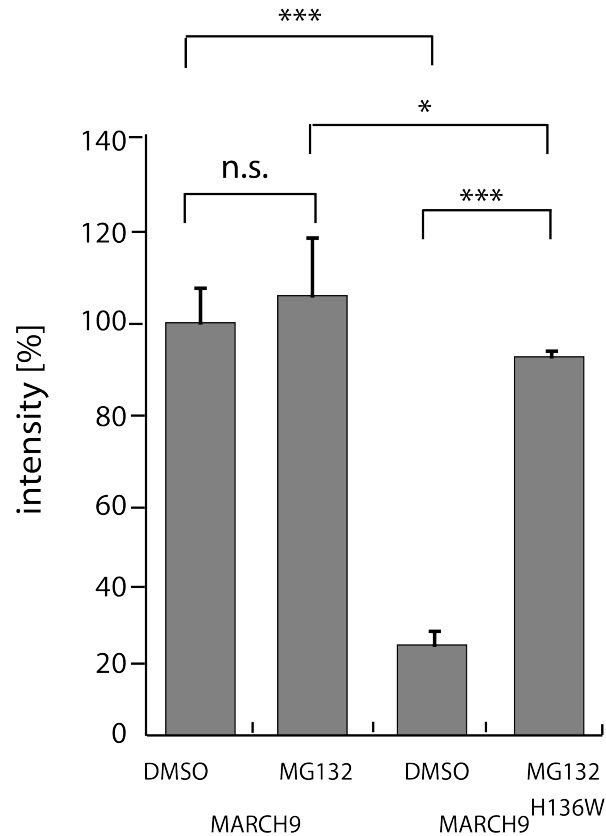
Figure 11: MARCH9 is a substrate for proteasomal degradation
Cells stably expressing MARCH9 or MARCH9^{H136W} were induced using tetracycline for 24 hours and treated for 6 hours with the proteasome inhibitor MG132 (50 μM/ml) or DMSO as a control. Protein lysates were analyzed by quantitative Western blot using α-MARCH9 antibody. Actin was used as a loading control. Error bars correspond to SEM. *** highlights p<0.001, ** highlights p<0.01, * highlights p<0.05 and n.s. highlights p>0.05 (unpaired, two-tailed Student's t-test, Microsoft Excel). This figure shows the average of three individual assays.

To further study the turnover of MARCH9 and MARCH9^{H136W}, protein levels of MARCH9 and MARCH9^{H136W} after treatment with the protein synthesis inhibitor cycloheximide were measured. To this end, HeLa cells were transfected with plasmids encoding either MARCH9 or MARCH9^{H136W}, respectively. Protein levels were analyzed after cycloheximide treatment using quantitative Western blot. Figure 12 shows measured half-lives of the proteins using quantitative Western blot. It was confirmed that MARCH9 is a relatively unstable protein with a half-life of around 90 minutes. However, MARCH9^{H136W} was even more unstable with a half-life around 45 minutes. These findings support the previous result in section 3.1.2. regarding the instability of MARCH9^{H136W}, and indicate that MARCH9 levels are not regulated by auto-ubiquitination alone, because inactivation of MARCH9 does not stabilize it.
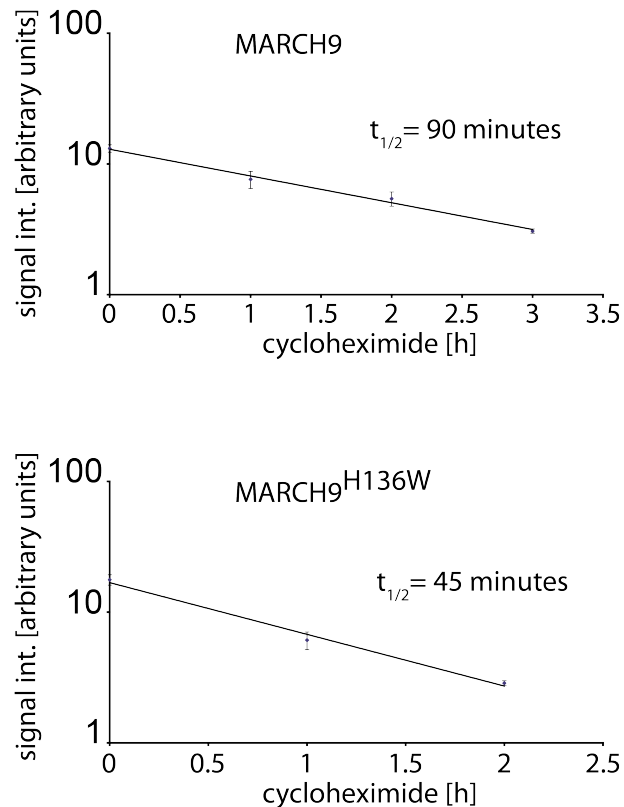
Figure 12: Half-life of MARCH9 and inactive MARCH9
HeLa cells were transfected with plasmids encoding MARCH9^{YFP} or MARCH9^{H136WYFP} and protein levels of MARCH9^{YFP} and MARCH9^{H136WYFP} were measured after treatment with cycloheximide (0-6 h, 50 μg/ml) using mouse α-GFP antibodies and quantitative Western blot. GAPDH was used as loading control and for normalization. Half-lives were calculated with the formula: $t_{1/2}= \ln (2)/\lambda$. Error bars correspond to SEM. This figure shows the average of three individual experiments.

3.1.3. MARCH9 is part of a homomeric complex

Based on the observed dominant-negative activity of MARCH9^{H136W} in terms of regulating mitochondrial morphology (Neutzner- personal communication), it is conceivable that MARCH9 is part of a homomeric complex as dominant-negative mechanisms oftentimes imply physical interaction. In the case of an ubiquitin ligase this might imply inter-molecular ubiquitination, potentially explaining the instability of MARCH9^{H136W} compared to wildtype MARCH9. To evaluate the potential of MARCH9 for self-interaction, the oligomeric state of MARCH9 was studied. To this end, HeLa cells were co-transfected with plasmids encoding MARCH9^{YFP} and MARCH9^{3xMyc} or with plasmids encoding MARCH9^{YFP} and control. Using α-GFP antibody, MARCH9^{YFP} was immunopurified and co-purifying MARCH9^{3xMyc} was detected using α-myc antibodies. It was found that MARCH9^{3xMyc} specifically co-purifies with MARCH9^{YFP} (Figure 13, lower panel, lane 2) when compared to control transfected cells (Figure 13, lower panel, lane 4). This result

strongly supports a physical MARCH9/MARCH9 interaction and might explain the observed dominant-negative effect of MARCH9^{H136W}.
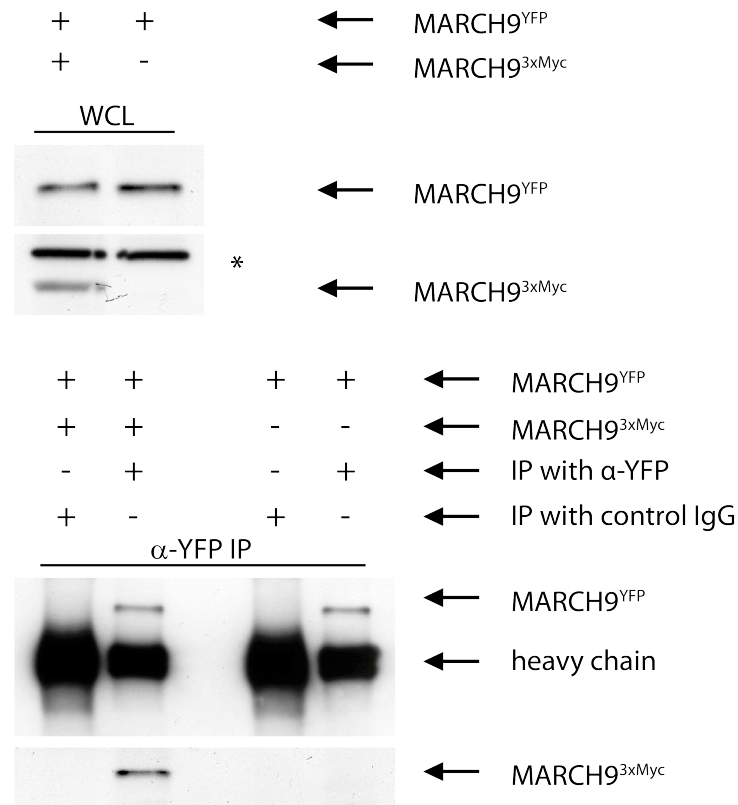
Figure 13: MARCH9 is part of a homomeric complex
HeLa cells were co-transfected with plasmids encoding MARCH9^{YFP} and MARCH9^{3xMyc} or vector control. Cells were lysed using digitonin lysis buffer and immunopurified using mouse α-GFP antibody. Immunoprecipitates of MARCH9^{YFP} were analyzed by Western blot using α-myc antibodies for the presence of MARCH9^{3xMyc}. This figure shows a representative experiment of three individual assays.

3.1.4. Potential role of MARCH9 as an ubiquitin ligase

Ubiquitination is involved in many cellular processes and is mediated by the action of an enzymatic cascade involving ubiquitin activating enzyme (E1), conjugating enzyme (E2) and ligating enzyme (E3). This cascade results in the formation of an ubiquitin chain on the specific substrate (*100*). RING finger domains were shown to play an important role in the transfer of ubiquitin to a substrate protein intended for proteasomal degradation (*96*). In mammalian genomes, several hundred ubiquitin ligases are found and their large number illustrates the specificity of the ubiquitination process. RING finger variant domains (RINGv), which are found in all MARCH proteins, were also shown to have ubiquitin ligase activity (*209*). Thus, the presence of a RING finger domain makes an ubiquitin ligase activity of MARCH9 conceivable. To evaluate this hypothesis of a potential ubiquitin

ligase activity for MARCH9, *in vitro* ubiquitin ligase measurements were performed. While MARCH9 did not display specific ubiquitination activity with the E2 enzymes UBE2D1, UBE2C, UBE2B or UBEJ2, previous preliminary studies from our laboratory suggested a functional interaction between MARCH9 with the Ubc7 ortholog E2 UBE2G2 (Neutzner-personal communication).

3.1.4.1. Bacterial *in vivo* ubiquitination assay

To test the potential role of MARCH9 as an ubiquitin ligase, an *in vivo* ubiquitination system was employed where E1, E2, E3 and ubiquitin are co-expressed in *E.coli* to reconstitute the ubiquitination machinery in a prokaryotic cell. Two different vectors were used, controlled by separate T7 promoters, each expressing two separate target genes (Figure 14) (*203*). Specifically, pCDFDuet-1 vector expressing *Uba1/Ube1* (E1) gene and *UBE2G2* (E2) gene, whereas a pACYCDuet-1 vector was used to produce a soluble version of MARCH9 or inactive MARCH9^{H136W} (E3) as well as FLAG-tagged ubiquitin. As MARCH9 is a transmembrane protein and as such insoluble, only amino acid 1-182 of MARCH9 containing the RING finger domain but omitting the two transmembrane domains were used.
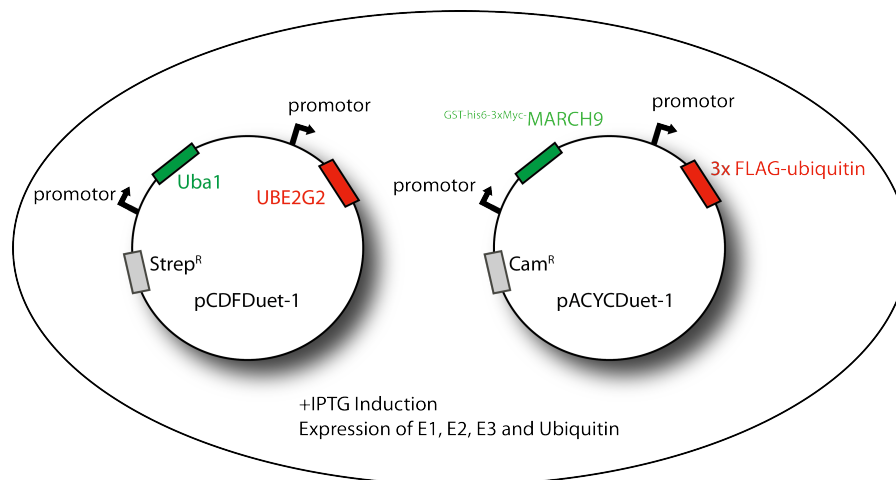
Figure 14: Expression system for reconstituting ubiquitination in *E. coli*
The employed pCDFDuet-1 and pACYCDuet-1 vectors contain two IPTG- dependent T7 promoters capable of driving each the expression of two different genes of interest allowing for the simultaneous production of four different genes. IPTG-induction of *E. coli* strains containing both plasmids results in the simultaneous production of E1, E2, E3 as well as ubiquitin.

To provide MARCH9 with an intramolecular substrate for auto-ubiquitination and to allow for easy purification and detection, MARCH9$^{AA1-182}$ was fused to gluthatione S-transferase (GST) as well as to a 3xmyc epitope tag, respectively. To detect potential ubiquitination, both $^{GST-3xMyc}$MARCH9$^{AA1-182}$ and $^{GST-3xMyc}$MARCH9$^{AA1-182H136W}$ were expressed in *E.coli*

together with E1, E2 and ubiquitin, and purified by affinity chromatography using glutathione-sepharose-beads. Figure 15 shows the expression and the *in vivo* ubiquitination of $^{\text{GST-3xMyc}}$MARCH9$^{\text{AA1-182}}$ compared to $^{\text{GST-3xMyc}}$MARCH9$^{\text{AA1-182H136W}}$ with the upper panel displaying the whole cell lysates and the lower panel displaying purified MARCH9. Using α-Flag antibodies to detect ubiquitination, no significant difference in auto-ubiqitination of $^{\text{GST-3xMyc}}$MARCH9$^{\text{AA1-182}}$ (lane 3), when compared to $^{\text{GST-3xMyc}}$MARCH9$^{\text{AA1-182H136W}}$ (lane 4), was observed. Interestingly, also $^{\text{GST-3xMyc}}$MARCH9$^{\text{AA1-182-H136W}}$ displayed some ubiquitination in this assay
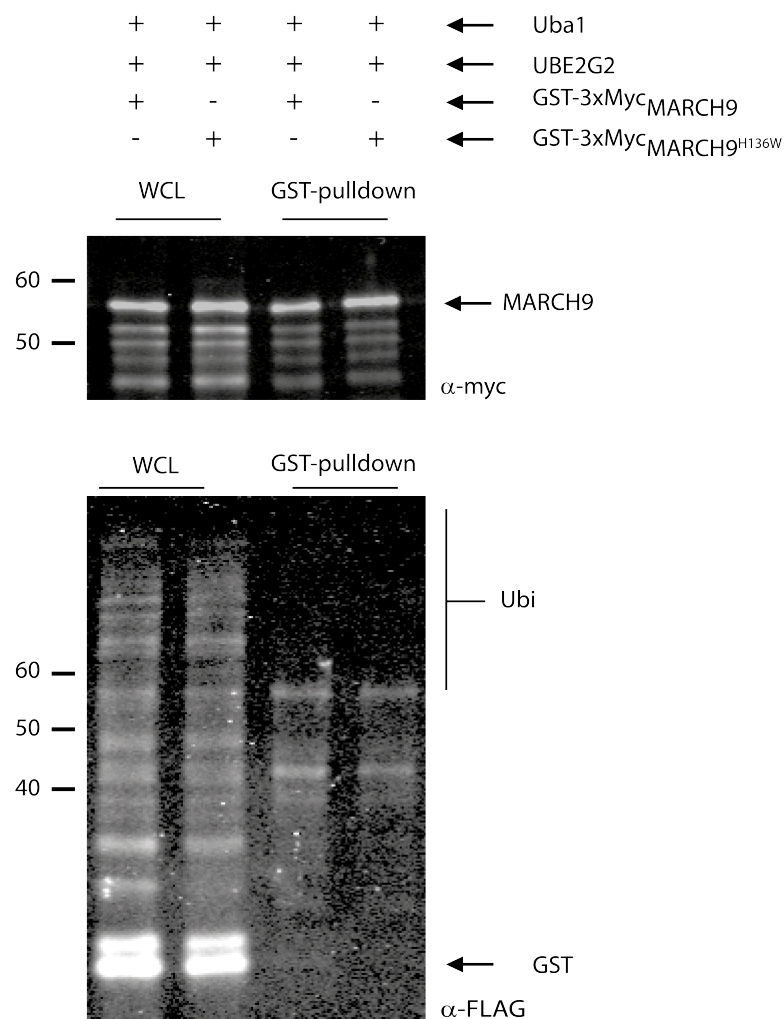
Figure 15: MARCH9 expression in a bacterial *in vivo* system
E.coli NEB T7 express was transformed with two compatible dual expression plasmids containing Uba1 (E1 enzyme), UBE2G2 (E2 enzyme), FLAG-ubiquitin and $^{\text{GST-3xMyc}}$MARCH9$^{\text{AA1-182}}$ or $^{\text{GST-3xMyc-}}$MARCH9$^{\text{AA1-182H136W}}$. All open reading frames were under the control of an IPTG-inducible T7 promoter. Bacteria were induced for 3 hours with IPTG, lysed in B-Per buffer and GST-tagged proteins were affinity purified using gluthation-sepharose-beads. Whole cell lysate (lane 1 and 2) was analyzed by quantitative Western blot using α-myc antibody. α-FLAG was used to analyze purified $^{\text{GST-3xMyc}}$MARCH9 or $^{\text{GST-3xMyc}}$MARCH9$^{\text{H136W}}$ (lane 3 and 4). No specific ubiquitination of MARCH9 with UBE2G2 was noticed. This figure shows a representative experiment of three individual assays.

To study this further and to exclude unspecific auto-ubiquitination, $^{\text{GST-3xMyc-}}\text{MARCH9}^{\text{AA1-182}}$ and $^{\text{GST-3xMyc}}\text{MARCH9}^{\text{AA1-182H136W}}$ were expressed alone without Uba1 and E2 (Figure 16A). In the GST pull-down no difference in modification was observed. To further exclude unspecific auto-ubiquitination, GST alone as additional control were expressed separately from E1 and E2 activity (Figure 16B). Figure 16B indicates a similar modification pattern between MARCH9 and MARCH9$^{\text{H136W}}$ even in the absence of E1 and E2 expression (Figure 16B). These data are consistent with the notion that a certain read-through between the two open reading frames on the pACYC-Duet vector occurred causing the generation of a MARCH9-ubiquitin in-frame fusion protein. To avoid this unspecific ubiquitination of MARCH9, the employed bacterial expression system was improved by placing MARCH9 and ubiquitin on separate expression vectors (section 3.1.4.2.).
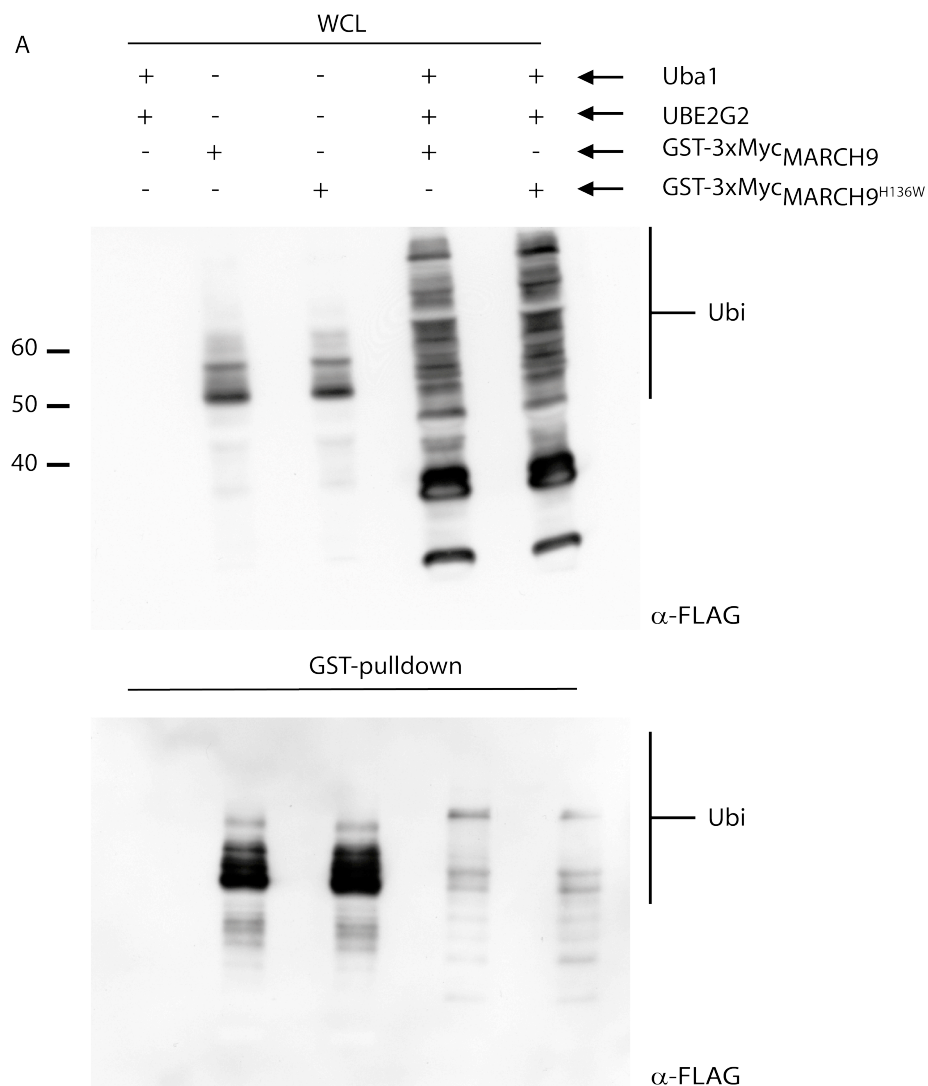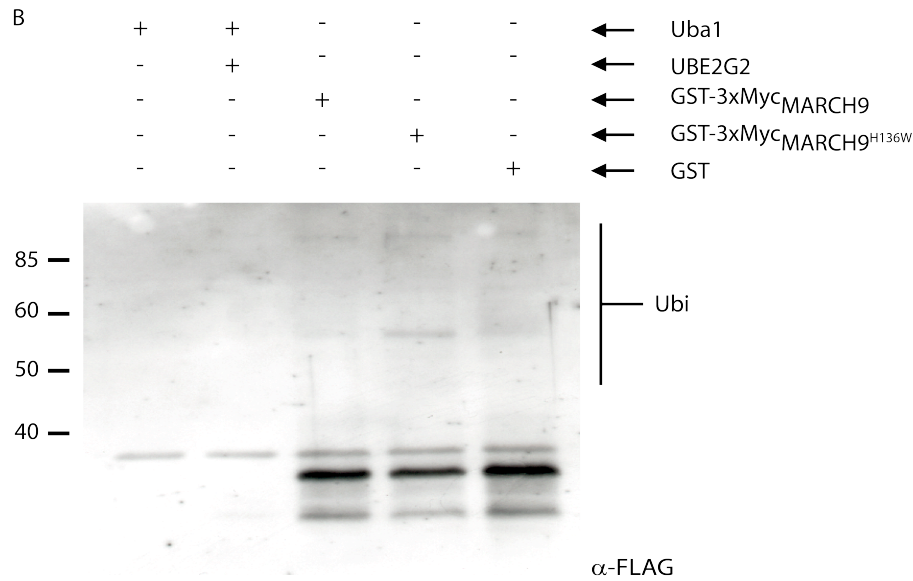
Figure 16: MARCH9 expression in a bacterial *in vivo* system
A: Expression of $^{GST-3xMyc}$MARCH9 and $^{GST-3xMyc}$MARCH9^{H136W} without Uba1 and E2. **B:** To exclude unspecific ubiquitination, the plasmid expressing GST gene alone and the plasmid encoding Uba1 and UBE2G2 were analyzed (lane 5). The affinity purified $^{GST-3xMyc}$MARCH9 and $^{GST-3xMyc}$MARCH9^{H136W} was analyzed using α-FLAG antibody. The lanes 3-5 indicate the same pattern of ubiquitination in each condition. This figure shows a representative experiment of three individual assays.

3.1.4.2. Improved bacterial *in vivo* ubiquitination assay

As the previous *in vitro* assay was inconclusive (3.1.4.1.) and the formation of an in-frame fusion protein between MARCH9 and ubiquitin was suspected, the employed bacterial expression system was further improved by placing MARCH9 and ubiquitin on separate expression vectors, thus preventing the formation of a MARCH9-ubiquitin fusion protein (Figure 17).
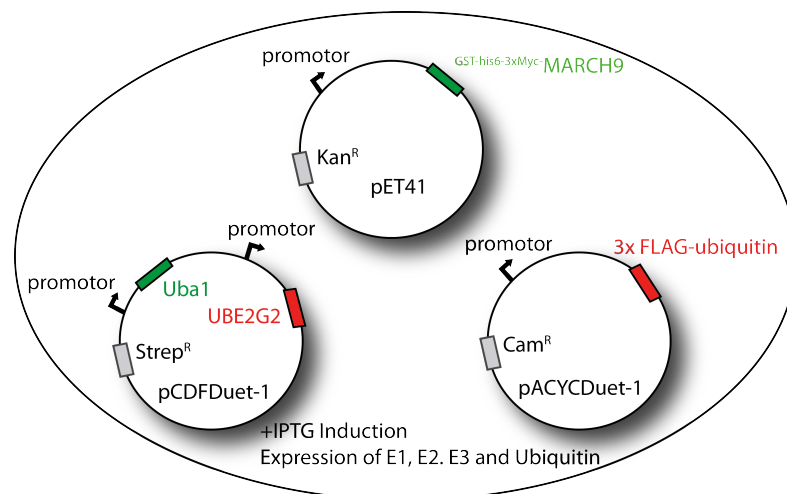
Figure 17: Prokaryotic expression system with three expression vectors for bacterial ubiquitination
Improved prokaryotic system with three expression vectors pCDFDuet-1, pACYCDuet-1 and pET41 for the expression of Uba1, UBE2G2, ^{3xFLAG}ubiquitin and $^{GST-3xMyc}$MARCH9 genes. The new construct contains three different expression vectors encoding separately $^{GST-3xMyc}$MARCH9 genes, ^{3xFLAG}ubiquitin genes and both UBE1 genes and UBE2G2 genes.

In vivo ubiquitination assay was performed as described in section 3.1.4.1 using the expression of GST as a control for unspecific ubiquitination. As seen previously, there was no detectable difference in ubiquitination between MARCH9 and MARCH9^{H136W} (Figure 18, lanes 4 and 6). However, in this experimental setup, GST alone was targeted for ubiquitination. Thus, an ubiquitin ligase activity of MARCH9 could neither be confirmed nor excluded.

+	+	+	+	+	+	←	Uba1
+	+	+	+	+	+	←	UBE2G2
-	-	+	+	-	-	←	GST-3xMyc$_{MARCH9}$
-	-	-	-	+	+	←	GST-3xMyc$_{MARCH9}$^{H136W}
-	+	-	+	-	+	←	FLAG-ubiquitin
+	+	-	-	-	-	←	GST
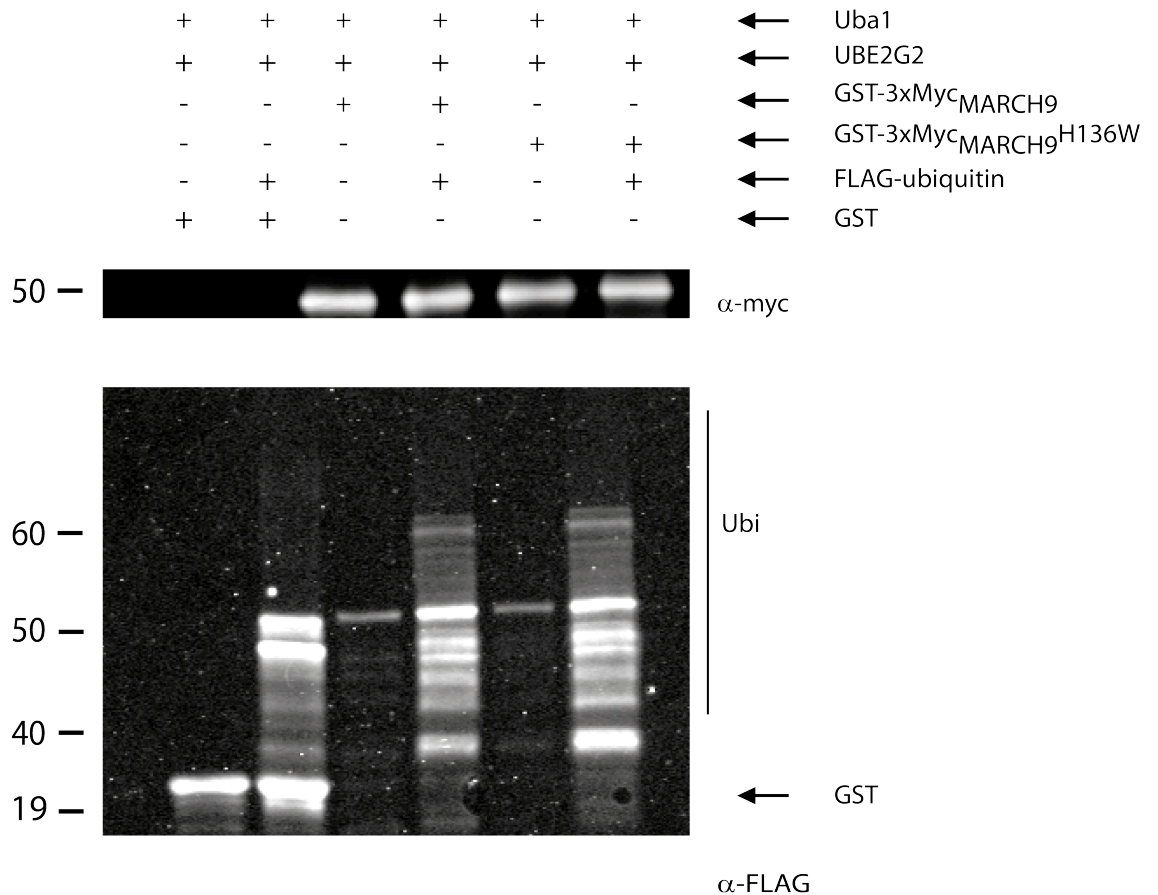
Figure 18: MARCH9 expression in a bacterial *in vivo* system
E.coli NEB T7 express was transformed with one pET41 expression vector encoding Uba1 (E1 enzyme) gene, UBE2G2 (E2 enzyme) gene and two compatible dual expression vectors encoding ^{3xFLAG}ubiquitin and $^{GST-3xMyc}$MARCH9$^{AA1-182}$ or $^{GST-3xMyc}$MARCH9$^{AA1-182H136W}$ genes. All genes are under control of an IPTG-inducible T7 promoter. Expression was induced for 3 hours with IPTG, bacteria were lysed in B-Per buffer and GST-tagged proteins were affinity purified using gluthation-sepharose-beads. Whole cell lysate was analyzed by Western blot using α-myc antibody. α-FLAG was used to analyze purified $^{GST-3xMyc}$MARCH9$^{AA1-182}$ or $^{GST-3xMyc}$MARCH9$^{AA1-182H136W}$. No specific ubiquitination of MARCH9 with UBE2G2 was evident. This figure shows a representative experiment of three individual assays.

3.1.4.3. Purification of MARCH9 or MARCH9^{H136W} for *in vitro* ubiquitination

To further address a potential ubiquitin ligase activity for MARCH9, an *in vitro* ubiquitination assay was performed. To avoid unspecific ubiquitination of GST fusion proteins as seen above, maltose binding protein (MBP) was employed as fusion partner for MARCH9$^{AA1-182}$. In addition and instead of the above used bacterial *in vivo* ubiquitination system, *in vitro* reconstitution of ubiquitination was performed. To this end, ^{MBP}MARCH9$^{AA1-182-his6}$ or ^{MBP}MARCH9$^{AA1-182H136W-his6}$ were purified using nickel-affinity chromatography. As seen in Figure 19, purification of MARCH9 fusion proteins was successful and resulted in a single peak of purified ^{MBP}MARCH9$^{AA1-182-his6}$ or ^{MBP}MARCH9$^{AA1-182H136W-his6}$.
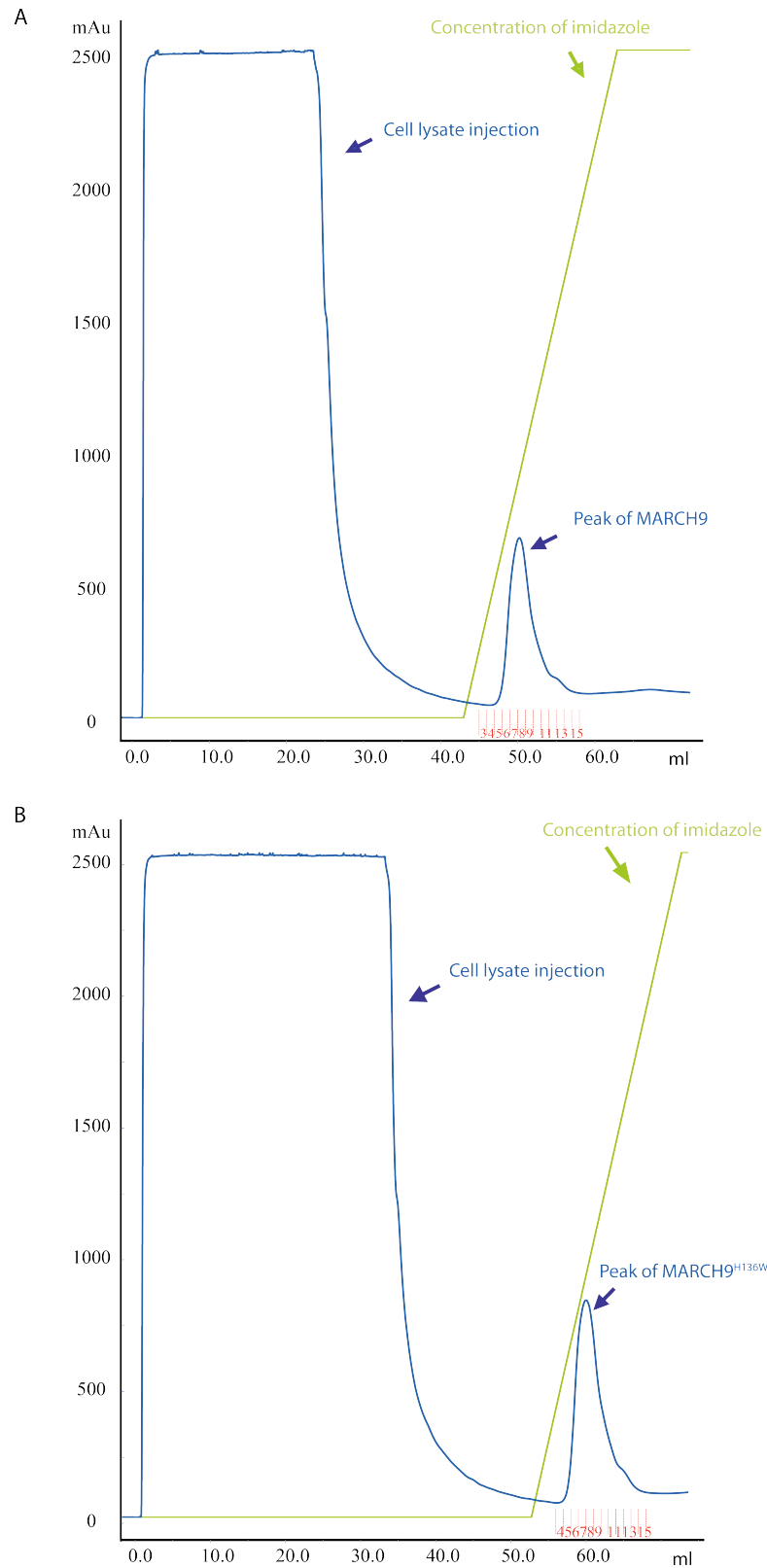
Figure 19: Chromatogram of nickel-NTA affinity purification of ^{MBP}MARCH9$^{AA1-182-his6}$ and ^{MBP}MARCH9$^{AA1-182H136W-his6}$

A and **B**: Green line shows the linear gradient of imidazole concentration, while the blue line depicts protein concentration (absorbance at 280 nm).

Proteins from the fractions with the highest concentration were analyzed using SDS-PAGE and Coomassie staining (Figure 20), and fraction 9 and 10 with the highest concentration of ^{MBP}MARCH9$^{AA1-182-his6}$ or ^{MBP}MARCH9$^{AA1-182H136W-his6}$ was dialyzed overnight against buffer C (section 2.3.9.) and used as E3 for the *in vitro* ubiquitination assay (section 3.1.4.4.) (Figure 20A, red-rimmed band and Figure 20B).
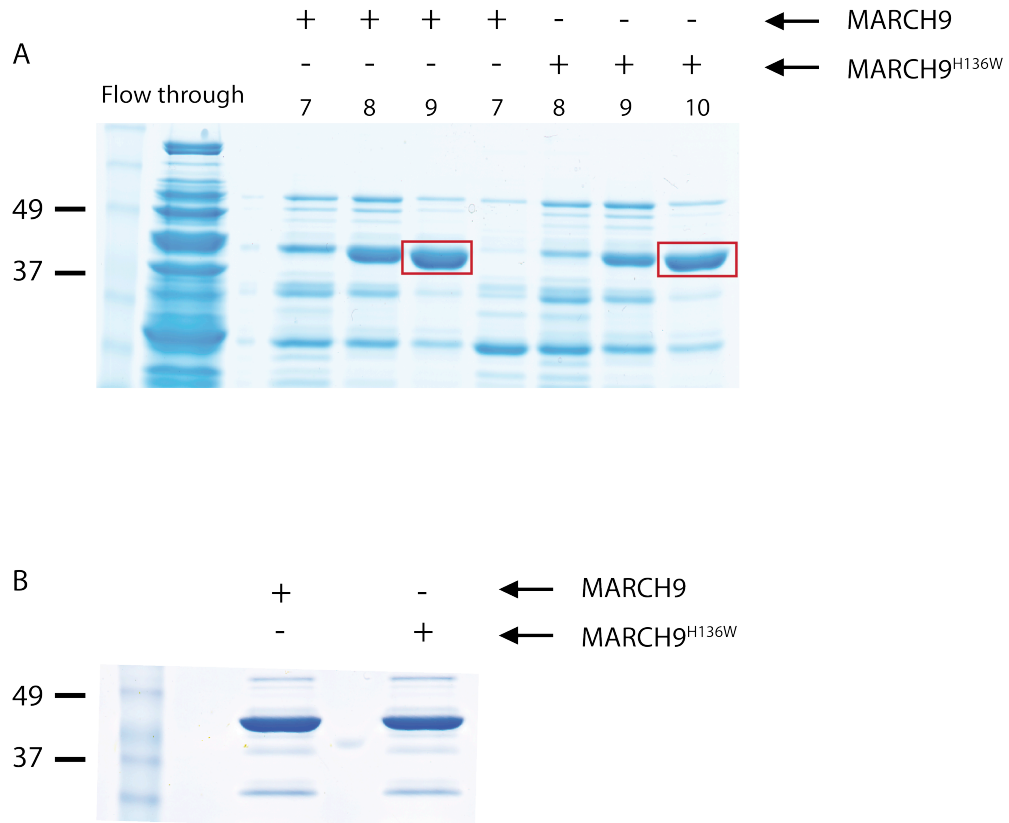
Figure 20: SDS-PAGE of purification of MARCH9 and MARCH9^{H136W}
A: The collected fractions (7-10) corresponding to the peak of maximal absorbance were run on a SDS-PAGE for verification of protein size and purity. The red-rimmed band indicates the purest protein with the highest concentration. This fraction was chosen for overnight dialysis. **B:** After dialysis ^{MBP}MARCH9$^{AA1-182-his6}$ and ^{MBP}MARCH9$^{AA1-182H136W-his6}$ were separated on SDS-PAGE. ^{MBP}MARCH9$^{AA1-182-his6}$ and ^{MBP}MARCH9$^{AA1-182H136W-his6}$ run at their predicted molecular weight of 43 kDa.

3.1.4.4. *In vitro* ubiquitination assay

Using purified ^{MBP}MARCH9$^{AA1-182-his6}$ and ^{MBP}MARCH9$^{AA1-182H136W-his6}$, an *in vitro* ubiquitination assay was performed, to examine whether ^{MBP}MARCH9 catalyzes auto-ubiquitination in the presence of ATP, E1, E2 and ubiquitin. As a source of E1 and E2, rabbit reticulocyte lysate was used, as it is known to contain ubiquitin-dependent proteolytic activity (*210*) and is a good source for a wide variety of different E2 activities. To this end, ^{MBP}MARCH9$^{AA1-182-his6}$, ^{MBP}MARCH9$^{AA1-182H136W-his6}$ or MBP as control were incubated for 1 hour at 37°C and modification of MARCH9 was detected by Western blot

using α-MARCH9 antibodies. As shown in Figure 21, incubation of ^{MBP}MARCH9$^{AA1-182-his6}$ and ^{MBP}MARCH9$^{AA1-182H136W-his6}$ with reticulocyte lysate and ubiquitin did not alter the molecular weight of ^{MBP}MARCH9$^{AA1-182-his6}$ and ^{MBP}MARCH9$^{AA1-182H136W-his6}$. However, it was apparent that one-step nickel-affinity purification was not sufficient to obtain protein of sufficient purity for this assay.

-	-	+	-	-	+	-	-	← MBP
-	-	-	+	-	-	+	-	← MBP-MARCH9-his6
-	-	-	-	+	-	-	+	← MBP-MARCH9^{H136W}his6
-	+	-	-	-	+	+	+	← reticulocyte lysate
+	+	+	+	+	+	+	+	← ubiquitin
+	+	+	+	+	+	+	+	← ATP
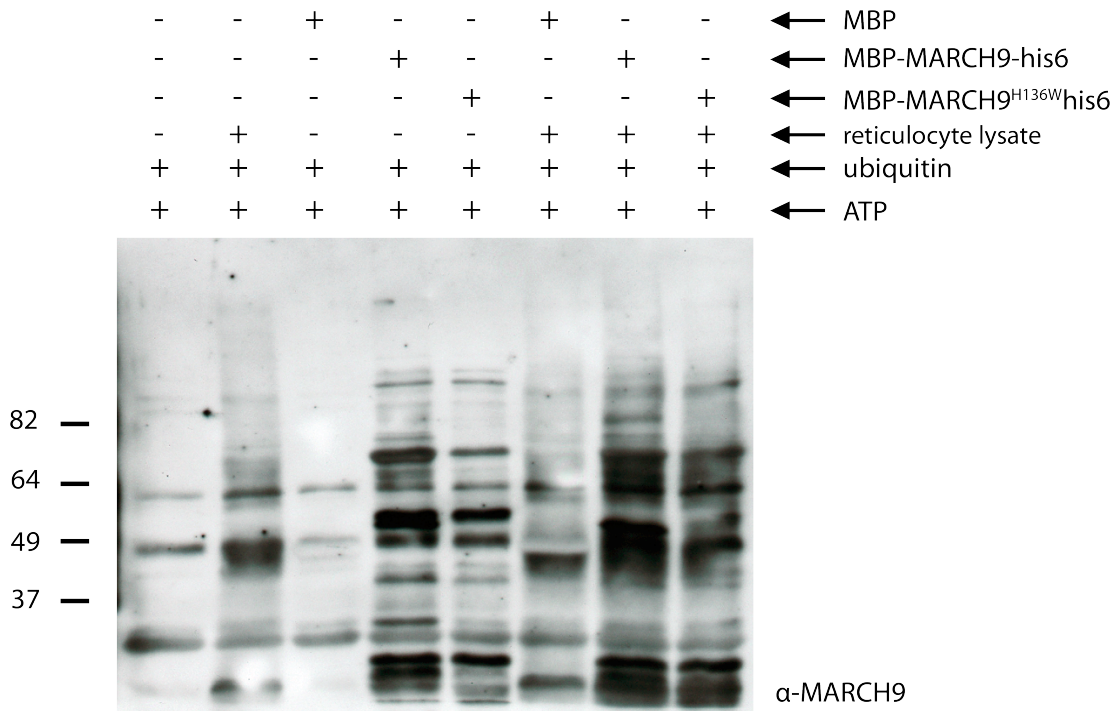
α-MARCH9

Figure 21: *In vitro* **Ubiquitination assay**
Both ^{MBP}MARCH9$^{AA1-182-his6}$ and ^{MBP}MARCH9$^{AA1-182H136W-his6}$ were incubated for 1 hour at 37°C in the presence of ATP, ubiquitin and reticulocyte lysate. MBP served as control. This figure shows a representative experiment of three individual assays.

3.1.4.5. Dual-affinity purification of MARCH9 or MARCH9^{H136W}

To achieve a purer form of the protein a dual-affinity purification was performed. MARCH9 was first purified using nickel-NTA affinity chromatography (Figure 22A) followed by maltose binding protein purification (Figure 22B, 22C). ^{MBP}MARCH9 was immobilized on the amylose resin and eluted using 10 mM maltose. The collected fractions were analyzed by Coomassie staining and the pooled fractions were dialyzed overnight against buffer C (Figure 22D). These dialyzed proteins were used for the following *in vitro* ubiquitination assay (section 3.1.4.6.).
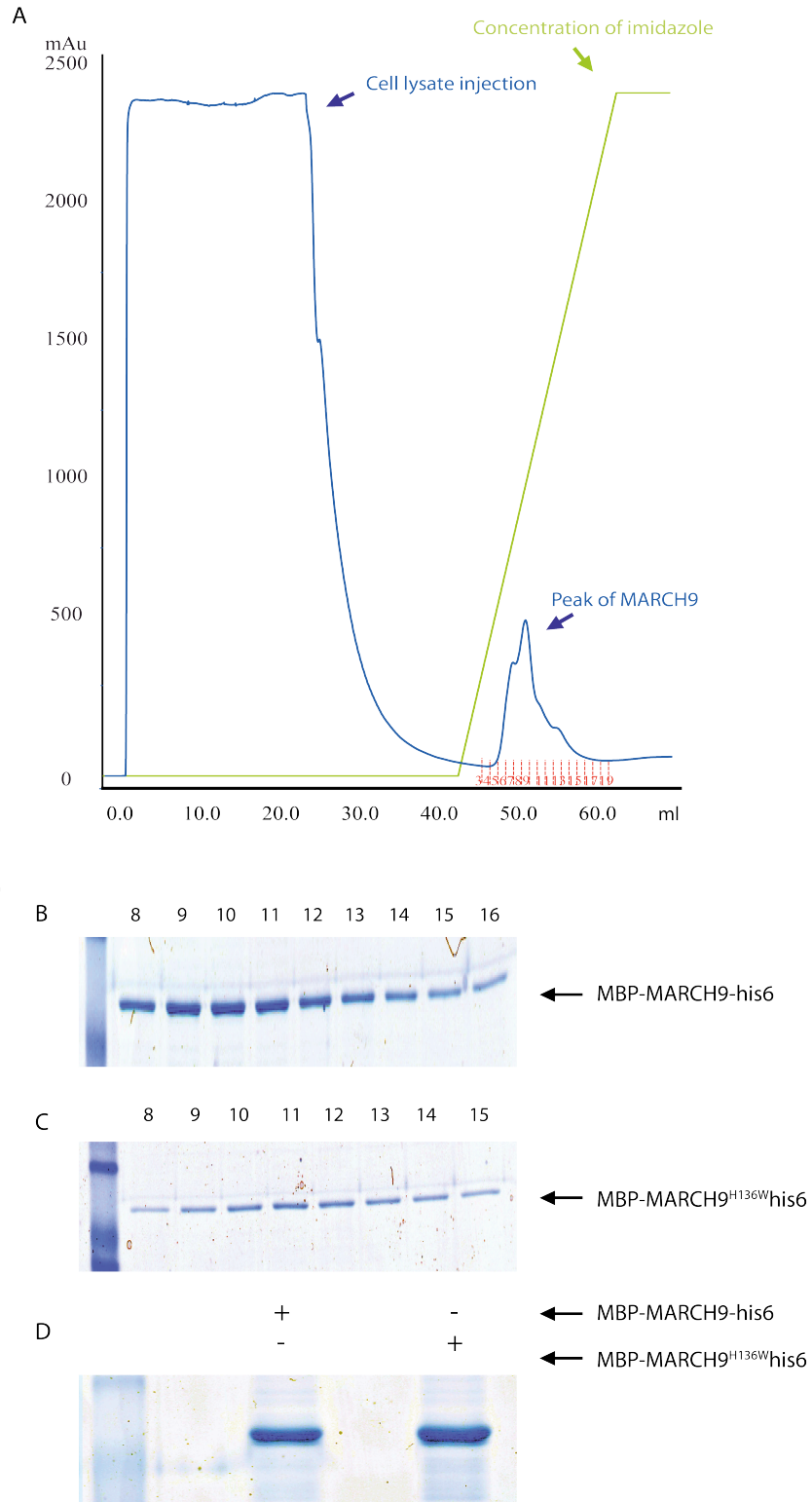
Figure 22: Dual-affinity purification of $^{\text{MBP}}$**MARCH9**$^{\text{AA1-182-his6}}$ **and** $^{\text{MBP}}$**MARCH9**$^{\text{AA1-182H136W-his6}}$
A: Chromatogram of $^{\text{MBP}}$MARCH9$^{\text{-his6}}$ nickel affinity chromatography. Green line shows the linear gradient of imidazole concentration and blue line shows absorbance at 280 nm. **B** and **C:** SDS-PAGE and Coommassie staining of the samples from the nickel-affinity purification peak fractions (8-15). **D:** SDS-PAGE and Coommassie staining of the pooled fractions following amylose-affinity chromatography and overnight dialysis. Please note the high purity of the fusion proteins especially in comparison to single affinity purification (section 3.1.4.3.).

3.1.4.6. *In vitro* ubiquitination assay using dual-affinity purified MARCH9

Dual-affinity purified MARCH9 and MARCH9^{H136W} was used in an *in vitro* ubiquitination assay. To ensure the presence of a broad spectrum of different E2 enzymes rabbit reticulocyte lysate was used as a source of E1 and E2 *(211)*. The reaction mixture containing ATP, reticulocyte lysate, ubiquitin and either MARCH9 or MARCH9^{H136W} or MBP as control, was incubated at 37°C for 1 hour as described before in section 3.1.4.4. After incubation, samples were analyzed by Western blot using α-MBP antibodies. As shown in Figure 23 there was no difference in ubiquitination between MARCH9 and MARCH9^{H136W} after analyzing using α-MBP antibody (lane 5 and 6). However, a clear ladder-like modification of MBP consistent with polyubiquitination was seen (lane 4) and with MBP itself being a target for modification in this experimental setting.

In summary, neither *in vivo* nor *in vitro* ubiquitination experiments (sections 3.1.4.1., 3.1.4.2., 3.1.4.4., 3.1.4.6.) support ubiquitin ligase activity for MARCH9, however neither do they disprove E3 activity for MARCH9.

Figure 23: Ubiquitination-assay after using dual-affinity purification
In vitro ubiquitination assay using purified MARCH9 after dual-affinity purification. Samples were analyzed by Western blot using α-MBP antibody. Lane 5 shows the MBP control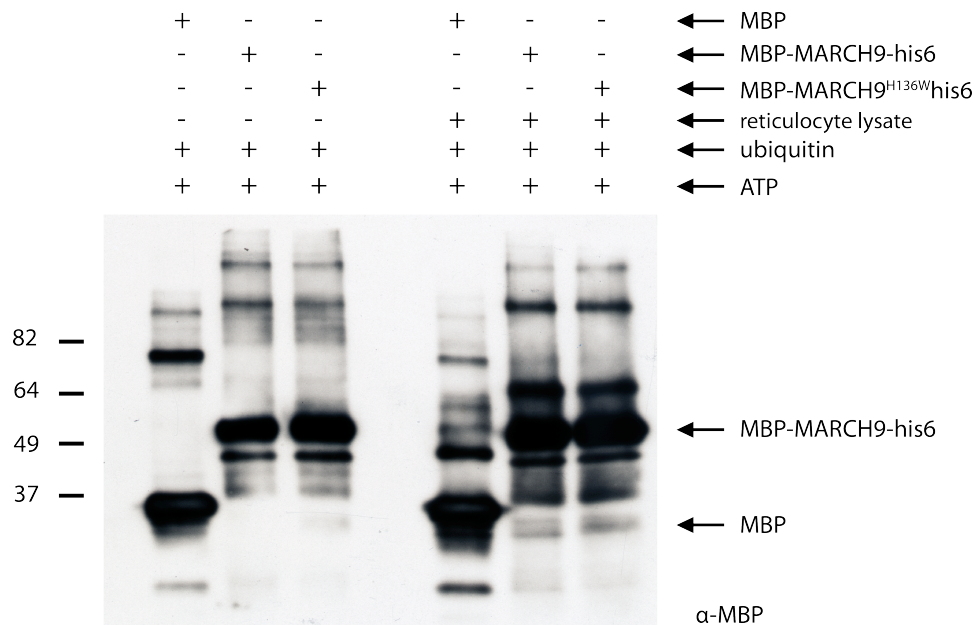 ubiquitination. Lane 6 and 7 demonstrate the ubiquitination of MARCH9. This figure shows a representative experiment of three individual assays.

3.1.5. The potential role of MARCH9 in the fusion machinery

Previous work indicated that MARCH9 might have a role in the regulation of mitochondrial morphology, in particular in the fusion of mitochondria tubules. Cells expressing dominant-negative MARCH9^{H136W} displayed a strong fragmentation of the mitochondrial network after immunostaining with α-cytochrome *c* antibody when compared to control cells (Neutzner- personal communication). To further substantiate a possible role of MARCH9 as a regulator of the fusion machinery, interaction between MARCH9 and known mediators of mitochondrial fusion were analyzed. To this end, co-immunoprecipitation studies were performed between MARCH9 and the two mitofusins Mnf1 and Mfn2 (*117*).

For this purpose, cells were tranfected with plasmids encoding Mfn1^{YFP} and MARCH9^{YFP}. Ectopically expressed Mfn1 or endogenous Mfn2, respectively, were immunopurified from whole cell lysates prepared using Triton X-100, CHAPS or digitonin containing buffers using specific α-Mfn2 and α-GFP antibodies. While no interaction between MARCH9 and mitofusins was detectable in buffers containing either Triton X-100 or CHAPS detergent, MARCH9 specifically co-purified with Mfn1 (Figure 24A) and Mfn2 (Figure 24B) in digitonin containing buffer. To ensure of complete solubilization of the mitochondrial membrane and thus co-purification of mitofusins with MARCH9 based on a real physical interaction and not on micelle formation due do incomplete solubilization of the mitochondrial membranes, immunoprecipitates were analyzed for the presence of the outer mitochondrial protein VDAC (voltage-dependent anion channel). Consistent with a complete solubilization of the mitochondrial membrane, VDAC was not detected in these mitofusin precipitates. The observed physical interaction of MARCH9 with both mitofusins and the observed impact of dominant-negative MARCH9^{H136W} on mitochondrial morphology strongly support a role of MARCH9 in the regulation of the mitochondrial fusion process.
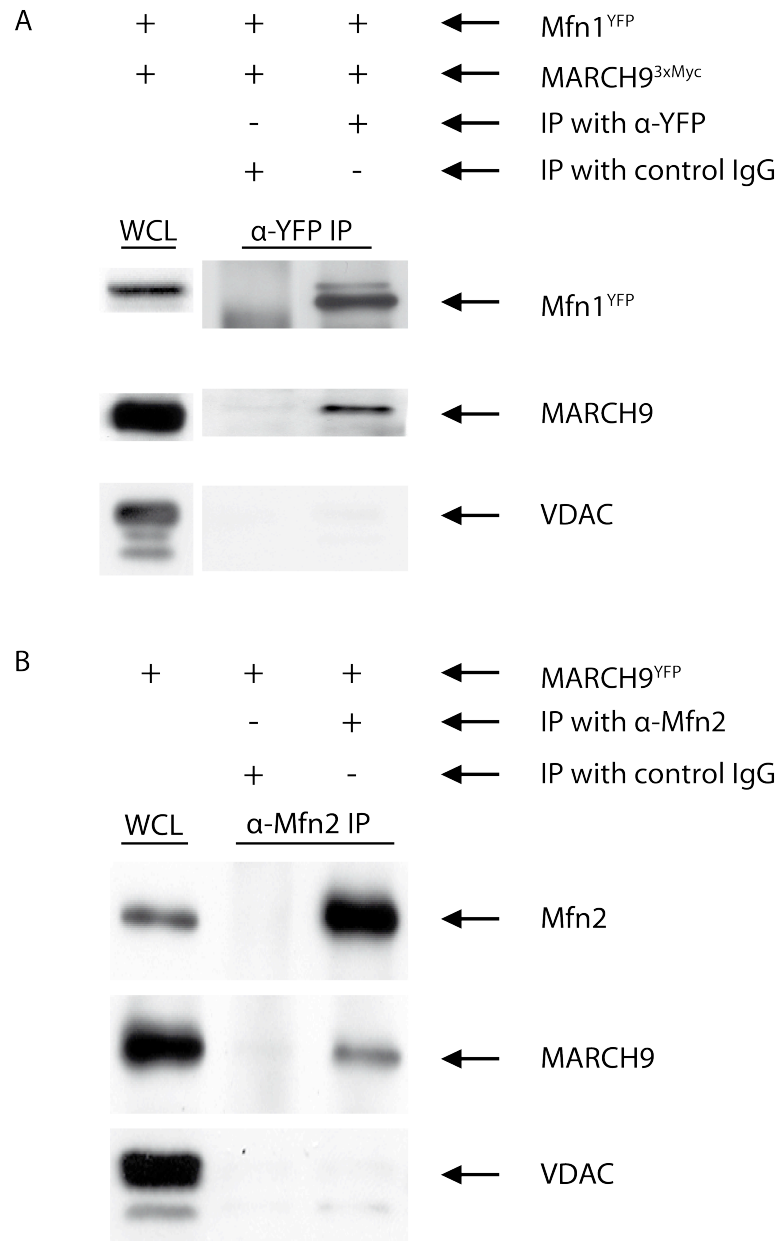
Figure 24: Interaction of MARCH9 with Mfn1 and Mfn2
A: HeLa cells transfected with plasmids encoding MARCH9^{3xMyc} or MARCH9^{YFP} and Mfn1^{YFP} were lysed in buffer containing digitonin. After centrifugation lysates were incubated with α-GFP antibody or an unspecific IgG antibody. After 2 hours of incubation with the antibody, A/G sepharose beads were added to the lysate and incubated overnight at 4°C. The interaction of Mfn1^{YFP} and MARCH9^{3xMyc} was detected using α-GFP or α-MARCH9 antibodies **B:** HeLa cells were transfected with plasmids encoding MARCH9^{YFP} and lysed using digitonin-containing lysis buffer. Whole cell lysates were immunopurified using α-Mfn2 antibody. This figure shows one representative experiment of three individual assays.

3.2. S-nitrosylation

3.2.1. S-Nitrosylated proteins

Nitric oxide (NO) can lead to S-nitrosylation, a chemical reaction resulting in the addition of NO to a cysteine-thiol (-SH) group on a target protein forming a nitrosothiol (SNO) (*43*). S-nitrosylation of proteins can be detected using the so called biotin-switch technique (*206*), where nitrosothiols are specifically labeled with a biotin moiety to allow detection of SNO-proteins using streptavidin-coupled HRP. To produce exogenous nitric oxide the NO donor sodium nitroprusside (SNP) was used, as it is known that SNP induces S-nitrosylated proteins (*212*). Furthermore, to test the potential role of the proteasome in the degradation of SNO-proteins, a proteasome inhibitor was used. Thus, HeLa cells were treated for 6 hours with 100 µM SNP or with the proteasome inhibitor MG132 (Figure 25). The whole cell lysate was prepared using RIPA buffer and following biotin-switch, SNO proteins were detected by Western blot using streptavidin HRP. In the presence of the NO donor the level of SNO-proteins was increased compared to the untreated control cells (Figure 25, lane 1 and 2). Interestingly, SNO protein levels of MG132 treated cells in the absence of exogenous NO were also increased (Figure 25, lane 3). This result shows that many proteins are a target for S-nitrosylation and that the degradation of such proteins is most likely proteasome-dependent.
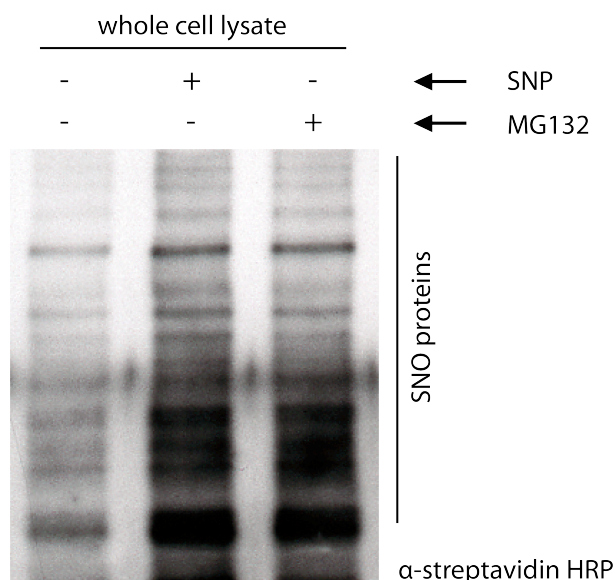
Figure 25: S-nitrosylated proteins in the whole cell lysate

HeLa cells were treated either with the NO donor SNP (100 μM) or the proteasome inhibitor MG132 (50 μg/ml) or left untreated as control, whole cell lysates were prepared, biotin-switch was performed and SNO proteins were detected using streptavidin HRP. This figure shows one representative experiment of three individual assays.

3.2.2. Turnover of S-nitrosylated proteins on mitochondria

To address the question whether mitochondrial proteins are also a target for S-nitrosylation, enriched mitochondrial fractions were studied. To this end, HeLa cells were treated with 100 μM SNP or MG132 for 6 hours and mitochondria-enriched heavy membrane fractions were generated using differential centrifugation. After mitochondrial isolation, mitochondria were solubilized using RIPA buffer and biotin switch was performed. As shown in Figure 26 (lane 2 and 3) both SNP and the proteasome inhibitor MG132 caused increased levels of SNO-proteins compared to unstressed cells (lane 1). Again, proteasomal inhibition resulted in similar SNO protein levels compared to low level NO stress due to SNP treatment. This result suggests the presence of S-nitrosylated proteins on mitochondria and their degradation via the proteasomal dependent pathway.
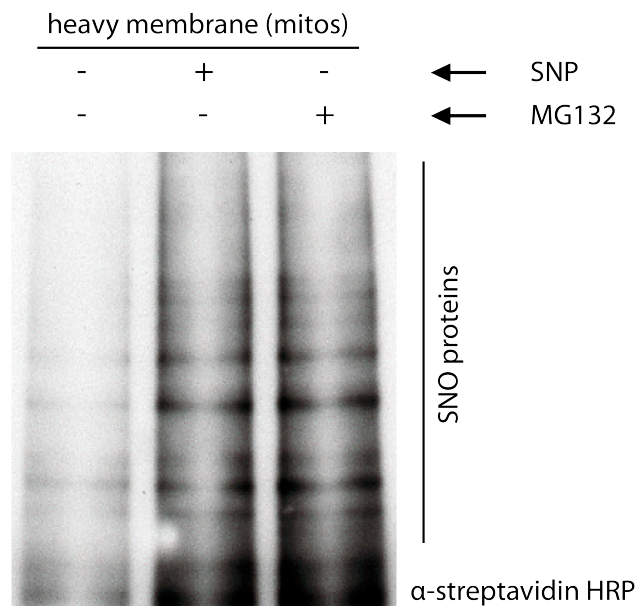
Figure 26: Turnover of S-nitrosylated mitochondrial proteins
Mitochondria were isolated from HeLa cells and treated with the NO donor SNP (100 μM) or the proteasome inhibitor MG132 or left untreated. After 6 hours of treatment cells were lysed, biotin switch was performed and S-nitrosylated proteins were analyzed by Western blot using streptavidin HRP. Note the different levels of SNO proteins (lane 2 and 3) compared to untreated cells (lane 1). This figure shows one representative experiment of three individual assays.

3.2.3. S-nitrosylated proteins on highly purified mitochondria

In the previous experiment (section 3.2.2.), levels of S-nitrosylated proteins after treatment with SNP and MG132 were compared. The result showed an increase of SNO-proteins after SNP and MG132 treatments (Figure 26) indicating a continuous turnover of SNO-proteins on mitochondria in a proteasome-dependent manner even in unstressed cells. To further investigate the involvement of the ubiquitin-proteasome system in the removal of SNO modified proteins from mitochondria, highly purified mitochondria were analyzed to exclude the possibility of contamination of the mitochondrial fractions with non-mitochondrial proteins. To obtain highly purified mitochondria, which exclude cytosol and other proteins, α-Tom22 antibodies coupled to super-paramagnetic beads were used. The highly purified mitochondria were free of lysosome and contained only a minor ER-resident proteins impurity (Charles Hemion- personal communication). For this propose, HeLa cells were treated either with 100 μM SNP, or the highly specific irreversible protease inhibitor epoxomicin. In contrast to MG132, epoxomicin does not inhibit the LON protease, which is involved in the degradation of matrix proteins (*213*). Highly purified mitochondria were lysed in RIPA buffer and S-nitrosylated proteins were analyzed by Western blot using streptavidin HRP antibody (Figure 27A). Using biotin-switch analysis, the levels of S-nitrosylated proteins in cells treated with the proteasomal inhibitor epoxomicin were found to be similar to the level in SNP treated cells and increased compared to the levels found in untreated control cells (Figure 27A, lane 2, 4 and 6). To confirm these results in another cell line, 293 HEK cells were used. As with HeLa cells, after treatment with the NO donor SNP or with the proteasome inhibitor epoxomicin, an increase in SNO-proteins in HEK 293 cells was observed compared to untreated control cells (Figure 27B, lane 2, 4 and 6). These findings strongly support an involvement of the ubiquitin proteasome system in the degradation of mitochondrial SNO-proteins.
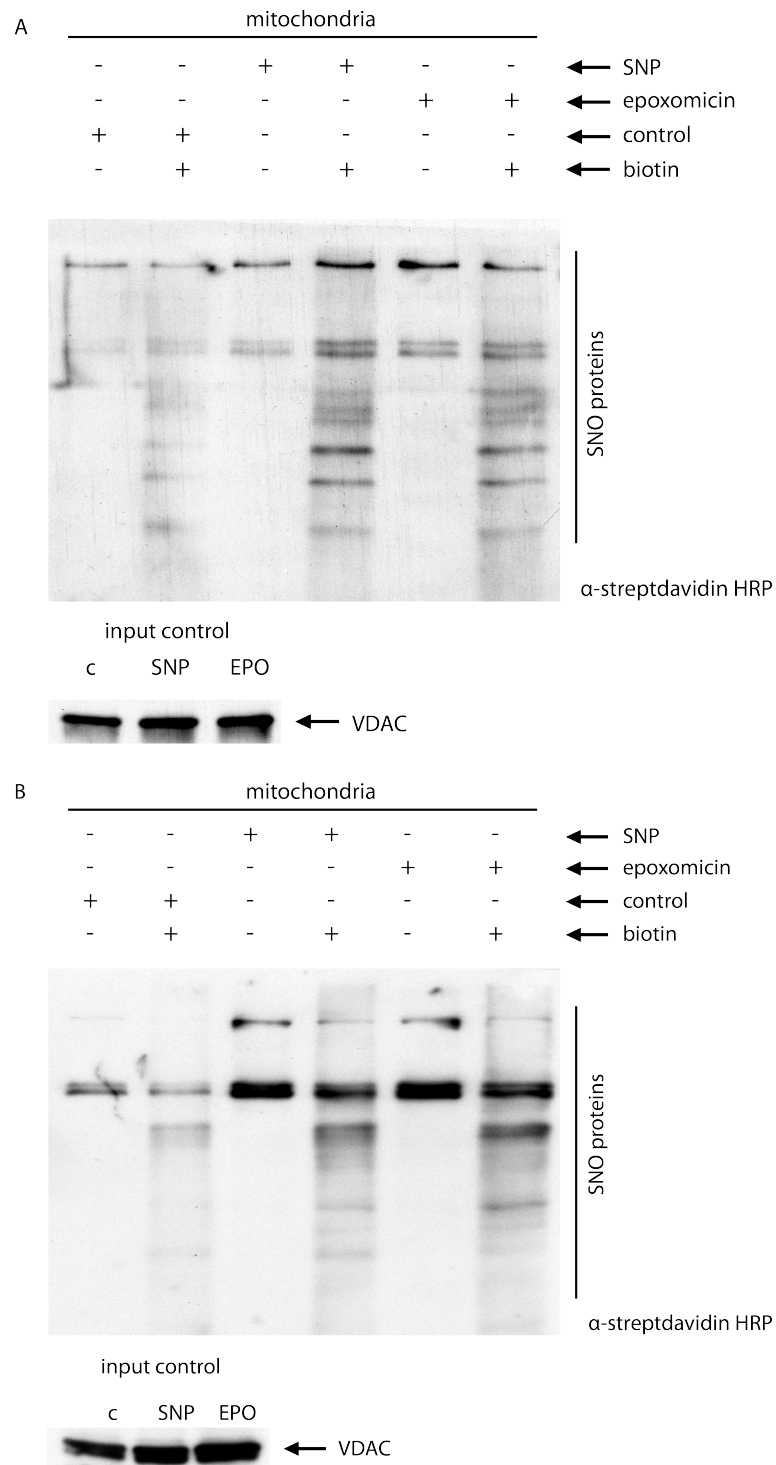
Figure 27: S-nitrosylated proteins on highly purified mitochondria
S-nitrosylated proteins were detected by biotin-switch using Western blot and streptdavidin-coupled HRP. **A:** Biotin-switch analysis of SNO proteins was performed on highly purified mitochondria of HeLa cells either treated with the proteasome inhibitor epoxomicin or NO-donor SNP. As shown in lane 4 there is a marked increase in SNP proteins following SNP treatment. Treatment with epoxomicin also increases the level of S-nitrosylated proteins (lane 6). The lanes 1, 3, 5 served as a control (-biotin) for the biotin-labeling step during the biotin switch. **B:** Highly purified mitochondria of 293 HEK cells either treated with the proteasome inhibitor epoxomicin or NO-donor SNP were analyzed by biotin-switch. Lane 4 and 6 show an increase in modified proteins following SNP treatment. VDAC served as an input control before starting the biotin-switch. This figure shows one representative experiment of three individual assays.

3.2.4. Absence of mitophagy upon SNP treatment

Mitophagy is a quality control process where dysfunctional mitochondria are selectively eliminated by autophagy (*73*). There is one pathway of mitophagy, which is activated by the ubiquitin ligase Parkin after translocation from the cytosol to the dysfunctional mitochondria (*74*). To evaluate the possibility of induced mitophagy following low dose treatment with the NO-donor SNP, induction of mitophagy was analyzed by assessing Parkin translocation to mitochondria. To this end, HeLa cells were transfected with a plasmid encoding Parkin^{YFP} and treated for 20 hours either with 100 µM SNP or 1 mM SNP and compared to untreated cells and to cells treated with the mitochondrial uncoupler and known inducer of mitophagy carbonyl cyanide m-chlorophenylhydrazone (CCCP). CCCP is known to depolarize mitochondria by increasing membrane permeability to H^{+} (*214*) causing translocation of Parkin to mitochondria. Figure 28 shows the translocation of Parkin^{YFP} after treatment with 20 µM CCCP from the cytosol to the mitochondria in 47% +/- 10% of cells, while translocation of Parkin following treatment with 100 µM or 1 mM SNP was only evident in 1.2% +/- 0.8%, 0% +/-0% of cells, respectively (Figure 29). This data demonstrates, that SNP in the used concentration does not induce mitophagy.
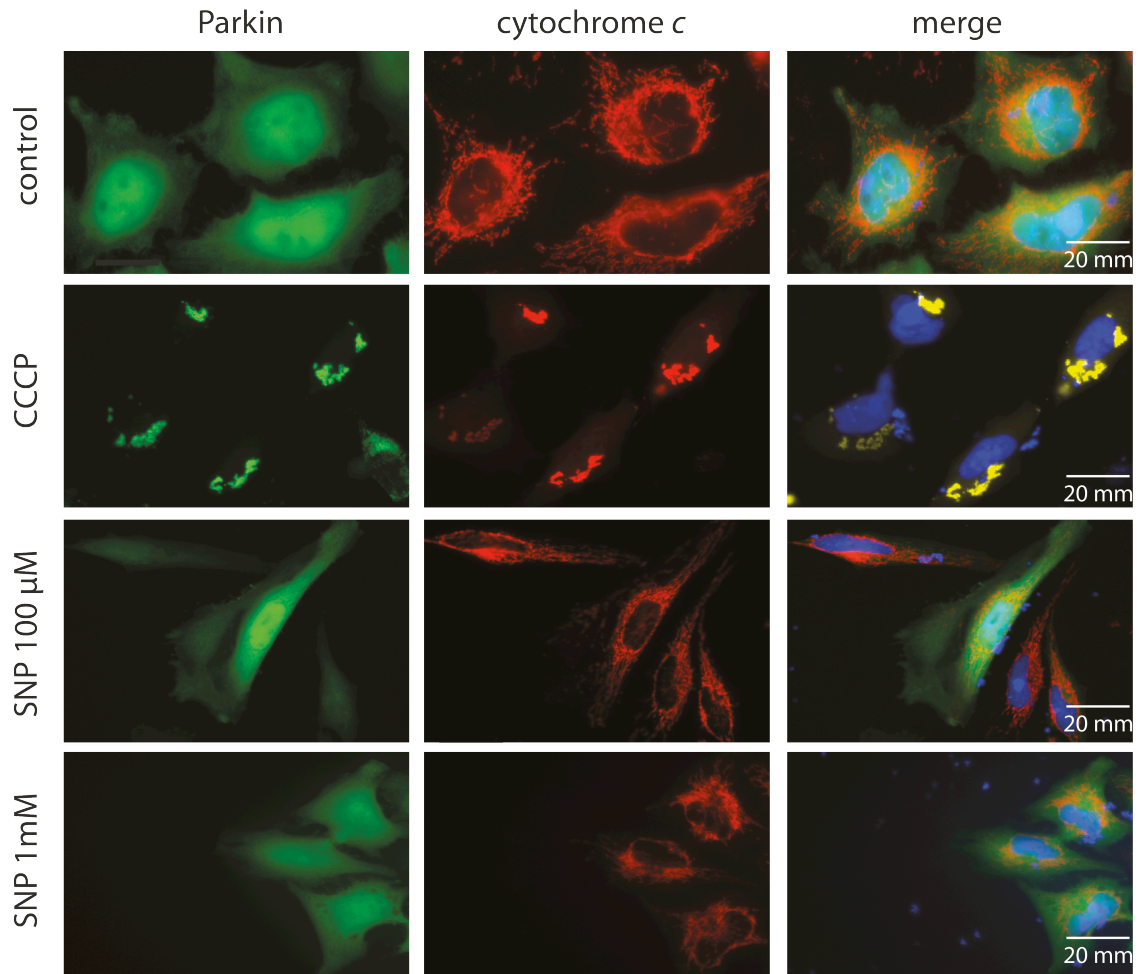
Figure 28: SNP does not promote mitophagy

HeLa cells were transfected with a plasmid encoding Parkin[YFP] (green) and treated for 20 hours either with 20 μM CCCP, 100 μM SNP, 1 mM SNP or untreated as control. Mitochondria were visualized using α-cytochrome *c* staining (red). DAPI (blue) stains the nucleus. Note the clear overlap of Parkin with the mitochondrial marker cytochrome *c* following treatment with CCCP indicative for mitophagic induction. Treatment with the NO-donor SNP in both concentrations showed no translocation of Parkin to the mitochondria similar to untreated control cells. This figure shows one representative experiment of three individual assays.
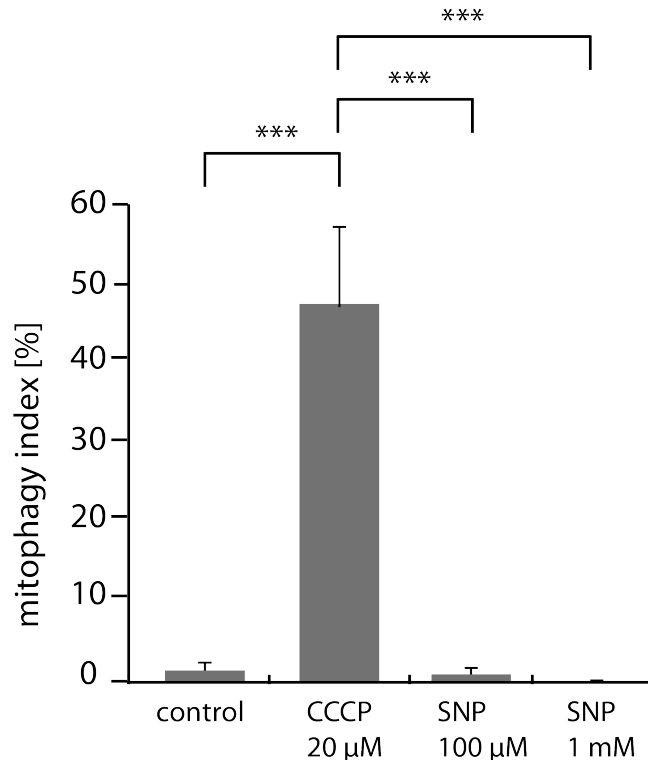
Figure 29: Quantification of mitophagy in HeLa cells
HeLa cells were transfected with a plasmid encoding Parkin^{YFP} followed by treatment with the mitophagy inducer CCCP or NO-donor SNP or left untreated as control. The translocation of Parkin to the mitochondria was quantified by counting >100 cells/condition. Error bars correspond to SEM. *** highlights $p<0.001$ (unpaired, two-tailed Student's t-test, Microsoft Excel). This figure shows the average of three individual assays.

3.2.5. Absence of cytochrome *c* release upon SNP treatment

It is known that NO-donors in high concentration are neurotoxic and induce apoptosis (*40*). Cytochrome *c* is a mitochondrial intermembrane space protein, which is released from the mitochondria into the cytosol in case of apoptosis (*215*). To test whether SNP induces apoptosis in the employed concentrations, cytochrome *c* release was quantified using immunocytochemistry. To this end, HeLa cells pretreated with the caspase inhibitor zVAD-fmk, were treated either with actinomycin D, a DNA transcription and replication inhibitor or 100 µM SNP or 1000 µM SNP. After 8 hours of treatment, cells were fixed, immunostained for cytochrome *c* and analyzed using fluorescence microscopy (Figure 30). As shown in Figure 31, cytochrome *c* was released into the cytosol in 32% +/- 6% of cells following actinomycin D treatment as expected. However, apoptotic induction following SNP treatment was only evident in 0% +/- 0% (100 µM), or 1.2% +/-0.6% of cells (1000 µM), respectively (Figure 31). This result illustrates that SNP treatment, as employed here, does not induce programmed cell death as no cytochrome *c* release during SNP treatments was observed.
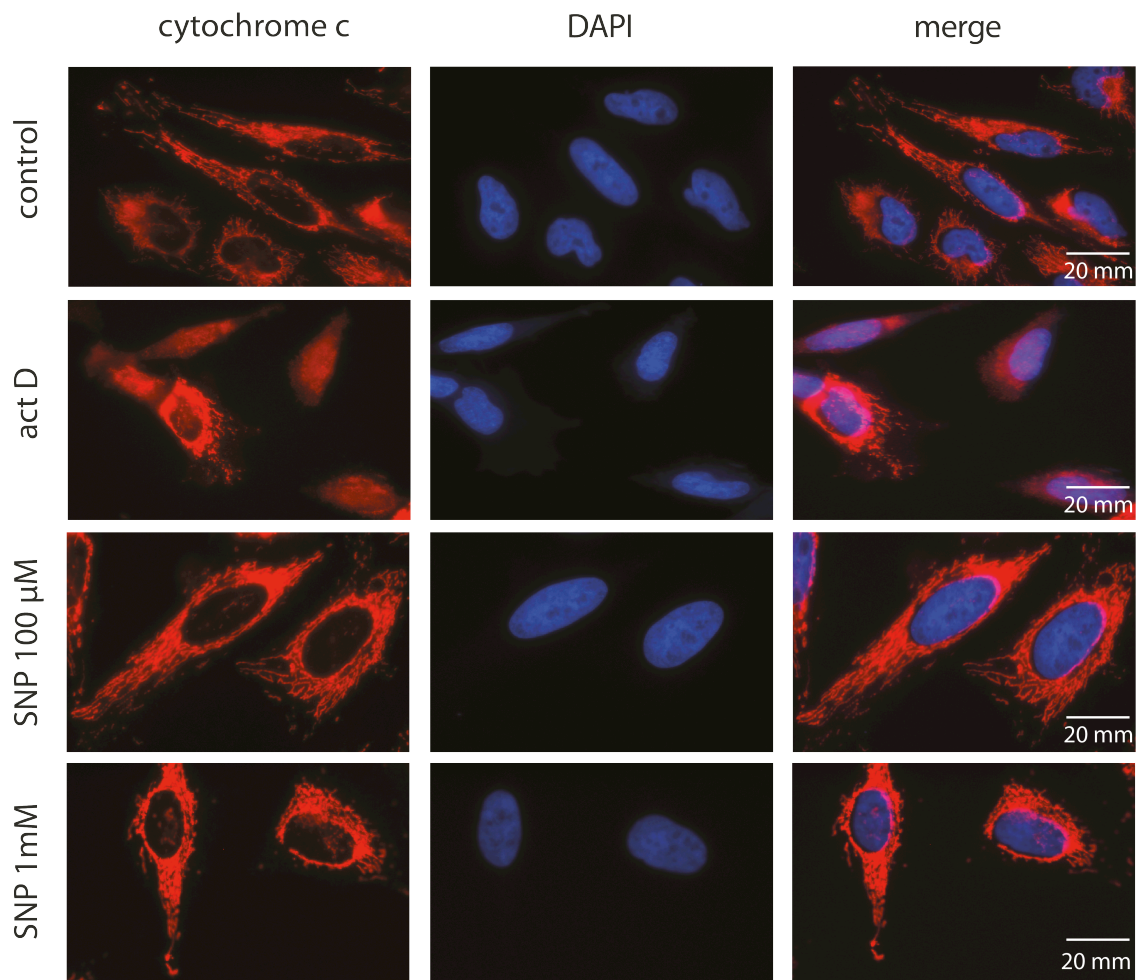
Figure 30: Cytochrome *c* release in HeLa cells
HeLa cells were pretreated for 30 minutes with 50 μM zVAD-fmk, followed by incubation with 20 μM ActD, 100 μM or 1 mM SNP for 8 hours or left untreated. Cells were stained using α-cytochrome *c* antibody (red), and cytochrome *c* release was visualized by fluorescence microscopy. Note in the group treated with ActD a markedly higher cytochrome *c* release was observed compared to the untreated control group or SNP groups. This figure shows one representative experiment of three individual assays.
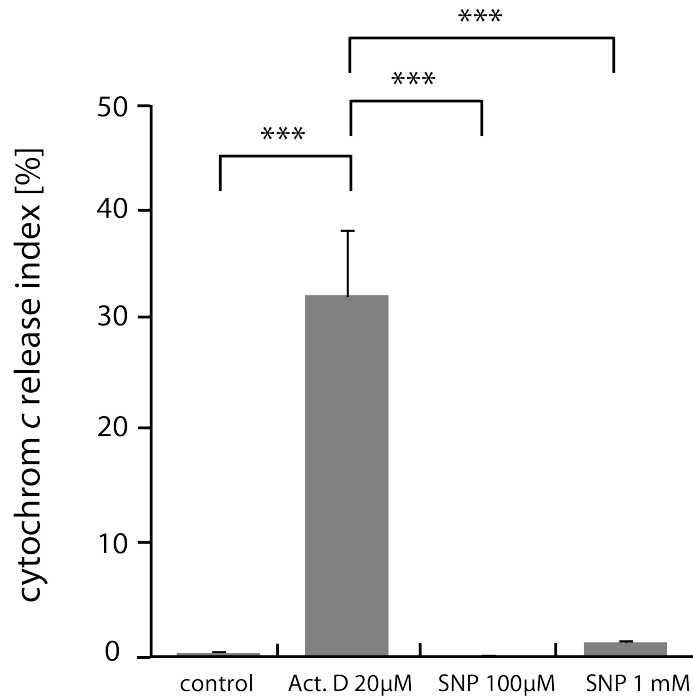
Figure 31: Quantification of cytochrome _c_ release in HeLa cells
HeLa cells were pretreated for 30 minutes with zVAD-mfk followed by treatment with the apoptosis inducer ActD or NO-donor SNP as described in Figure 30. Cytochrome _c_ release was quantified by counting >100 cells/condition. Error bars correspond to SEM. *** highlights $p<0.001$ (unpaired, two-tailed Student's t-test, Microsoft Excel). This figure shows the average of three individual assays.

3.2.6. Degradation of S-nitrosylated proteins by the ubiquitin-proteasome-system

To further investigate the role of proteasome-dependent SNO-proteins turnover, the levels of ubiquitinated proteins in absence or presence of the NO-donor SNP were studied. To this end, HeLa cells were transfected with a plasmid encoding HA-epitope tagged ubiquitin followed by treatment either with SNP, and/or epoxomicin for 6 hours. After treatment, highly purified mitochondria were prepared and analyzed by Western blot using α-ubiquitin antibody. Figure 32 shows that after treatment with SNP or epoxomicin the levels of S-nitrosylated proteins in highly purified mitochondria are increased even further (Figure 32, lane 2 and 3). However, treatment with SNP together with the proteasomal inhibitor epoxomicin increases the level of ubiquitinated mitochondrial proteins substantially (Figure 32, lane 4). This accumulation of ubiquitinated proteins on mitochondria following NO stress and under conditions of proteasomal inhibition strongly supports a role of the proteasome-dependent degradation pathway in the clearance of SNO proteins from mitochondria.
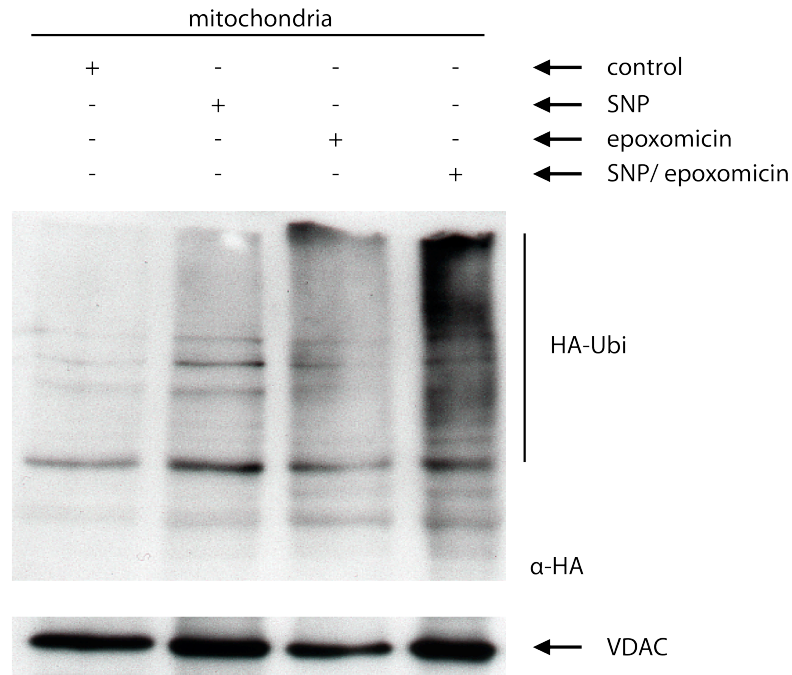
Figure 32: Ubiquitin-dependent degradation of S-nitrosylated proteins
HeLa cells were transfected with a plasmid encoding ubiquitin-HA and treated either with the proteasome inhibitor epoxomicin, 100 μM SNP or both together for 6 hours. Cells were harvested and highly purified mitochondria were prepared. Mitochondria pellets were resuspended in RIPA buffer and boiled at 95°C for 5 minutes. Ubiquitinated proteins were analyzed by Western blot using α-ubiquitin antibody. This result is consistent with the ubiquitin-dependent degradation of SNO-proteins. This figure shows one representative example of three individual experiments.

3.2.7. The AAA-ATPase p97 is involved in the degradation of SNO proteins

To allow the degradation of mitochondrial proteins by the cytosolic proteasome, substrate proteins must be extracted from mitochondria and retrotranslocated into the cytosol (*103*). Recent studies have shown that the cytosolic AAA-ATPase p97 is required for this protein retrotranslocation from the mitochondria into the cytosol (*111*). To investigate whether the AAA-ATPase p97 is involved in the proteasomal degradation of SNO mitochondrial proteins, SNO-protein levels in cell lines, stably expressing p97 or inactive p97^{QQ} (*216*) under the control of a tetracycline-inducible promoter, were analyzed. Both wildtype p97 and mutant p97^{QQ} expressing cells were either treated with SNP for 9 hours or left untreated. Highly purified mitochondria were prepared and biotin-switch was performed. Figure 33 shows the levels of SNO proteins after incubation with SNP. As expected, treatment with SNP caused elevated levels of SNO-proteins (lane 1) in cells expressing wildtype p97 compared to untreated control cells (lane 3). Interestingly, expression of

p97^{QQ} caused a marked increase of SNO-protein levels in the presence as well as in the absence of exogenous NO stress.

This result supports a role for p97 in the degradation and therefore likely in the retrotranslocation of SNO proteins from mitochondria into the cytosol for proteasomal degradation.
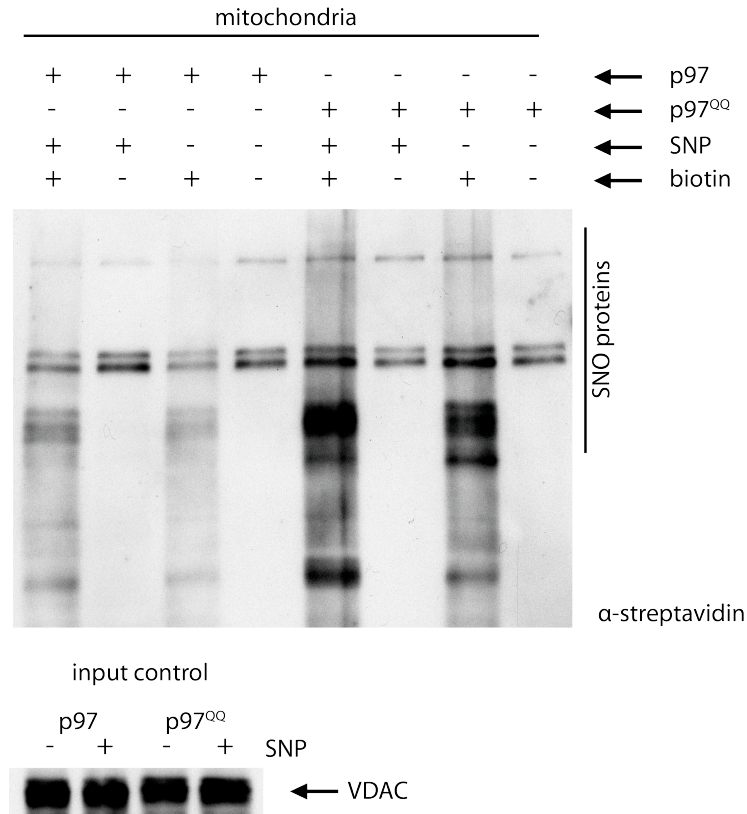
Figure 33: AAA-ATPase p97 dependent degradation of mitochondrial S-nitrosylated proteins
HEK 293 cells stably expressing tetracycline-inducible p97 or inactive p97^{QQ} were treated with SNP for 9 hours or left untreated. Levels of SNO-proteins were analyzed in highly purified mitochondria. Note the strong increase in cells expressing inactive p97^{QQ} (lane 7) compared to cells expressing wildtype p97 (lane 3). More SNO proteins are detectable following SNP treatment (compare lane 1 with lane 5). These findings support a role of p97 in clearance of mitochondrial SNO proteins. This figure shows one representative experiment of three individual assays. Omission of biotin label served as control for the biotin-switch assay. Detection of VDAC served as input control. This figure shows one representative example of three individual experiments.

3.2.8. NO-dependent stabilization of MARCH9

To test the role of the potential mitochondrial ubiquitin ligase MARCH9 during NO stress, Western blot was performed to analyze expression levels of MARCH9 and MARCH9^{H136W} after treatment with the NO donor SNP. For this purpose, HeLa cells were transfected with a plasmid encoding MARCH9^{YFP} or MARCH9^{H136WYFP} and incubated for 12 hours with 10 μM SNP, 100 μM SNP or left untreated. Levels of MARCH9 were detected by Western blot using α-GFP antibody (Figure 34).
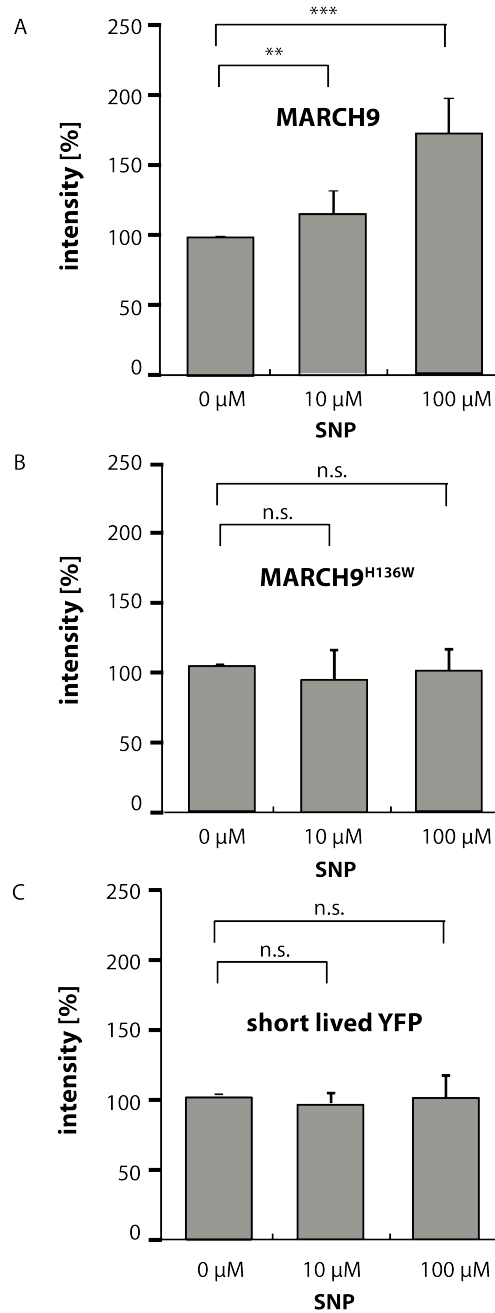
Figure 34: MARCH9 stabilization after SNP incubation
A: : HeLa cells were transfected with a plasmid encoding MARCH9^{YFP} and treated for 12 hours with the NO-donor SNP at concentrations of 10 μM SNP, 100 μM SNP or left untreated. Protein lysates were analyzed by quantitative Western blot using α-GFP antibody. GAPDH was used as a loading control. Note the increase of MARCH9 levels following SNP treatment compared to control cells (bar 2 and 3). **B:** HeLa cells were transfected with a plasmid encoding MARCH9^{H136WYFP} and treated for 12 hours with the NO-donor SNP in the concentrations of 10 μM SNP, 100 μM SNP or left untreated. Protein lysates were analyzed by quantitative Western blot using α-GFP antibody. GAPDH was used as a loading control. Note there is no increase of levels of MARCH9^{H136W} following SNP treatments when compared to untreated controls. **C:** HeLa cells were transfected with a plasmid encoding short-lived GFP and treated for 12 hours with the NO-donor SNP in the concentrations of 10 μM SNP, 100 μM SNP or left untreated. Protein lysates were analyzed by quantitative Western blot using α-GFP antibody. GAPDH was used as a loading control. Note there is no increase of short-lived GFP levels. Error bars correspond to SEM. *** highlights $p<0.01$, ** highlights $p<0.05$ and n.s. highlights $p>0.05$ (unpaired, two-tailed Student's t-test, Microsoft Excel). This figure shows the average of three individual assays.

These data are consistent with a stabilization of MARCH9 under NO stress conditions based on increased stability of MARCH9 rather than decreased proteasomal degradation of this protein. While no direct connection between levels of mitochondrial SNO-proteins and the expression of MARCH9 was found (data not shown), these observations hint towards a potential role for MARCH9 during NO stress. Increased stability of an ubiquitin ligase suggests the presence of substrate proteins, which in turn would diminish auto-degradation of such an ubiquitin ligase. Whether such a mechanism explaining the observed stabilization of MARCH9 remains unclear, however, it is tempting to speculate that MARCH9 might have a role in resolving NO stress conditions.

4. Discussion

Mitochondrial dysfunction is virtually at the core of all neurodegenerative disorders and connected to the aging processes. Therefore multiple mitochondrial quality control mechanisms are an essential part of maintaining cellular function to prevent aging and untimely death of neuronal cells. Keeping mitochondria in a healthy state is a complex process and has to be tightly regulated (*218*). Recent studies support the idea that mitochondrial fusion and fission machinery as well as mitochondrial quality control play an important role in maintaining mitochondrial integrity and the survival of neurons (*219*).

4.1. Degradation of mitochondrial proteins by OMMAD

Ubiquitination plays an essential role in virtually all cellular processes, and especially in the quality control of proteins. Recently, the role of ubiquitination and ubiquitin-dependent protein degradation in mitochondrial physiology became clearer. Mitochondrial morphology seems to be under control of the UPS, with the mitofusins as well as the fission protein Drp1 being a target for ubiquitination.

The special topology of mitochondria requires specialized protein degradation mechanisms. As the UPS is mainly cytosolic, ubiquitin-dependent degradation of mitochondrial proteins necessitates the presence of factors able to interface the UPS to mitochondria. OMM-anchored RING finger ubiquitin ligases such as MARCH5 (*105*), MULAN/MAPL (*220*) and IBRDC2 (*106*) might provide this interfacing function. These observations suggest an involvement of the UPS on mitochondrial quality control. Recent observations suggest a role for proteasomal degradation of outer mitochondrial proteins, similar to the process of ER-associated protein degradation (ERAD) (*221*). As mitochondria, the ER is a membrane-bound organelle with highly active protein import mechanisms. Also like mitochondria, the ER is impacted by misfolded and/or damaged proteins. Thus, one might postulate that mitochondrial proteins are under the control of a process termed OMM-associated degradation (OMMAD) as the ER is maintained by ERAD. ER-associated degradation consists of three different steps. Ubiquitin ligases, embedded in the ER membrane, interact with accessory recognition factors to recognize misfolded proteins. Two mammalian ubiquitin ligases were identified, HRD1 and gp78 (*222*). Specific ubiquitination of the

substrate is catalyzed by such membrane-anchored ubiquitin ligases. As the proteasome is located in the cytosol, the ubiquitinated substrates have to be extracted from the ER membrane to the cytosol for proteasomal degradation. For ERAD it was shown that the AAA-ATPase p97 provides the mechanical force necessary to extract substrate proteins and cause retrotranslocation of proteins into the cytosol (*223*). After translocation, the substrate is then escorted to the 26S proteasome for degradation (*224*). Interestingly, while OMMAD and ERAD are governed by different membrane-anchored ubiquitin ligases, both mechanisms share their retrotranslocation mechanism. It was shown that p97 is able to extract and retrotranslocate ubiquitinated mitochondrial proteins from the outer mitochondrial membrane to the cytosol for subsequent proteasomal degradation (*225*). It is currently unknown whether misfolded or damaged mitochondrial proteins are processed by OMMAD in the same manner as misfolded ER proteins. However, the presence of ubiquitin ligases on the outer mitochondrial membrane and the involvement of p97 in protein retrotranslocation greatly support this notion.

4.2. MARCH9 and mitochondrial maintenance

Ubiquitination plays an essential role in all critical cellular processes, especially in the quality control of proteins, and recent findings strongly connect the UPS to mitochondrial maintenance. MARCH9 was identified in a screen for new factors regulating mitochondrial morphology and mitochondrial integrity, where potential membrane-anchored ubiquitin ligases, based on the presence of a RING finger domain and at least one transmembrane domain, were localized to subcellular compartments (*105*). Together with MARCH5, IBRDC2 and MAPL/MULAN, MARCH9 was found to localize to the outer mitochondrial membrane (Neutzner- personal communication). However, the function of MARCH9 remained unclear and warranted further examination.

4.3. RING finger domain of MARCH9

As MARCH9 belongs to the MARCH family of proteins and encompasses a RINGv and as most MARCH proteins were shown to possess E3 activity, this suggests also an ubiquitin ligase activity for MARCH9 (*99*). To further investigate whether MARCH9 indeed possesses E3 activity, several attempts were made to reconstitute MARCH9-mediated ubiquitination *in vitro* or to ascertain E3 activity for MARCH9 *in vivo*. It is a prominent feature of RING finger ubiquitin ligases to regulate the enzymatic activity *in vitro* via auto-ubiquitination wherein they catalyze the addition of ubiquitin to themselves to form a

polyubiquitin chain and initiate their own proteasomal degradation (*208*). In a first attempt, mutation in the RING finger domain by substitution of histidine 136 with tryptophan predicted to inhibit Zn^{2+} coordination, thereby inactivation of MARCH9 was performed. While inactivation of the RING finger domain lead to the stabilization of most RING finger proteins, the RING finger mutation of MARCH9 did not stabilize as predicted, but rather destabilized and promoted proteasomal degradation of inactive MARCH9 mutant (Figure 11). Measurement of protein levels (Figure 12) also confirmed the instability of MARCH9[H136W]. These data do not readily support ubiquitin ligase activity for MARCH9. While it is unlikely that the introduced RING finger mutation did not inhibit but rather increase MARCH9 activity towards itself, it cannot completely exclude the possibility that the H136W mutation does not render MARCH9 completely inactive. However, a similar mutation in MARCH5 (H43W) was shown to block E3 activity (*105*). In addition, analysis of wildtype MARCH9 levels in the presence and absence of proteasomal inhibition did not result in a massive stabilization of MARCH9, suggesting that wildtype MARCH9 only has minor auto-ubiquitination activity. This leaves the question of why the H136W mutation leads to a destabilization of MARCH9. It is conceivable, that MARCH9[H136W] constitutes a novel substrate for mitochondrial protein quality control or OMMAD. Thus, unknown ubiquitin ligase or endogenous MARCH9 target MARCH9[H136W] for proteasomal degradation. As many ubiquitin ligases form dimers, such as MARCH9-dependent ubiquitination could also occur *in trans (226)*. The notion that MARCH9 might be involved in the degradation of MARCH9[H136W] is supported by the observation that MARCH9 interacts with itself and likely forms dimers (Figure 13). These observations are consistent with a model were MARCH9 would control its stability in a regulatory feedback loop. However, another still unknown ubiquitin ligase could be responsible for the degradation of MARCH9[H136W] as result for protein quality mechanism, responsible for the removal of damaged proteins. In summary, the analysis of MARCH9[H136W] stability neither proved nor disproved an ubiquitin ligase activity for MARCH9.

To identify ubiquitin ligase activity of MARCH9, a bacterial system was used that allows expression of multiple genes to reconstitute the ubiquitination reaction *in vivo*. To this end, E1, E2, and ubiquitin, as well as MARCH9, were expressed in a bacterial host and auto-ubiquitination of MARCH9 was analyzed. As prokaryotes do not have posttranslational modification by ubiquitin like eukaryotic cells, background nonspecific ubiquitin reactions are absent in such systems. Using this bacterial *in vivo* ubiquitination assay did not result in

specific ubiquitination of MARCH9. As discussed above, MARCH9 might not possess major auto-ubiquitination activity. In the bacterial assay a GST-fusion of MARCH9 was employed, supposedly providing an intra-molecular substrate for MARCH9. While this method proved useful for other ubiquitin ligases, the low auto-ubiquitination activity of MARCH9 might hamper this approach.

Also, MARCH9 is a membrane protein, making the purification of the full-length protein highly difficult, and in this case all such attempts failed. Thus, a soluble version of MARCH9 including the RING finger domain, lacking the two transmembrane domains and the entire C-terminus, was used for these assays. This might explain the lack of ubiquitin ligase activity of truncated MARCH9 seen in the experiments. While it was shown that a RING finger domain might be sufficient to support *in vitro* ubiquitin ligase activity (*227*), it cannot be exclude that other parts of the protein domains, even the transmembrane domains, might be involved in the ubiquitination reaction.

Another reason for the failure to detect ubiquitin ligase activity might lie with employment of ubiquitin-conjugating enzyme E2 and MARCH9. MARCH9 did not show specific ubiquitination with UBE2G2, UBE2D1, UBE2B, UBE2B and UBEJ2. An ubiquitin ligase function results only with a specific E2 enzyme, therefore the compatibility between E3 and E2 is a critical aspect of the enzyme cascade. MARCH9 might require another E2 such as a mitochondrial-anchored ubiquitin-conjugating enzyme E2. For example, during the last step of ERAD it was demonstrated that substrates are polyubiquitinated by membrane-bound E2 enzymes Ubc1, Ubc6 and Cue1-associated Ubc7 (*228, 229*). However, MARCH9's requirement of an as yet unknown E2, is a subject for another investigation. Construction of an E2 library could serve as a tool to identify a specific E2 for MARCH9 (*230*). The library would contain both full-length and core UBC domain versions of all 40 *H. sapiens* E2 proteins. This entire E2 panel could then be used in an *in vitro* ubiquitination assay with MARCH9.

Although it is suspected that MARCH9 is a potential ubiquitin ligase, it cannot be excluded that MARCH9 has as well some another function. It was recently shown that the mitochondrial RING finger containing ubiquitin ligase MAPL (*104*) possess SUMO ligase activity, MARCH9 might also act as a SUMO ligase. SUMOylation is, like ubiquitination, a multi-step process involving E1, E2 and a SUMO ligase. The question whether MARCH9

possesses ubiquitin ligase activity, or may act as a SUMO ligase remains open to further specific investigation.

4.4. A potential role for MARCH9 in the mitochondrial fusion process

Previous observations suggested a role for MARCH9 in the regulation of mitochondrial fusion. It was found that expression of inactive MARCH9^{H136W} caused extensive mitochondrial fragmentation, while expression of wildtype MARCH9 did not seem to influence the balance between mitochondrial fusion and fission. These findings indicate a role for MARCH9 as either a fusion process activator or a fission process inhibitor. Interestingly, no shift in mitochondrial morphology was observed after 70% knockdown of MARCH9 using RNA interference (Neutzner- personal communication). Assuming the achieved knockdown was sufficient, MARCH9 seems not to be an essential part of the mitochondrial fusion machinery. However, these findings indicate a dominant-negative action of MARCH9^{H136W} likely blocking mitochondrial fusion through a titration effect. One mode of action for dominant-negative mutations is through unproductive interaction between a mutated protein and an essential factor of the affected process (*231*). Consequently, the existence of a MARCH9 activator has not been postulated and would explain why only dominate-negative mutant affect mitochondrial morphology. Consistent with this notion, we found that MARCH9 physically interacts with both Mfn1 and Mfn2, both of which are essential for the mitochondrial fusion process as no other mitofusins are present in mammalian cells (Figure 24). It is also conceivable that MARCH9 directly or indirectly regulates the stability of mitofusins thereby blocking the fusion process. While Mfn1 is not a target of proteasomal degradation, Mfn2 is a substrate for proteasomal degradation (*232*) and MARCH9 seems to influence Mfn2 stability under certain conditions (Neutzner- personal communication). A model seems attractive where MARCH9 causes the degradation of Mfn2 during the actual fusion process. During fusion, mitochondrial tubules show a so called kiss-and-run behavior (*233*). The degradation of Mfn2 might be essential to change from the kiss-and-run pattern into a permanent fusion of two mitochondria. This scenario is supported by recent studies in yeast, where the Ugo-1 and Mdm30- dependent degradation of the mitofusin Fzo1 is necessary for the irreversibility of the outer mitochondrial membrane fusion (*138*). However, to substantiate this hypothesis, the role of MARCH9 in modulating Mfn2 stability, and its involvement in the mitochondrial fusion machinery needs, further investigation.

4.5. Additional potential role of MARCH9

The RING-CH proteins were initially described, following the identification of the K3 family or viral E3 ligases in γ-herpesvirus. While showing little sequence homology with the viral E3 ligases, the mammalian MARCH E3 ligases share similar structural organization and contain both, a RING domain and several transmembrane domains (*234*). It was also shown that other MARCH proteins such as MARCH1 and MARCH8 modulate the levels of immune regulatory molecules either directly or indirectly. Interestingly, it was also shown that mitochondrial-localized MARCH5 catalyzes the K63-linked polyubiquitination of TANK, a modulator of innate immunity, thus promoting toll like receptor 7 responses in viral defense (*235*). These observations suggest a function of MARCH proteins in the immune response.

Recent studies have suggested that MARCH9 modulates the stability of immunological cell surface markers such as ICAM-1 (*236*), CD4 and HLA-DOβ (*237*). Indeed, MARCH9, as a MARCH protein, shows homology to the viral ubiquitin ligase K3 and K5, supporting the idea that MARCH9 is involved in the degradation of immune-modulatory surface proteins (*234*). Considering that MARCH9 is closely related to MARCH5, and other mitochondrial proteins such as MAVS (*238*) and NLRX1 (*239*) are involved in immune response, a role for MARCH9, as an immune modulator is conceivable. Thus, similarly to MARCH5, MARCH9 might also have dual functions in modulating mitochondrial morphology and the immune response.

4.6. Mitochondria and S-nitrosylation

Nitric oxide has normal physiological functions and influences a wide variety of cellular processes (*40, 240*). Mitochondrial physiology is impacted by NO and NO-mediated protein modification. Although NO has many physiological functions, once excessive NO is generated, it reacts with oxygen to form very reactive nitrogen species (RNS), such as nitrogen dioxide (NO_2), dinitrogen trioxide (N_2O_3) and peroxynitrite ($ONOO^-$) (*241*). Such RNS are known to cause damage to proteins such as excessive S-nitrosylation and nitration. Mitochondria are especially prone to RNS damage as these organelles are major producers of RNS via ROS production. The question, when does mitochondrial nitric oxide (NO)

become harmful, remains open. The answer may depend on different factors, such as the type of target protein, location of target protein and function of target protein. Also the issue of where mitochondrial NO originates from is still controversial. Some studies have reported that one of the isoforms of NO synthase is located in the inner mitochondrial membrane. Bates et al. (*242*) has identified the first NO synthase in liver and rat brain mitochondria. This observation has opened the possibility that nitric oxide could be a regulator of mitochondrial respiration. Indeed, the activity of mtNOS has been proven by the measurement of mitochondrial NO production in liver mitochondria (*243*). Aside of the mitochondrial NO synthase, NO can impact mitochondria in other ways. As NO is a soluble and uncharged molecule it can diffuse easily across membranes (*244*). A well-established model for excessive NO production in neuronal cells is the activation of *N*-methyl-D-aspartate (NMDA)-type glutamate receptor. Activation of the glutamate receptor leads to an influx of Ca^{2+}, which in turn activates neuronal NO synthase (nNOS) leading to elevated NO levels in case of exocitotoxicity finally causing mitochondrial dysfunction (*245*).

4.7. Quality control of S-nitrosylated mitochondrial proteins

Mitochondrial proteins are the target of S-nitrosylation either during normal regulatory processes or as result of a stressor induced insult. While several mechanisms such as thioredoxin or S-nitrosogluthation reductase (section 1.2.3.) are in place to reverse S-nitrosylation, it is unclear whether these systems are able to revert all S-nitrosylation of mitochondrial proteins or whether, especially during increased NO stress, S-nitrosylated proteins accumulate with potentially deleterious effects on mitochondrial function.

Therefore it is conceivable, that degradation of such S-nitrosylated proteins plays a role in the clearance of such proteins, thus maintaining mitochondrial fidelity. While several proteolytic systems such as membrane-anchored as well as matrix localized proteases are active in mitochondria, the UPS might also provide quality control for extraneous S-nitrosylated proteins. Indeed, we found that proteasome inhibition increased the levels of S-nitrosylated proteins in whole cell lysates, and most importantly, in highly purified mitochondrial fractions (Figures 26, 27, 32). The accumulation of ubiquitinated proteins in response to NO stress under treatment with the proteasome inhibitor is indicative of an ubiquitin-dependent, proteasomal degradation of mitochondrial S-nitrosylated proteins. Interestingly, proteasome-dependent degradation of S-nitrosylated proteins was evident in NO-stressed as well as unstressed cells. Thus, even under normal physiological conditions,

in the absence of exogenous NO, S-nitrosylation is resolved via protein degradation. While de-nitrosylation might still be the main pathway to deal with S-nitrosylated proteins, UPS-mediated clearance of S-nitrosylated proteins clearly plays a role under unstressed conditions. Proteasomal degradation of S-nitrosylated proteins also occurs during low NO stress conditions.

These observations are further supported by the involvement of p97 in the clearance of S-nitrosylated proteins from mitochondria. We found increased levels of S-nitrosylated proteins in cells expressing p97 when compared to control cells (Figure 33). Based on this result, it is reasonable to assume that mitochondrial S-nitrosylated proteins are retrotranslocated by p97 from the mitochondria to the cytosol to prevent accumulation of S-nitrosylated proteins and to aid their proteasomal degradation. As p97 was previously shown to be a part of OMMAD, these findings support the involvement of OMMAD in the quality control of S-nitrosylated proteins.

Recently, the importance of Parkin-mediated mitophagic clearance of damaged mitochondrial subunits was recognized (*246*). While NO seems to be connected to the induction of mitophagy (*247*), under low level NO stress, as employed by us, proteasomal degradation seems more prevalent than mitophagic clearance as no Parkin recruitment to mitochondria was seen. Also, induction of apoptosis was not present under low level NO stress, thus, no involvement of programmed cell death in the clearance of S-nitrosylated proteins is evident (Figure 28 and 30). Therefore, we suggest that the degradation of S-nitrosylated mitochondrial proteins by the proteasome is an additional element in protection against low level nitrosative stress and might be an important player in the defense against aging and neurodegeneration.

This notion is further supported by the link between the mitochondrial ubiquitin ligase MARCH5 and S-nitrosylated microtubules-associated protein 1B (MAP1B). S-nitrosylated MAP1B (SNO-MAP1B) in mitochondria is degraded by the mitochondria-anchored ubiquitin ligase MARCH5. MARCH5-dependent degradation of SNO-MAP1B protects neurons from mitochondrial dysfunction and subsequent cell death (*248*). In addition, the ubiquitin ligase Parkin that participates the ubiquitin proteasome system is a target for S-nitrosylation. Upon S-nitrosylation, the activity of Parkin initially increases but is subsequently inhibited. This might be of the increased auto-ubiquitintation. This inhibition

of ubiquitin ligase activity leads to impairment of ubiquitination and degradation of substrate protein (*54*).

Further support for the connection between OMMAD and quality control of S-nitrosylated proteins comes from our finding that the stability of the mitochondrial RING finger protein MARCH9 was increased in response to low level NO stress (Figure 34A). It is conceivable that MARCH9 levels are upregulated in response to the presence of potential S-nitrosylated substrate proteins. Thus, MARCH9, as a possible OMMAD ubiquitin ligase, could play a role in the clearance of S-nitrosylated proteins. However, no direct impact of MARCH9 on the levels of S-nitrosylated proteins was seen. If S-nitrosylation can also directly inhibit the 26S proteasome activity by targeting cysteine residues in the catalytic core, one might speculate that the observed stabilization of MARCH9 can be attributed to a decreased turnover of MARCH9 in response to proteasomal degradation (*249*). However, using a short-lived GFP protein, which is degraded by the proteasome, did not result in protein stabilization after treatment with NO (Figure 34C), discounting the idea of proteasomal inhibition under low level stress conditions as used by us.

Thus, reversal of S-nitrosylation or denitrosylation resulting in restoration of protein function and protein degradation seems to work hand in hand to protect mitochondria from the deleterious action of excessive NO levels. As the detoxification systems are a target for S-nitrosylation-dependent inactivation themselves, the ubiquitin proteasome system likely also plays a role in maintaining denitrosylation capacity.

Considering these data, the ubiquitin proteasome system is probably an additional part in defending mitochondria against nitrosative stress and therefore prevention of mitochondrial dysfunction and associated neurodegenerative diseases. Our data supports a new role for p97-mediated, ubiquitin-dependent proteasomal degradation for S-nitrosylated proteins. In addition, our findings may connect the potential OMMAD ubiquitin ligase MARCH9 with the clearance of S-nitrosylated proteins from mitochondria. OMMAD may therefore provide an additional mitochondrial quality control for the clearance of S-nitrosylated proteins and help to keep mitochondria in a healthy state during constant low level nitrosative stress conditions.

4.8. Summary

In summary, recent findings have expanded the understanding of the importance of mitochondrial maintenance. One central part, in keeping mitochondria healthy is the removal of damaged proteins, which potentially interfere with normal mitochondrial function. Such damages are caused by ROS and RNS, leading to modifications such as protein carbonylation and S-nitrosylation. These modifications result in inactivation of proteins, thus it is important to remove such proteins preventing mitochondrial dysfunction. Several different mitochondrial quality control levels are involved to maintain the mitochondrial functions. On the molecular level, the repair systems deal with damaged proteins, mitochondrial DNA or lipids. On the organellar level the combined functions of mitochondrial fusion and fission together with mitophagy are established as essential quality control mechanisms. On the cellular level, programmed cell death is responsible for the removal of entire mitochondrial networks (*82*). Similar to the ERAD, the ubiquitin proteasome system in form of OMMAD controls proteins, which are localized on mitochondria. Based on our data, the ubiquitin proteasome system provides mitochondrial quality control and is involved in the clearance of mitochondrial S-nitrosylated proteins. Furthermore, based on our data a role for MARCH9 in this process is conceivable, we do not want to exclude the possibility of another as yet unknown ubiquitin ligase being involved in this process. However, the involvement of the OMMAD-component p97 in the retrotranslocation and degradation of mitochondrial S-nitrosylated proteins is well supported by our findings. Thus, the ubiquitin proteasome system in form of OMMAD seems to be important for the elimination of S-nitrosylated proteins from the mitochondria, further connecting ubiquitination to mitochondrial maintenance.

References

1. J. E. Vance, Phospholipid synthesis in a membrane fraction associated with mitochondria. *The Journal of biological chemistry* **265**, 7248 (May 5, 1990).
2. T. E. Gunter, D. R. Pfeiffer, Mechanisms by which mitochondria transport calcium. *The American journal of physiology* **258**, C755 (May, 1990).
3. D. D. Newmeyer, D. M. Farschon, J. C. Reed, Cell-free apoptosis in Xenopus egg extracts: inhibition by Bcl-2 and requirement for an organelle fraction enriched in mitochondria. *Cell* **79**, 353 (Oct 21, 1994).
4. E. V. Koonin, The origin and early evolution of eukaryotes in the light of phylogenomics. *Genome biology* **11**, 209 (2010).
5. M. W. Gray, G. Burger, B. F. Lang, Mitochondrial evolution. *Science* **283**, 1476 (Mar 5, 1999).
6. L. Margulis, D. Bermudes, Symbiosis as a mechanism of evolution: status of cell symbiosis theory. *Symbiosis* **1**, 101 (1985).
7. S. E. Horvath, G. Daum, Lipids of mitochondria. *Progress in lipid research* **52**, 590 (Sep 2, 2013).
8. M. Zick, R. Rabl, A. S. Reichert, Cristae formation-linking ultrastructure and function of mitochondria. *Biochimica et biophysica acta* **1793**, 5 (Jan, 2009).
9. J. A. Alberts B, Lewis J, et al. , *Molecular Biology of the Cell, 4th edition.* (2002).
10. D. F. Bogenhagen, D. Rousseau, S. Burke, The layered structure of human mitochondrial DNA nucleoids. *The Journal of biological chemistry* **283**, 3665 (Feb 8, 2008).
11. W. J. Koopman, F. Distelmaier, J. A. Smeitink, P. H. Willems, OXPHOS mutations and neurodegeneration. *The EMBO journal* **32**, 9 (Jan 9, 2013).
12. D. Acuna-Castroviejo *et al.*, Melatonin, mitochondria, and cellular bioenergetics. *Journal of pineal research* **30**, 65 (Mar, 2001).
13. M. H. Irwin, K. Parameshwaran, C. A. Pinkert, Mouse models of mitochondrial complex I dysfunction. *The international journal of biochemistry & cell biology* **45**, 34 (Jan, 2013).
14. C. Hagerhall, Succinate: quinone oxidoreductases. Variations on a conserved theme. *Biochimica et biophysica acta* **1320**, 107 (Jun 13, 1997).
15. J. Hirst, Mitochondrial complex I. *Annual review of biochemistry* **82**, 551 (2013).
16. Y. Hatefi, Y. M. Galante, Isolation of cytochrome b560 from complex II (succinateubiquinone oxidoreductase) and its reconstitution with succinate dehydrogenase. *The Journal of biological chemistry* **255**, 5530 (Jun 25, 1980).
17. C. L. Quinlan *et al.*, Mitochondrial complex II can generate reactive oxygen species at high rates in both the forward and reverse reactions. *The Journal of biological chemistry* **287**, 27255 (Aug 3, 2012).
18. I. Arnold, H. Folsch, W. Neupert, R. A. Stuart, Two distinct and independent mitochondrial targeting signals function in the sorting of an inner membrane protein, cytochrome c1. *The Journal of biological chemistry* **273**, 1469 (Jan 16, 1998).
19. T. A. Link, H. Schagger, G. von Jagow, Analysis of the structures of the subunits of the cytochrome bc1 complex from beef heart mitochondria. *FEBS letters* **204**, 9 (Aug 11, 1986).
20. A. R. Crofts, The cytochrome bc1 complex: function in the context of structure. *Annual review of physiology* **66**, 689 (2004).

21. I. Hassinen, in *Mitochondria,* S. Schaffer, M. S. Suleiman, Eds. (Springer New York, 2007), vol. 2, pp. 3-25.

22. S. Srinivasan, N. G. Avadhani, Cytochrome c oxidase dysfunction in oxidative stress. *Free radical biology & medicine* **53**, 1252 (Sep 15, 2012).

23. J. P. Abrahams, A. G. Leslie, R. Lutter, J. E. Walker, Structure at 2.8 A resolution of F1-ATPase from bovine heart mitochondria. *Nature* **370**, 621 (Aug 25, 1994).

24. G. Oster, H. Wang, Rotary protein motors. *Trends in cell biology* **13**, 114 (Mar, 2003).

25. M. Yoshida, E. Muneyuki, T. Hisabori, ATP synthase--a marvellous rotary engine of the cell. *Nature reviews. Molecular cell biology* **2**, 669 (Sep, 2001).

26. E. L. Chan, J. Rujiviphat, G. A. McQuibban, in *Mitochondrial Dynamics and Neurodegeneration,* B. Lu, Ed. (Springer Netherlands, 2011), pp. 1-46.

27. M. K. Shigenaga, T. M. Hagen, B. N. Ames, Oxidative damage and mitochondrial decay in aging. *Proceedings of the National Academy of Sciences of the United States of America* **91**, 10771 (Nov 8, 1994).

28. L. Farout, B. Friguet, Proteasome function in aging and oxidative stress: implications in protein maintenance failure. *Antioxidants & redox signaling* **8**, 205 (Jan-Feb, 2006).

29. D. Harman, Aging: a theory based on free radical and radiation chemistry. *Journal of gerontology* **11**, 298 (Jul, 1956).

30. I. Juranek, S. Bezek, Controversy of free radical hypothesis: reactive oxygen species--cause or consequence of tissue injury? *General physiology and biophysics* **24**, 263 (Sep, 2005).

31. M. F. Alexeyev, S. P. Ledoux, G. L. Wilson, Mitochondrial DNA and aging. *Clin Sci (Lond)* **107**, 355 (Oct, 2004).

32. J. Miquel, A. C. Economos, J. Fleming, J. E. Johnson, Jr., Mitochondrial role in cell aging. *Experimental gerontology* **15**, 575 (1980).

33. A. Hiona, C. Leeuwenburgh, The role of mitochondrial DNA mutations in aging and sarcopenia: implications for the mitochondrial vicious cycle theory of aging. *Experimental gerontology* **43**, 24 (Jan, 2008).

34. A. Sanz, P. Caro, J. Gomez, G. Barja, Testing the vicious cycle theory of mitochondrial ROS production: effects of H2O2 and cumene hydroperoxide treatment on heart mitochondria. *Journal of bioenergetics and biomembranes* **38**, 121 (Apr, 2006).

35. G. C. Kujoth *et al.*, Mitochondrial DNA mutations, oxidative stress, and apoptosis in mammalian aging. *Science* **309**, 481 (Jul 15, 2005).

36. A. Trifunovic *et al.*, Somatic mtDNA mutations cause aging phenotypes without affecting reactive oxygen species production. *Proceedings of the National Academy of Sciences of the United States of America* **102**, 17993 (Dec 13, 2005).

37. V. L. Dawson, T. M. Dawson, E. D. London, D. S. Bredt, S. H. Snyder, Nitric oxide mediates glutamate neurotoxicity in primary cortical cultures. *Proceedings of the National Academy of Sciences of the United States of America* **88**, 6368 (Jul 15, 1991).

38. M. A. Marletta, Nitric oxide synthase structure and mechanism. *The Journal of biological chemistry* **268**, 12231 (Jun 15, 1993).

39. C. F. Nathan, J. B. Hibbs, Jr., Role of nitric oxide synthesis in macrophage antimicrobial activity. *Current opinion in immunology* **3**, 65 (Feb, 1991).

40. J. S. Stamler, Redox signaling: nitrosylation and related target interactions of nitric oxide. *Cell* **78**, 931 (Sep 23, 1994).

41. J. S. Beckman, T. W. Beckman, J. Chen, P. A. Marshall, B. A. Freeman, Apparent hydroxyl radical production by peroxynitrite: implications for endothelial injury from nitric oxide and superoxide. *Proceedings of the National Academy of Sciences of the United States of America* **87**, 1620 (Feb, 1990).

42. S. A. Lipton *et al.*, A Redox-Based Mechanism for the Neuroprotective and Neurodestructive Effects of Nitric-Oxide and Related Nitroso-Compounds. *Nature* **364**, 626 (Aug 12, 1993).

43. T. Nakamura *et al.*, Aberrant protein s-nitrosylation in neurodegenerative diseases. *Neuron* **78**, 596 (May 22, 2013).

44. Y. B. Choi *et al.*, Molecular basis of NMDA receptor-coupled ion channel modulation by S-nitrosylation. *Nature neuroscience* **3**, 15 (Jan, 2000).

45. Z. Q. Shi *et al.*, S-nitrosylated SHP-2 contributes to NMDA receptor-mediated excitotoxicity in acute ischemic stroke. *Proceedings of the National Academy of Sciences of the United States of America* **110**, 3137 (Feb 19, 2013).

46. J. Garthwaite, S. L. Charles, R. Chess-Williams, Endothelium-derived relaxing factor release on activation of NMDA receptors suggests role as intercellular messenger in the brain. *Nature* **336**, 385 (Nov 24, 1988).

47. S. Z. Lei *et al.*, Effect of nitric oxide production on the redox modulatory site of the NMDA receptor-channel complex. *Neuron* **8**, 1087 (Jun, 1992).

48. S. L. Budd, L. Tenneti, T. Lishnak, S. A. Lipton, Mitochondrial and extramitochondrial apoptotic signaling pathways in cerebrocortical neurons. *Proceedings of the National Academy of Sciences of the United States of America* **97**, 6161 (May 23, 2000).

49. Q. L. Deveraux *et al.*, Cleavage of human inhibitor of apoptosis protein XIAP results in fragments with distinct specificities for caspases. *The EMBO journal* **18**, 5242 (Oct 1, 1999).

50. T. Nakamura *et al.*, Transnitrosylation of XIAP regulates caspase-dependent neuronal cell death. *Molecular cell* **39**, 184 (Jul 30, 2010).

51. L. Tenneti, D. M. D'Emilia, S. A. Lipton, Suppression of neuronal apoptosis by S-nitrosylation of caspases. *Neuroscience letters* **236**, 139 (Nov 7, 1997).

52. M. M. Lyles, H. F. Gilbert, Catalysis of the oxidative folding of ribonuclease A by protein disulfide isomerase: pre-steady-state kinetics and the utilization of the oxidizing equivalents of the isomerase. *Biochemistry* **30**, 619 (Jan 22, 1991).

53. T. Uehara *et al.*, S-nitrosylated protein-disulphide isomerase links protein misfolding to neurodegeneration. *Nature* **441**, 513 (May 25, 2006).

54. K. K. Chung *et al.*, S-nitrosylation of parkin regulates ubiquitination and compromises parkin's protective function. *Science* **304**, 1328 (May 28, 2004).

55. D. P. Narendra, R. J. Youle, Targeting mitochondrial dysfunction: role for PINK1 and Parkin in mitochondrial quality control. *Antioxidants & redox signaling* **14**, 1929 (May 15, 2011).

56. D. Yao *et al.*, Nitrosative stress linked to sporadic Parkinson's disease: S-nitrosylation of parkin regulates its E3 ubiquitin ligase activity. *Proceedings of the National Academy of Sciences of the United States of America* **101**, 10810 (Jul 20, 2004).

57. D. H. Cho *et al.*, S-nitrosylation of Drp1 mediates beta-amyloid-related mitochondrial fission and neuronal injury. *Science* **324**, 102 (Apr 3, 2009).

58. R. Sengupta, A. Holmgren, Thioredoxin and thioredoxin reductase in relation to reversible S-nitrosylation. *Antioxidants & redox signaling* **18**, 259 (Jan 20, 2013).

59. L. Liu *et al.*, Essential roles of S-nitrosothiols in vascular homeostasis and endotoxic shock. *Cell* **116**, 617 (Feb 20, 2004).

60. M. Benhar, M. T. Forrester, J. S. Stamler, Protein denitrosylation: enzymatic mechanisms and cellular functions. *Nature reviews. Molecular cell biology* **10**, 721 (Oct, 2009).

61. J. S. Paige, G. Xu, B. Stancevic, S. R. Jaffrey, Nitrosothiol reactivity profiling identifies S-nitrosylated proteins with unexpected stability. *Chemistry & biology* **15**, 1307 (Dec 22, 2008).

62. C. H. Lillig, A. Holmgren, Thioredoxin and related molecules--from biology to health and disease. *Antioxidants & redox signaling* **9**, 25 (Jan, 2007).

63. D. A. Stoyanovsky *et al.*, Thioredoxin and lipoic acid catalyze the denitrosation of low molecular weight and protein S-nitrosothiols. *Journal of the American Chemical Society* **127**, 15815 (Nov 16, 2005).

64. M. Benhar, M. T. Forrester, D. T. Hess, J. S. Stamler, Regulated protein denitrosylation by cytosolic and mitochondrial thioredoxins. *Science* **320**, 1050 (May 23, 2008).

65. M. Trujillo, M. N. Alvarez, G. Peluffo, B. A. Freeman, R. Radi, Xanthine oxidase-mediated decomposition of S-nitrosothiols. *The Journal of biological chemistry* **273**, 7828 (Apr 3, 1998).

66. C. B. Thompson, Apoptosis in the pathogenesis and treatment of disease. *Science* **267**, 1456 (Mar 10, 1995).

67. D. W. Choi, Excitotoxic cell death. *Journal of neurobiology* **23**, 1261 (Nov, 1992).

68. B. Hoffman, D. A. Liebermann, Molecular controls of apoptosis: differentiation/growth arrest primary response genes, proto-oncogenes, and tumor suppressor genes as positive & negative modulators. *Oncogene* **9**, 1807 (Jul, 1994).

69. R. E. Ellis, J. Y. Yuan, H. R. Horvitz, Mechanisms and functions of cell death. *Annual review of cell biology* **7**, 663 (1991).

70. A. Ashkenazi, V. M. Dixit, Death receptors: signaling and modulation. *Science* **281**, 1305 (Aug 28, 1998).

71. H. Y. Chang, X. Yang, Proteases for cell suicide: functions and regulation of caspases. *Microbiology and molecular biology reviews : MMBR* **64**, 821 (Dec, 2000).

72. C. Wang, R. J. Youle, The role of mitochondria in apoptosis*. *Annual review of genetics* **43**, 95 (2009).

73. J. J. Lemasters, Selective mitochondrial autophagy, or mitophagy, as a targeted defense against oxidative stress, mitochondrial dysfunction, and aging. *Rejuvenation research* **8**, 3 (Spring, 2005).

74. D. P. Narendra *et al.*, PINK1 is selectively stabilized on impaired mitochondria to activate Parkin. *PLoS biology* **8**, e1000298 (Jan, 2010).

75. I. E. Clark *et al.*, Drosophila pink1 is required for mitochondrial function and interacts genetically with parkin. *Nature* **441**, 1162 (Jun 29, 2006).

76. R. J. Youle, D. P. Narendra, Mechanisms of mitophagy. *Nature reviews. Molecular cell biology* **12**, 9 (Jan, 2011).

77. I. Kissova, M. Deffieu, S. Manon, N. Camougrand, Uth1p is involved in the autophagic degradation of mitochondria. *The Journal of biological chemistry* **279**, 39068 (Sep 10, 2004).

78. R. L. Schweers *et al.*, NIX is required for programmed mitochondrial clearance during reticulocyte maturation. *Proceedings of the National Academy of Sciences of the United States of America* **104**, 19500 (Dec 4, 2007).

79. J. K. Ngo, K. J. Davies, Importance of the lon protease in mitochondrial maintenance and the significance of declining lon in aging. *Annals of the New York Academy of Sciences* **1119**, 78 (Nov, 2007).

80. S. G. Kang *et al.*, Functional proteolytic complexes of the human mitochondrial ATP-dependent protease, hClpXP. *The Journal of biological chemistry* **277**, 21095 (Jun 7, 2002).

81. D. Korbel, S. Wurth, M. Kaser, T. Langer, Membrane protein turnover by the m-AAA protease in mitochondria depends on the transmembrane domains of its subunits. *EMBO reports* **5**, 698 (Jul, 2004).

82. T. Tatsuta, T. Langer, Quality control of mitochondria: protection against neurodegeneration and ageing. *The EMBO journal* **27**, 306 (Jan 23, 2008).

83. E. Reinstein, A. Ciechanover, Narrative review: protein degradation and human diseases: the ubiquitin connection. *Annals of internal medicine* **145**, 676 (Nov 7, 2006).

84. M. H. Glickman, A. Ciechanover, The ubiquitin-proteasome proteolytic pathway: destruction for the sake of construction. *Physiological reviews* **82**, 373 (Apr, 2002).

85. E. B. Taylor, J. Rutter, Mitochondrial quality control by the ubiquitin-proteasome system. *Biochemical Society transactions* **39**, 1509 (Oct, 2011).

86. D. Chhangani, A. P. Joshi, A. Mishra, E3 ubiquitin ligases in protein quality control mechanism. *Molecular neurobiology* **45**, 571 (Jun, 2012).

87. N. Livnat-Levanon, M. H. Glickman, Ubiquitin-proteasome system and mitochondria - reciprocity. *Biochimica et biophysica acta* **1809**, 80 (Feb, 2011).

88. I. Amm, T. Sommer, D. H. Wolf, Protein quality control and elimination of protein waste: The role of the ubiquitin-proteasome system. *Biochimica et biophysica acta*, (Jul 10, 2013).

89. S. Zhao, H. D. Ulrich, Distinct consequences of posttranslational modification by linear versus K63-linked polyubiquitin chains. *Proceedings of the National Academy of Sciences of the United States of America* **107**, 7704 (Apr 27, 2010).

90. A. Williamson *et al.*, Identification of a physiological E2 module for the human anaphase-promoting complex. *Proceedings of the National Academy of Sciences of the United States of America* **106**, 18213 (Oct 27, 2009).

91. M. Neutzner, A. Neutzner, Enzymes of ubiquitination and deubiquitination. *Essays in biochemistry* **52**, 37 (2012).

92. C. M. Pickart, Mechanisms underlying ubiquitination. *Annual review of biochemistry* **70**, 503 (2001).

93. J. M. Huibregtse, M. Scheffner, S. Beaudenon, P. M. Howley, A family of proteins structurally and functionally related to the E6-AP ubiquitin-protein ligase. *Proceedings of the National Academy of Sciences of the United States of America* **92**, 5249 (May 23, 1995).

94. M. Scheffner, U. Nuber, J. M. Huibregtse, Protein ubiquitination involving an E1-E2-E3 enzyme ubiquitin thioester cascade. *Nature* **373**, 81 (Jan 5, 1995).

95. P. S. Freemont, I. M. Hanson, J. Trowsdale, A novel cysteine-rich sequence motif. *Cell* **64**, 483 (Feb 8, 1991).

96. C. A. Joazeiro, A. M. Weissman, RING finger proteins: mediators of ubiquitin ligase activity. *Cell* **102**, 549 (Sep 1, 2000).

97. R. J. Deshaies, C. A. Joazeiro, RING domain E3 ubiquitin ligases. *Annual review of biochemistry* **78**, 399 (2009).

98. E. Ozkan, H. Yu, J. Deisenhofer, Mechanistic insight into the allosteric activation of a ubiquitin-conjugating enzyme by RING-type ubiquitin ligases. *Proceedings of the National Academy of Sciences of the United States of America* **102**, 18890 (Dec 27, 2005).

99. M. Ohmura-Hoshino *et al.*, A novel family of membrane-bound E3 ubiquitin ligases. *Journal of biochemistry* **140**, 147 (Aug, 2006).

100. M. B. Metzger, J. N. Pruneda, R. E. Klevit, A. M. Weissman, RING-type E3 ligases: Master manipulators of E2 ubiquitin-conjugating enzymes and ubiquitination. *Biochimica et biophysica acta*, (Jun 6, 2013).

101. A. Schreiber *et al.*, Structural basis for the subunit assembly of the anaphase-promoting complex. *Nature* **470**, 227 (Feb 10, 2011).

102. M. Tyers, P. Jorgensen, Proteolysis and the cell cycle: with this RING I do thee destroy. *Current opinion in genetics & development* **10**, 54 (Feb, 2000).

103. A. Neutzner, R. J. Youle, M. Karbowski, Outer mitochondrial membrane protein degradation by the proteasome. *Novartis Foundation symposium* **287**, 4 (2007).

104. E. Braschi, R. Zunino, H. M. McBride, MAPL is a new mitochondrial SUMO E3 ligase that regulates mitochondrial fission. *EMBO reports* **10**, 748 (Jul, 2009).

105. M. Karbowski, A. Neutzner, R. J. Youle, The mitochondrial E3 ubiquitin ligase MARCH5 is required for Drp1 dependent mitochondrial division. *The Journal of cell biology* **178**, 71 (Jul 2, 2007).

106. G. Benard *et al.*, IBRDC2, an IBR-type E3 ubiquitin ligase, is a regulatory factor for Bax and apoptosis activation. *The EMBO journal* **29**, 1458 (Apr 21, 2010).

107. M. Karbowski, R. J. Youle, Regulating mitochondrial outer membrane proteins by ubiquitination and proteasomal degradation. *Current opinion in cell biology* **23**, 476 (Aug, 2011).

108. S. S. Vembar, J. L. Brodsky, One step at a time: endoplasmic reticulum-associated degradation. *Nature reviews. Molecular cell biology* **9**, 944 (Dec, 2008).

109. J. Bordallo, R. K. Plemper, A. Finger, D. H. Wolf, Der3p/Hrd1p is required for endoplasmic reticulum-associated degradation of misfolded lumenal and integral membrane proteins. *Molecular biology of the cell* **9**, 209 (Jan, 1998).

110. V. Denic, E. M. Quan, J. S. Weissman, A luminal surveillance complex that selects misfolded glycoproteins for ER-associated degradation. *Cell* **126**, 349 (Jul 28, 2006).

111. Y. Ye, H. H. Meyer, T. A. Rapoport, The AAA ATPase Cdc48/p97 and its partners transport proteins from the ER into the cytosol. *Nature* **414**, 652 (Dec 6, 2001).

112. J. S. Bonifacino, A. M. Weissman, Ubiquitin and the control of protein fate in the secretory and endocytic pathways. *Annual review of cell and developmental biology* **14**, 19 (1998).

113. R. Yonashiro *et al.*, A novel mitochondrial ubiquitin ligase plays a critical role in mitochondrial dynamics. *The EMBO journal* **25**, 3618 (Aug 9, 2006).

114. V. Azzu, M. D. Brand, Degradation of an intramitochondrial protein by the cytosolic proteasome. *Journal of cell science* **123**, 578 (Feb 15, 2010).

115. Q. Zhong, W. Gao, F. Du, X. Wang, Mule/ARF-BP1, a BH3-only E3 ubiquitin ligase, catalyzes the polyubiquitination of Mcl-1 and regulates apoptosis. *Cell* **121**, 1085 (Jul 1, 2005).

116. M. P. Yaffe, Dynamic mitochondria. *Nature cell biology* **1**, E149 (Oct, 1999).

117. B. Westermann, Molecular machinery of mitochondrial fusion and fission. *The Journal of biological chemistry* **283**, 13501 (May 16, 2008).

118. V. P. Skulachev, Mitochondrial filaments and clusters as intracellular power-transmitting cables. *Trends in biochemical sciences* **26**, 23 (Jan, 2001).

119. G. Szabadkai *et al.*, Mitochondrial dynamics and Ca2+ signaling. *Biochimica et biophysica acta* **1763**, 442 (May-Jun, 2006).

120. R. S. Balaban, S. Nemoto, T. Finkel, Mitochondria, oxidants, and aging. *Cell* **120**, 483 (Feb 25, 2005).

121. D. C. Chan, Mitochondria: dynamic organelles in disease, aging, and development. *Cell* **125**, 1241 (Jun 30, 2006).

122. H. Chen, D. C. Chan, Physiological functions of mitochondrial fusion. *Annals of the New York Academy of Sciences* **1201**, 21 (Jul, 2010).

123. S. J. Park *et al.*, Mitochondrial fragmentation caused by phenanthroline promotes mitophagy. *FEBS letters* **586**, 4303 (Dec 14, 2012).

124. S. Frank *et al.*, The role of dynamin-related protein 1, a mediator of mitochondrial fission, in apoptosis. *Developmental cell* **1**, 515 (Oct, 2001).

125. T. Weber *et al.*, SNAREpins: minimal machinery for membrane fusion. *Cell* **92**, 759 (Mar 20, 1998).

126. K. G. Hales, M. T. Fuller, Developmentally regulated mitochondrial fusion mediated by a conserved, novel, predicted GTPase. *Cell* **90**, 121 (Jul 11, 1997).

127. H. Sesaki, R. E. Jensen, Ugo1p links the Fzo1p and Mgm1p GTPases for mitochondrial fusion. *The Journal of biological chemistry* **279**, 28298 (Jul 2, 2004).

128. S. Fritz, N. Weinbach, B. Westermann, Mdm30 is an F-box protein required for maintenance of fusion-competent mitochondria in yeast. *Molecular biology of the cell* **14**, 2303 (Jun, 2003).

129. E. E. Griffin, S. A. Detmer, D. C. Chan, Molecular mechanism of mitochondrial membrane fusion. *Biochimica et biophysica acta* **1763**, 482 (May-Jun, 2006).

130. M. Ranieri *et al.*, Mitochondrial fusion proteins and human diseases. *Neurology research international* **2013**, 293893 (2013).

131. A. Santel, M. T. Fuller, Control of mitochondrial morphology by a human mitofusin. *Journal of cell science* **114**, 867 (Mar, 2001).

132. S. Meeusen, J. M. McCaffery, J. Nunnari, Mitochondrial fusion intermediates revealed in vitro. *Science* **305**, 1747 (Sep 17, 2004).

133. T. Koshiba *et al.*, Structural basis of mitochondrial tethering by mitofusin complexes. *Science* **305**, 858 (Aug 6, 2004).

134. N. Ishihara, Y. Eura, K. Mihara, Mitofusin 1 and 2 play distinct roles in mitochondrial fusion reactions via GTPase activity. *Journal of cell science* **117**, 6535 (Dec 15, 2004).

135. M. Rojo, F. Legros, D. Chateau, A. Lombes, Membrane topology and mitochondrial targeting of mitofusins, ubiquitous mammalian homologs of the transmembrane GTPase Fzo. *Journal of cell science* **115**, 1663 (Apr 15, 2002).

136. B. Westermann, Mitochondrial membrane fusion. *Biochimica et biophysica acta* **1641**, 195 (Aug 18, 2003).

137. O. M. de Brito, L. Scorrano, Mitofusin 2 tethers endoplasmic reticulum to mitochondria. *Nature* **456**, 605 (Dec 4, 2008).

138. F. Anton *et al.*, Ugo1 and Mdm30 act sequentially during Fzo1-mediated mitochondrial outer membrane fusion. *Journal of cell science* **124**, 1126 (Apr 1, 2011).

139. M. M. Cohen *et al.*, Sequential requirements for the GTPase domain of the mitofusin Fzo1 and the ubiquitin ligase SCFMdm30 in mitochondrial outer membrane fusion. *Journal of cell science* **124**, 1403 (May 1, 2011).

140. P. Belenguer, L. Pellegrini, The dynamin GTPase OPA1: more than mitochondria? *Biochimica et biophysica acta* **1833**, 176 (Jan, 2013).

141. C. Delettre *et al.*, Mutation spectrum and splicing variants in the OPA1 gene. *Human genetics* **109**, 584 (Dec, 2001).

142. V. R. Akepati *et al.*, Characterization of OPA1 isoforms isolated from mouse tissues. *Journal of neurochemistry* **106**, 372 (Jul, 2008).

143. L. Griparic, T. Kanazawa, A. M. van der Bliek, Regulation of the mitochondrial dynamin-like protein Opa1 by proteolytic cleavage. *The Journal of cell biology* **178**, 757 (Aug 27, 2007).

144. O. Guillery *et al.*, Metalloprotease-mediated OPA1 processing is modulated by the mitochondrial membrane potential. *Biology of the cell / under the auspices of the European Cell Biology Organization* **100**, 315 (May, 2008).

145. B. Head, L. Griparic, M. Amiri, S. Gandre-Babbe, A. M. van der Bliek, Inducible proteolytic inactivation of OPA1 mediated by the OMA1 protease in mammalian cells. *The Journal of cell biology* **187**, 959 (Dec 28, 2009).

146. S. Ehses *et al.*, Regulation of OPA1 processing and mitochondrial fusion by m-AAA protease isoenzymes and OMA1. *The Journal of cell biology* **187**, 1023 (Dec 28, 2009).

147. S. Cipolat, O. Martins de Brito, B. Dal Zilio, L. Scorrano, OPA1 requires mitofusin 1 to promote mitochondrial fusion. *Proceedings of the National Academy of Sciences of the United States of America* **101**, 15927 (Nov 9, 2004).

148. L. Griparic, N. N. van der Wel, I. J. Orozco, P. J. Peters, A. M. van der Bliek, Loss of the intermembrane space protein Mgm1/OPA1 induces swelling and localized constrictions along the lengths of mitochondria. *The Journal of biological chemistry* **279**, 18792 (Apr 30, 2004).

149. A. Olichon *et al.*, Loss of OPA1 perturbates the mitochondrial inner membrane structure and integrity, leading to cytochrome c release and apoptosis. *The Journal of biological chemistry* **278**, 7743 (Mar 7, 2003).

150. C. Frezza *et al.*, OPA1 controls apoptotic cristae remodeling independently from mitochondrial fusion. *Cell* **126**, 177 (Jul 14, 2006).

151. W. Bleazard *et al.*, The dynamin-related GTPase Dnm1 regulates mitochondrial fission in yeast. *Nature cell biology* **1**, 298 (Sep, 1999).

152. E. Smirnova, D. L. Shurland, S. N. Ryazantsev, A. M. van der Bliek, A human dynamin-related protein controls the distribution of mitochondria. *The Journal of cell biology* **143**, 351 (Oct 19, 1998).

153. S. M. Ferguson, P. De Camilli, Dynamin, a membrane-remodelling GTPase. *Nature reviews. Molecular cell biology* **13**, 75 (Feb, 2012).

154. Y. J. Lee, S. Y. Jeong, M. Karbowski, C. L. Smith, R. J. Youle, Roles of the mammalian mitochondrial fission and fusion mediators Fis1, Drp1, and Opa1 in apoptosis. *Molecular biology of the cell* **15**, 5001 (Nov, 2004).

155. E. Bossy-Wetzel, M. J. Barsoum, A. Godzik, R. Schwarzenbacher, S. A. Lipton, Mitochondrial fission in apoptosis, neurodegeneration and aging. *Current opinion in cell biology* **15**, 706 (Dec, 2003).

156. A. D. Mozdy, J. M. McCaffery, J. M. Shaw, Dnm1p GTPase-mediated mitochondrial fission is a multi-step process requiring the novel integral membrane component Fis1p. *The Journal of cell biology* **151**, 367 (Oct 16, 2000).

157. D. C. Chan, Fusion and fission: interlinked processes critical for mitochondrial health. *Annual review of genetics* **46**, 265 (2012).

158. R. C. Wells, L. K. Picton, S. C. Williams, F. J. Tan, R. B. Hill, Direct binding of the dynamin-like GTPase, Dnm1, to mitochondrial dynamics protein Fis1 is negatively regulated by the Fis1 N-terminal arm. *The Journal of biological chemistry* **282**, 33769 (Nov 16, 2007).

159. S. Gandre-Babbe, A. M. van der Bliek, The novel tail-anchored membrane protein Mff controls mitochondrial and peroxisomal fission in mammalian cells. *Molecular biology of the cell* **19**, 2402 (Jun, 2008).

160. H. Otera *et al.*, Mff is an essential factor for mitochondrial recruitment of Drp1 during mitochondrial fission in mammalian cells. *The Journal of cell biology* **191**, 1141 (Dec 13, 2010).

161. C. S. Palmer *et al.*, MiD49 and MiD51, new components of the mitochondrial fission machinery. *EMBO reports* **12**, 565 (Jun, 2011).

162. O. C. Loson, Z. Song, H. Chen, D. C. Chan, Fis1, Mff, MiD49, and MiD51 mediate Drp1 recruitment in mitochondrial fission. *Molecular biology of the cell* **24**, 659 (Mar, 2013).

163. X. J. Han *et al.*, CaM kinase I alpha-induced phosphorylation of Drp1 regulates mitochondrial morphology. *The Journal of cell biology* **182**, 573 (Aug 11, 2008).

164. W. Wang *et al.*, Mitochondrial fission triggered by hyperglycemia is mediated by ROCK1 activation in podocytes and endothelial cells. *Cell metabolism* **15**, 186 (Feb 8, 2012).

165. I. R. Boldogh, H. C. Yang, L. A. Pon, Mitochondrial inheritance in budding yeast. *Traffic* **2**, 368 (Jun, 2001).

166. J. H. Wu *et al.*, RNAi screening identifies GSK3beta as a regulator of DRP1 and the neuroprotection of lithium chloride against elevated pressure involved in downregulation of DRP1. *Neuroscience letters* **554**, 99 (Oct 25, 2013).

167. J. D. Wikstrom *et al.*, AMPK regulates ER morphology and function in stressed pancreatic beta-cells via phosphorylation of DRP1. *Mol Endocrinol* **27**, 1706 (Oct, 2013).

168. G. M. Cereghetti *et al.*, Dephosphorylation by calcineurin regulates translocation of Drp1 to mitochondria. *Proceedings of the National Academy of Sciences of the United States of America* **105**, 15803 (Oct 14, 2008).

169. H. Wang *et al.*, Parkin ubiquitinates Drp1 for proteasome-dependent degradation: implication of dysregulated mitochondrial dynamics in Parkinson disease. *The Journal of biological chemistry* **286**, 11649 (Apr 1, 2011).

170. Z. Harder, R. Zunino, H. McBride, Sumo1 conjugates mitochondrial substrates and participates in mitochondrial fission. *Current biology : CB* **14**, 340 (Feb 17, 2004).

171. R. Zunino, A. Schauss, P. Rippstein, M. Andrade-Navarro, H. M. McBride, The SUMO protease SENP5 is required to maintain mitochondrial morphology and function. *Journal of cell science* **120**, 1178 (Apr 1, 2007).

172. S. Frank, Dysregulation of mitochondrial fusion and fission: an emerging concept in neurodegeneration. *Acta neuropathologica* **111**, 93 (Feb, 2006).

173. M. Karbowski *et al.*, Quantitation of mitochondrial dynamics by photolabeling of individual organelles shows that mitochondrial fusion is blocked during the Bax activation phase of apoptosis. *The Journal of cell biology* **164**, 493 (Feb 16, 2004).

174. E. A. Schon, S. Przedborski, Mitochondria: the next (neurode)generation. *Neuron* **70**, 1033 (Jun 23, 2011).

175. H. M. McBride, M. Neuspiel, S. Wasiak, Mitochondria: more than just a powerhouse. *Current biology : CB* **16**, R551 (Jul 25, 2006).

176. A. B. Knott, E. Bossy-Wetzel, Impairing the mitochondrial fission and fusion balance: a new mechanism of neurodegeneration. *Annals of the New York Academy of Sciences* **1147**, 283 (Dec, 2008).

177. M. H. Yan, X. Wang, X. Zhu, Mitochondrial defects and oxidative stress in Alzheimer disease and Parkinson disease. *Free radical biology & medicine* **62**, 90 (Sep, 2013).

178. V. Campuzano *et al.*, Friedreich's ataxia: autosomal recessive disease caused by an intronic GAA triplet repeat expansion. *Science* **271**, 1423 (Mar 8, 1996).

179. P. Gonzalez-Cabo, F. Palau, Mitochondrial pathophysiology in Friedreich's ataxia. *Journal of neurochemistry* **126 Suppl 1**, 53 (Aug, 2013).

180. D. C. Wallace *et al.*, Mitochondrial DNA mutation associated with Leber's hereditary optic neuropathy. *Science* **242**, 1427 (Dec 9, 1988).

181. V. Carelli, F. N. Ross-Cisneros, A. A. Sadun, Mitochondrial dysfunction as a cause of optic neuropathies. *Progress in retinal and eye research* **23**, 53 (Jan, 2004).

182. E. Kirches, LHON: Mitochondrial Mutations and More. *Current genomics* **12**, 44 (Mar, 2011).

183. J. A. Fraser, V. Biousse, N. J. Newman, The neuro-ophthalmology of mitochondrial disease. *Survey of ophthalmology* **55**, 299 (Jul-Aug, 2010).

184. Q. Li *et al.*, ALS-linked mutant superoxide dismutase 1 (SOD1) alters mitochondrial protein composition and decreases protein import. *Proceedings of the National Academy of Sciences of the United States of America* **107**, 21146 (Dec 7, 2010).

185. P. Shi, J. Gal, D. M. Kwinter, X. Liu, H. Zhu, Mitochondrial dysfunction in amyotrophic lateral sclerosis. *Biochimica et biophysica acta* **1802**, 45 (Jan, 2010).

186. M. Karbowski, A. Neutzner, Neurodegeneration as a consequence of failed mitochondrial maintenance. *Acta neuropathologica* **123**, 157 (Feb, 2012).

187. R. Yonashiro *et al.*, Mitochondrial ubiquitin ligase MITOL ubiquitinates mutant SOD1 and attenuates mutant SOD1-induced reactive oxygen species generation. *Molecular biology of the cell* **20**, 4524 (Nov, 2009).

188. A. Sugiura *et al.*, A mitochondrial ubiquitin ligase MITOL controls cell toxicity of polyglutamine-expanded protein. *Mitochondrion* **11**, 139 (Jan, 2011).

189. E. M. Valente *et al.*, Hereditary early-onset Parkinson's disease caused by mutations in PINK1. *Science* **304**, 1158 (May 21, 2004).

190. J. Park *et al.*, Mitochondrial dysfunction in Drosophila PINK1 mutants is complemented by parkin. *Nature* **441**, 1157 (Jun 29, 2006).

191. A. C. Poole, R. E. Thomas, S. Yu, E. S. Vincow, L. Pallanck, The mitochondrial fusion-promoting factor mitofusin is a substrate of the PINK1/parkin pathway. *PloS one* **5**, e10054 (2010).

192. C. Delettre *et al.*, Nuclear gene OPA1, encoding a mitochondrial dynamin-related protein, is mutated in dominant optic atrophy. *Nature genetics* **26**, 207 (Oct, 2000).

193. C. Zanna *et al.*, OPA1 mutations associated with dominant optic atrophy impair oxidative phosphorylation and mitochondrial fusion. *Brain : a journal of neurology* **131**, 352 (Feb, 2008).

194. L. Chen, Q. Gong, J. P. Stice, A. A. Knowlton, Mitochondrial OPA1, apoptosis, and heart failure. *Cardiovascular research* **84**, 91 (Oct 1, 2009).

195. S. Zuchner *et al.*, Mutations in the mitochondrial GTPase mitofusin 2 cause Charcot-Marie-Tooth neuropathy type 2A. *Nature genetics* **36**, 449 (May, 2004).

196. K. W. Chung *et al.*, Early onset severe and late-onset mild Charcot-Marie-Tooth disease with mitofusin 2 (MFN2) mutations. *Brain : a journal of neurology* **129**, 2103 (Aug, 2006).

197. H. R. Waterham *et al.*, A lethal defect of mitochondrial and peroxisomal fission. *The New England journal of medicine* **356**, 1736 (Apr 26, 2007).

198. C. T. Chung, S. L. Niemela, R. H. Miller, One-step preparation of competent Escherichia coli: transformation and storage of bacterial cells in the same solution. *Proceedings of the National Academy of Sciences of the United States of America* **86**, 2172 (Apr, 1989).

199. K. Mullis *et al.*, Specific enzymatic amplification of DNA in vitro: the polymerase chain reaction. *Cold Spring Harbor symposia on quantitative biology* **51 Pt 1**, 263 (1986).

200. U. K. Laemmli, Cleavage of structural proteins during the assembly of the head of bacteriophage T4. *Nature* **227**, 680 (Aug 15, 1970).

201. H. Towbin, T. Staehelin, J. Gordon, Electrophoretic transfer of proteins from polyacrylamide gels to nitrocellulose sheets: procedure and some applications. *Proceedings of the National Academy of Sciences of the United States of America* **76**, 4350 (Sep, 1979).

202. A. Neutzner *et al.*, A systematic search for endoplasmic reticulum (ER) membrane-associated RING finger proteins identifies Nixin/ZNRF4 as a regulator of calnexin stability and ER homeostasis. *The Journal of biological chemistry* **286**, 8633 (Mar 11, 2011).

203. L. Su, N. Lineberry, Y. Huh, L. Soares, C. G. Fathman, A novel E3 ubiquitin ligase substrate screen identifies Rho guanine dissociation inhibitor as a substrate of gene related to anergy in lymphocytes. *J Immunol* **177**, 7559 (Dec 1, 2006).

204. Y. Fukumoto *et al.*, Cost-effective gene transfection by DNA compaction at pH 4.0 using acidified, long shelf-life polyethylenimine. *Cytotechnology* **62**, 73 (Jan, 2010).

205. M. M. Bradford, A rapid and sensitive method for the quantitation of microgram quantities of protein utilizing the principle of protein-dye binding. *Analytical biochemistry* **72**, 248 (May 7, 1976).

206. S. R. Jaffrey, H. Erdjument-Bromage, C. D. Ferris, P. Tempst, S. H. Snyder, Protein S-nitrosylation: a physiological signal for neuronal nitric oxide. *Nature cell biology* **3**, 193 (Feb, 2001).

207. K. L. Lorick *et al.*, RING fingers mediate ubiquitin-conjugating enzyme (E2)-dependent ubiquitination. *Proceedings of the National Academy of Sciences of the United States of America* **96**, 11364 (Sep 28, 1999).

208. Y. Amemiya, P. Azmi, A. Seth, Autoubiquitination of BCA2 RING E3 ligase regulates its own stability and affects cell migration. *Molecular cancer research : MCR* **6**, 1385 (Sep, 2008).

209. G. Hassink *et al.*, TEB4 is a C4HC3 RING finger-containing ubiquitin ligase of the endoplasmic reticulum. *The Biochemical journal* **388**, 647 (Jun 1, 2005).

210. J. D. Etlinger, A. L. Goldberg, A soluble ATP-dependent proteolytic system responsible for the degradation of abnormal proteins in reticulocytes. *Proceedings of the National Academy of Sciences of the United States of America* **74**, 54 (Jan, 1977).

211. N. Matsuda, T. Suzuki, K. Tanaka, A. Nakano, Rma1, a novel type of RING finger protein conserved from Arabidopsis to human, is a membrane-bound ubiquitin ligase. *Journal of cell science* **114**, 1949 (May, 2001).

212. L. Shargorodsky *et al.*, The nitric oxide donor sodium nitroprusside requires the 18 kDa Translocator Protein to induce cell death. *Apoptosis : an international journal on programmed cell death* **17**, 647 (Jul, 2012).

213. K. Kita, T. Suzuki, T. Ochi, Diphenylarsinic acid promotes degradation of glutaminase C by mitochondrial Lon protease. *The Journal of biological chemistry* **287**, 18163 (May 25, 2012).

214. K. Gilmore, M. Wilson, The use of chloromethyl-X-rosamine (Mitotracker red) to measure loss of mitochondrial membrane potential in apoptotic cells is incompatible with cell fixation. *Cytometry* **36**, 355 (Aug 1, 1999).

215. R. M. Kluck, E. Bossy-Wetzel, D. R. Green, D. D. Newmeyer, The release of cytochrome c from mitochondria: a primary site for Bcl-2 regulation of apoptosis. *Science* **275**, 1132 (Feb 21, 1997).

216. Y. Ye, H. H. Meyer, T. A. Rapoport, Function of the p97-Ufd1-Npl4 complex in retrotranslocation from the ER to the cytosol: dual recognition of nonubiquitinated

polypeptide segments and polyubiquitin chains. *The Journal of cell biology* **162**, 71 (Jul 7, 2003).

217. N. P. Dantuma, K. Lindsten, R. Glas, M. Jellne, M. G. Masucci, Short-lived green fluorescent proteins for quantifying ubiquitin/proteasome-dependent proteolysis in living cells. *Nature biotechnology* **18**, 538 (May, 2000).

218. H. D. Osiewacz, D. Bernhardt, Mitochondrial quality control: impact on aging and life span - a mini-review. *Gerontology* **59**, 413 (2013).

219. A. M. van der Bliek, Q. Shen, S. Kawajiri, Mechanisms of mitochondrial fission and fusion. *Cold Spring Harbor perspectives in biology* **5**, (Jun, 2013).

220. W. Li *et al.*, Genome-wide and functional annotation of human E3 ubiquitin ligases identifies MULAN, a mitochondrial E3 that regulates the organelle's dynamics and signaling. *PloS one* **3**, e1487 (2008).

221. M. H. Smith, H. L. Ploegh, J. S. Weissman, Road to ruin: targeting proteins for degradation in the endoplasmic reticulum. *Science* **334**, 1086 (Nov 25, 2011).

222. M. Kikkert *et al.*, Human HRD1 is an E3 ubiquitin ligase involved in degradation of proteins from the endoplasmic reticulum. *The Journal of biological chemistry* **279**, 3525 (Jan 30, 2004).

223. S. Jentsch, S. Rumpf, Cdc48 (p97): a "molecular gearbox" in the ubiquitin pathway? *Trends in biochemical sciences* **32**, 6 (Jan, 2007).

224. C. Hirsch, R. Gauss, S. C. Horn, O. Neuber, T. Sommer, The ubiquitylation machinery of the endoplasmic reticulum. *Nature* **458**, 453 (Mar 26, 2009).

225. S. Xu, G. Peng, Y. Wang, S. Fang, M. Karbowski, The AAA-ATPase p97 is essential for outer mitochondrial membrane protein turnover. *Molecular biology of the cell* **22**, 291 (Feb 1, 2011).

226. A. M. Weissman, N. Shabek, A. Ciechanover, The predator becomes the prey: regulating the ubiquitin system by ubiquitylation and degradation. *Nature reviews. Molecular cell biology* **12**, 605 (Sep, 2011).

227. S. Fang, A. M. Weissman, A field guide to ubiquitylation. *Cellular and molecular life sciences : CMLS* **61**, 1546 (Jul, 2004).

228. R. Friedlander, E. Jarosch, J. Urban, C. Volkwein, T. Sommer, A regulatory link between ER-associated protein degradation and the unfolded-protein response. *Nature cell biology* **2**, 379 (Jul, 2000).

229. E. Jarosch *et al.*, Protein dislocation from the ER requires polyubiquitination and the AAA-ATPase Cdc48. *Nature cell biology* **4**, 134 (Feb, 2002).

230. Y. Sheng *et al.*, A human ubiquitin conjugating enzyme (E2)-HECT E3 ligase structure-function screen. *Molecular & cellular proteomics : MCP* **11**, 329 (Aug, 2012).

231. H. Yu, P. M. Kim, E. Sprecher, V. Trifonov, M. Gerstein, The importance of bottlenecks in protein networks: correlation with gene essentiality and expression dynamics. *PLoS computational biology* **3**, e59 (Apr 20, 2007).

232. G. P. Leboucher *et al.*, Stress-induced phosphorylation and proteasomal degradation of mitofusin 2 facilitates mitochondrial fragmentation and apoptosis. *Molecular cell* **47**, 547 (Aug 24, 2012).

233. X. Liu, D. Weaver, O. Shirihai, G. Hajnoczky, Mitochondrial 'kiss-and-run': interplay between mitochondrial motility and fusion-fission dynamics. *The EMBO journal* **28**, 3074 (Oct 21, 2009).

234. P. J. Lehner, S. Hoer, R. Dodd, L. M. Duncan, Downregulation of cell surface receptors by the K3 family of viral and cellular ubiquitin E3 ligases. *Immunological reviews* **207**, 112 (Oct, 2005).

235. H. X. Shi *et al.*, Mitochondrial ubiquitin ligase MARCH5 promotes TLR7 signaling by attenuating TANK action. *PLoS pathogens* **7**, e1002057 (May, 2011).

236. B. van de Kooij *et al.*, Ubiquitination by the membrane-associated RING-CH-8 (MARCH-8) ligase controls steady-state cell surface expression of tumor necrosis factor-related apoptosis inducing ligand (TRAIL) receptor 1. *The Journal of biological chemistry* **288**, 6617 (Mar 1, 2013).

237. M. Jahnke, J. Trowsdale, A. P. Kelly, Ubiquitination of HLA-DO by MARCH family E3 ligases. *European journal of immunology* **43**, 1153 (Apr, 2013).

238. I. Scott, Mitochondrial factors in the regulation of innate immunity. *Microbes and infection / Institut Pasteur* **11**, 729 (Jul-Aug, 2009).

239. C. B. Moore *et al.*, NLRX1 is a regulator of mitochondrial antiviral immunity. *Nature* **451**, 573 (Jan 31, 2008).

240. M. W. Foster, D. T. Hess, J. S. Stamler, Protein S-nitrosylation in health and disease: a current perspective. *Trends in molecular medicine* **15**, 391 (Sep, 2009).

241. V. Calabrese *et al.*, Nitric oxide in cell survival: a janus molecule. *Antioxidants & redox signaling* **11**, 2717 (Nov, 2009).

242. T. E. Bates, A. Loesch, G. Burnstock, J. B. Clark, Immunocytochemical evidence for a mitochondrially located nitric oxide synthase in brain and liver. *Biochemical and biophysical research communications* **213**, 896 (Aug 24, 1995).

243. P. Ghafourifar, M. S. Parihar, R. Nazarewicz, W. J. Zenebe, A. Parihar, Detection assays for determination of mitochondrial nitric oxide synthase activity; advantages and limitations. *Methods in enzymology* **440**, 317 (2008).

244. J. R. Lancaster, Jr., A tutorial on the diffusibility and reactivity of free nitric oxide. *Nitric oxide : biology and chemistry / official journal of the Nitric Oxide Society* **1**, 18 (Feb, 1997).

245. T. Nakamura, S. A. Lipton, Cell death: protein misfolding and neurodegenerative diseases. *Apoptosis : an international journal on programmed cell death* **14**, 455 (Apr, 2009).

246. N. C. Chan *et al.*, Broad activation of the ubiquitin-proteasome system by Parkin is critical for mitophagy. *Human molecular genetics* **20**, 1726 (May 1, 2011).

247. K. Ozawa *et al.*, S-nitrosylation regulates mitochondrial quality control via activation of parkin. *Scientific reports* **3**, 2202 (2013).

248. R. Yonashiro *et al.*, Mitochondrial ubiquitin ligase MITOL blocks S-nitrosylated MAP1B-light chain 1-mediated mitochondrial dysfunction and neuronal cell death. *Proceedings of the National Academy of Sciences of the United States of America* **109**, 2382 (Feb 14, 2012).

249. M. R. Kapadia, J. W. Eng, Q. Jiang, D. A. Stoyanovsky, M. R. Kibbe, Nitric oxide regulates the 26S proteasome in vascular smooth muscle cells. *Nitric oxide : biology and chemistry / official journal of the Nitric Oxide Society* **20**, 279 (Jun, 2009).

Curriculum Vitae

Anne-Sophie Benischke

PERSONAL DETAILS

Name: Anne-Sophie Benischke
Address: CH 4054 Basel, Tiergartenrain 1
Date of Birth: 01.12.1983
Nationality: Swiss and Austrian
Mobile: 0041 78 830 37 23
Mail: anne-sophie.benischke@hotmail.com

EDUCATION

01/2010 – present	PhD student in Medical-Biological Research, Department of Biomedicine, Ocular Pharmacology and Physiology, University of Basel Supervisor: PD Dr. Albert Neutzner <u>Thesis title</u>: Ubiquitin-proteasome dependent mitochondrial protein quality control
08/2007 – 08/2009	Master of Science in Pharmacy, University of Basel Federal Diploma for Pharmacists
10/2004 – 08/2007	Bachelor of Science in Pharmaceutical Sciences, University of Basel
08/1998 – 07/2004	High School Diploma, Humanistisches Gymnasium, Typ A, Basel

WORKING EXPERIENCE

09/2011 – present	Part time pharmacist, emergency pharmacy Basel
09/2008 – 06/2009	Assistantship, pharmacy Amavita Stadelhofen Zürich
07/2005 – 07/2007	Pharmafocus Basel

LABORATORY SKILLS

General molecular biology techniques: western blotting, immunoprecipitation, isolation of mitochondria, biotin-switch for measurement of S-nitrosylated proteins, ubiquitination assays, RT-PCR, molecular cloning, live/death assay

Biochemistry: bacterial protein purification, FPLC, affinity chromatography

Cell culture: culture of mammalian cells, DNA transfection

Fluorescence microscopy: visualization of GTP-tagged proteins

Animals: introductory course in laboratory animal science

ADDITIONAL SKILLS

Languages: German (native language)
English (fluent speaking and writing)
French (advanced knowledge)

Curriculum Vitae

Anne-Sophie Benischke

Software: Microsoft Office (Word, Excel, Powerpoint)
Image processing: Adobe Photoshop, Adobe Illustrator, ImageJ
Clone Manager6

PUBLICATIONS

Hemion C[*], <u>Benischke AS</u>[*], Neutzner M, Norris K, Frank S, Santel A, Flammer J, Youle R, Karbowski M, Neutzner A. [*] contributed equally to this work
The mitochondrial RING finger protein MARCH9 modulates mitochondrial dynamics PLOS ONE (in revision)

Neutzner A, Neutzner M, <u>Benischke AS</u>, Ryu SW, Frank S, Youle RJ, Karbowski MA
Systematic search for endoplasmic reticulum (ER) membrane-associated RING finger proteins identifies Nixin/ZNRF4 as a regulator of calnexin stability and ER homeostasis. J Biol Chem. 2011, Mar 11;286(10):8633-43

<u>Benischke AS,</u> Hemion C, Flammer J, Neutzner A
Proteasome-mediated quality control of S-nitrosylated mitochondrial proteins
Mitochondrion (submitted)

MANUSCRIPTS IN PREPARATION

<u>Benischke AS</u>, Neutzner A, Tappeiner Ch, Goldblum D
In vitro toxicity of omalizumab in conjuctival epithelial cells

POSTER PRESENTATIONS

Systematic search for endoplasmic reticulum (ER) membrane-associated RING finger proteins identifies Nixin/ZNRF4 as a regulator of calnexin stability and ER homeostasis
Experimental Biology 2011, Washington DC

A novel mitochondrial ubiquitin ligase involved in the regulation of mitochondrial fusion
Experimental Biology 2012, San Diego

In vitro toxicity of omalizumab in conjuctival epithelial cells
ARVO 2013, Seattle

Grant

August Collin-Fonds Grant (Freiwillige Akademische Gesellschaft Basel, 2013)

PERSONAL REFERENCES

Dr. Albert Neutzner
Department of Biomedicine
University of Basel
Hebelstrasse 20
4031 Basel
albert.neutzner@unibas.ch

Prof. David Goldblum
Department of Ophthalmology
University Hospital Basel
Mittlere Strasse 91
4031 Basel
David.Goldblum@usb.ch